Fracture Stimulation by Nano-assisted Foam-based Fluids in High-Temperature Reservoirs

Tuan Huynh Minh Tran

B. Eng. (Hons)

A thesis submitted for the degree of Doctor of Philosophy (PhD.)

School of Chemical Engineering

Discipline of Petroleum Engineering

Faculty of Sciences, Engineering & Technology (SET)

The University of Adelaide, Australia

September 2023

Table of Contents

Abstract

Fracture stimulation, or hydraulic fracturing, has been increasingly implemented to extract and enhance oil and gas production from unconventional resources with very low permeability. In this stimulation technique, fracturing fluid is injected at very high pressure into the underground to initiate and propagate fractures at the target reservoir interval. Proppants, such as coated sands and ceramic, are mixed within the fracturing fluid and distributed inside the fractures to keep the fractures open and maintain the conductive pathways for oil and gas flows. Therefore, fracturing fluids must have sufficient stability and viscosity to suspend, transport and place proppants deep into the fracture system.

Liquid foam has been an attractive alternative to conventional water-based fracturing fluids, especially in water-sensitive or under-pressured reservoirs. Implementing fracturing foams offers several practical benefits, such as low water consumption, reduced formation damage, low leak-off rate and high efficiency in transporting and distributing proppants in the fractures. However, while surfactant agents are mainly used to generate and stabilize liquid foams, they tend to degrade very quickly at high temperatures and high salinity, resulting in reduced stability and poor performance of fracturing foams at reservoir conditions.

The main aim of this study is to develop an optimized foam-based fracturing fluid with sufficient stability and adequate proppant transportation capacity under harsh reservoir conditions. Furthermore, the stabilization effects of nanoparticles and surfactants on the properties of liquid foams are investigated by a wide range of surface and bulk-scale experiments and fracture simulation modelling.

The experimental results show that the synergy between surfactants and silica nanoparticles (SNP) has massive impacts on the properties of fracturing foams. At ambient and elevated temperatures, the combination of SNP and ionic surfactant leads to higher foam stability and foamability, compared to that of SNP and non-ionic surfactant. At sufficient surfactant concentrations, the electrostatic attraction between SNP and cationic surfactant results in a higher half-life, higher apparent viscosity and greater proppant-carrying capacity when compared with the electrostatic repulsion of the SNP-anionic surfactant system. The aggregation behaviour of SNP is promoted by either interacting with the oppositely charged surfactants or increasing the temperature and/or salinity. It is found that the SNP aggregates can either have positive or negative influences on the foams' properties, depending on their size and location of accumulation. The simulation results show that foams' stability, rheology and proppant suspension capacity are directly proportional to the propped area, fracture conductivity and well productivity. In the simulated tight gas reservoir models, the fracturing performance of SNP-surfactant-stabilized foams is significantly greater than that of the benchmark slickwater frac case.

The research presents remarkable insights into the synergistic interactions between surfactants and nanoparticles. Furthermore, it provides practical guidelines for designing an optimal nanoparticle-surfactant mixture to stabilize and enhance the properties of fracturing foams at high-temperature and high salinity reservoir conditions.

Declaration

I certify that this work contains no material which has been accepted for the award of any other degree or diploma in my name in any university or other tertiary institution and, to the best of my knowledge and belief, contains no material previously published or written by another person, except where due reference has been made in the text. In addition, I certify that no part of this work will, in the future, be used in a submission in my name for any other degree or diploma in any university or other tertiary institution without the prior approval of the University of Adelaide and where applicable, any partner institution responsible for the joint award of this degree.

The author acknowledges that the copyright of published works contained within this thesis resides with the copyright holder(s) of those works.

I give permission for the digital version of my thesis to be made available on the web, via the University's digital research repository, the Library Search and also through web search engines, unless permission has been granted by the University to restrict access for a period of time.

Tuan Huynh Minh Tran   22/09/2023

Acknowledgments

This thesis is not solely a result of my own work but a result of the shared work and supports from many amazing people around me. I would like to take the opportunity to express my appreciation to those who have supported me and contributed to my professional and personal development throughout the journey.

First and foremost, I would like to show my deep gratitude to my parents, Loan Huynh and Son Tran. Despite our physical distance, I have fully felt your strong love and support every single day since I first came to Australia. I am very thankful for all of your sacrifices so that I can follow my passion and chase my own dreams overseas. I would also like to extend my appreciation to my elder brother, Hung Mishar Tran, for his continued support and encouragement.

A very special thanks to my principal supervisor, Mrs. Maria Gonzalez, who has consistently and patiently supported me since the very first day. She has provided a huge amount of valuable input and advice and, more importantly, guided me to become an effective researcher. Thank you very much for your hard work and dedication, Mary!

I would also like to express my sincere appreciation to my first co-supervisor, Assoc. Professor Manouchehr Haghighi, for his significant technical contribution, motivating discussions and the knowledge shared.

I am very grateful to my second co-supervisor, Dr. Khalid Amrouch, for his supportive attitude and invaluable pieces of advice for personal and career growth. Thank you for raising me up at the toughest times and changing my mindset in a very positive way.

I am also grateful for the significant assistance that I received from the staff and administrative people at the Australian School of Petroleum and Energy Resources (ASPER) and at the University of Adelaide.

Besides that, I would like to especially thank my PhD colleagues at ASPER and my close friends in Australia for their enormous support. I will never forget all the fantastic memories that we had together in my candidature.

Last but not least, I would like to express my greatest appreciation to my partner, Phuong Dinh. Thank you for always being there, loving and taking very good care of me, and especially always believing in me even when sometimes I wasn't. I love every single food that you make, and I am extremely grateful to have your support and encouragement in the whole journey. I just couldn't imagine how my physical and mental health would be without you. You are the reason that I keep on working hard and improving myself every day. Because of you, I have been able to accomplish achievements and become the best version of myself. Thank you!

List of Publications

Published Peer-Reviewed Journal Papers:

- ➤ **Tran, T**, Gonzalez Perdomo, ME, Haghighi, M & Amrouch, K 2022, 'Study of the synergistic effects between different surfactant types and silica nanoparticles on the stability of liquid foams at elevated temperature', Fuel, vol. 315.

- ➤ **Tran, T**, Gonzalez Perdomo, ME, Wilk, K, Kasza, P & Amrouch, K 2020, 'Performance evaluation of synthetic and natural polymers in nitrogen foam-based fracturing fluids in the Cooper Basin, South Australia', Journal of the Australian Petroleum Production & Exploration Association (APPEA), vol. 60, no. 1.

- ➤ **Tran, T**, Gonzalez Perdomo, ME, Haghighi, M & Amrouch, K 2023, 'Experimental study of the effects of salinity on nanoparticle-surfactant foams for fracture stimulation application', Journal of Gas Science and Engineering, vol. 115.

- ➤ **Tran, T**, Gonzalez Perdomo, ME, Haghighi, M & Amrouch, K 2023, 'Effects of cationic and anionic surfactants on the stability, rheology and proppant suspension of nanoparticle-stabilized fracturing foams at elevated temperature', Journal of Geoenergy Science and Engineering, vol. 228.

Submitted Journal Papers:

- ➤ **Tran, T**, Nguyen, G, Gonzalez Perdomo, ME, Haghighi, M & Amrouch, K 2023, 'Simulation study of foam rheology and the effects on hydraulic fracture proppant placement', SPE Journal, submitted in August 2023.

List of Figures

List of Tables

Nomenclature

A	Hamaker constant
A_b	Bubble area
A_v	Exponential constant
D	Separation distance
d_p	Proppant particle diameter
E	Particle detachment energy
E_f	Activation energy
F_{drag}	Total drag force exerting on a settling particle
F^n	Network force exerting on a settling particle
F^p	Pressure force exerting on a settling particle
h_f	Film thickness
k	Flow consistency index
n	Flow behaviour index
Q	Foam quality
R	University gas constant
R_b	Bubble/film radius
R_p	Particle radius
P_c^{max}	Maximum capillary pressure of coalescence
P_{inside}	Pressure inside the bubble (gas phase)
$P_{outside}$	Pressure out the bubble (liquid phase)
T	Absolute temperature
$V_{drainage}$	Liquid drainage velocity
V_{gas}	Gas volume in foam
V_{liquid}	Liquid volume in foam
V_{foam}	Total foam volume
W	Total interaction energy
W_{EDL}	Electric double layer repulsive interaction energy
W_{VdW}	Van der Waals attractive interaction energy
β	Theoretical packing parameter
γ	Surface tension of the gas-liquid interface
γ_{aw}	Air-water interfacial tension
$\dot{\gamma}$	Shear rate
ΔP_f	Film pressure
ΔP	Pressure difference in gas bubble
ε	Relative dielectric constant of the liquid
ε_0	Permittivity of vacuum
ζ	Zeta potential
θ	Contact angle
κ^{-1}	Debye length
μ	Fluid viscosity
μ_a	Apparent viscosity
μ_e	Effective viscosity
ρ	Fluid density
σ	Surface tension
τ	Shear stress

τ_0 Yield stress
ϕ_g Foam quality
ψ_s Stern potential

1. Contextual Statement

1.1. Research background

In recent decades, due to the depletion of conventional hydrocarbon resources, there has been an increasing need for production from unconventional resources to satisfy the growing energy demand. These unconventional resources are challenging to extract because of their low permeability, usually less than 1 mD. Fracture stimulation, or hydraulic fracturing, was first introduced in Texas, USA, in the late 1940s (Speight, 2016). Since then, hydraulic fracturing has been a very effective stimulation technique, which injects fluids at high pressure into the underground to generate fractures in a target reservoir. Proppants, such as coated sands and ceramics, are mixed within the fracturing fluids to keep the fractures open after the treatment, creating a network of highly conductive pathways and enhancing the well productivity (Barati and Liang, 2014; Speight, 2016). Therefore, it is critically important that fracturing fluids have sufficient stability and viscosity to effectively transport and distribute proppants in the fracture system. With inadequate fluid viscosity or stability, proppant particles tend to quickly accumulate in the near-wellbore region, which eventually reduces the propped area in both vertical and horizontal directions and decreases the fracture conductivity.

Generally, conventional water-based fracturing fluids such as slickwater are the simplest and most inexpensive options to fracture a reservoir. However, they possess several practical limitations, such as high consumption of water, limited proppant transportation capacity, low flowback recovery, and water blocking in tight formations (Gupta, 2009) and especially, they cause clay swelling and permeability impairment when interacting with water-sensitive formations such as shale (Wang et al., 2016; Wanniarachchi et al., 2017; Yekeen et al., 2018; Fu and Liu, 2019; Fu and Liu, 2021). Multiple alternative fracturing fluid solutions have been developed and introduced to address these limitations, and foam-based fracturing fluid has been widely considered the most effective and successful one.

Since initially introduced in the early 1980s, liquid foams have been applied to stimulate some water-sensitive and depleted reservoirs (Harris et al., 1984). Throughout the decades, the advantages of foam-based fracturing fluids have been commonly reported and acknowledged. First, due to the dominant volume of gas in foams, the water consumption required in foam fracturing technology is only 10 – 30% compared to that of the conventional water-based fluids. In addition, the high apparent viscosity of liquid foams offers substantial benefits not only to the transportation and placement of proppants, but also to the low leak-off rate (Kong et al., 2016; Fei et al., 2018; Isah et al., 2021). These foams' properties are significant to decrease the chemical additive consumption, prevent formation damage from clay swelling, water blocking and reduce the environmental concerns on the fracturing operation (Yekeen et al., 2018). Moreover, as foams naturally break down by gas expansion over time, they offer a very effective and rapid fluid clean-up after the treatment. However, as fracturing foams must be produced on site before injection, there are some associated technical and logistical challenges to construct the facility and to transport and store the chemicals, gas and liquids separately (Wanniarachchi et al., 2015). Besides that, high surface pumping pressure is usually required due to the low density of the fracturing foam.

During fluid injection with high shear rates and fracturing closing with low shear rates, fracturing fluids should have sufficient stability and viscosity to transport and distribute proppants in the fracture system effectively. With inadequate fluid viscosity or stability, proppant particles tend to quickly accumulate in the near-wellbore region, which eventually reduces the propped area in both vertical and horizontal directions and decreases the fracture conductivity. Therefore, it is critically important that fracturing foams maintain highly stable and viscous under harsh reservoir conditions such as high temperature and high salinity.

Traditionally, surfactant has been mostly used as a foaming agent to improve liquid foams' rheology and proppant suspension capacity. It has been observed that surfactant-stabilized fracturing foams possess some superior properties in laboratory studies (Zhou et al., 2020). However, they have two major limitations in the field application, which include the adsorption of surfactants on the rock surface and, more severely, the degradation of surfactants at reservoir conditions with high temperature and/or high salinity (Kapetas et al., 2016; Faroughi et al., 2018; Abdelaal et al., 2021). This significantly reduces the stability and viscosity of the fracturing foams, leading to limited proppant transportation and poor performance of the stimulation treatment (Luo et al., 2014; Lv et al., 2015; Ahmed et al., 2018). While several approaches have been studied to enhance the foam durability, the combination of surfactant and nanotechnology has been widely accepted as the most viable and efficient solution to tackle these issues.

Although some previous research works have been conducted to study the effects of nanoparticles on liquid foams, the cooperative interaction between surfactants and nanoparticles has not been fully understood. Moreover, the synergistic effects between nanoparticles and surfactants on the properties of foam-based fracturing fluids have not been investigated before, especially at reservoir conditions. Therefore, a comprehensive study focusing on this topic is necessary to fill in the presented research gaps.

1.2. Research objectives

The properties of liquid foams are unfavourably affected by many external factors, such as temperature and salinity. The main aim of this study is to develop an optimized foam system which has high stability, high proppant transportation capacity and excellent effectiveness in the hydraulic fracturing application at reservoir conditions. Specifically, the combinations of nanoparticles, surfactants and polymers are considered to enhance the properties of foams. This research's primary purpose is to establish general guidelines for the petroleum industry in designing foam fracturing treatment. The following objectives are addressed in the study:

a) Develop a reproducible and reliable experimental technique to evaluate the properties of fracturing foams stabilized by surfactants and nanoparticles.

b) Determine the effects of surfactant type and concentration on the surface characteristics of nanoparticles.

c) Investigate the synergistic effects between surfactants and nanoparticles on the foamability, stability, viscosity and proppant-carrying capacity of the foam-based fracturing fluids.

d) Determine the interrelationship among the stability, rheological and proppant suspension properties of fracturing foams in the presence of nanoparticles.

e) Investigate the influences of temperature and salinity on the properties of nanoparticle-surfactant-stabilized fracturing foams.

f) Integrate experimental results with numerical modelling to simulate and assess the fracturing performance of liquid foams at reservoir conditions.

1.3. Thesis structure

This is a PhD thesis by publication. Five journal papers are included in the thesis, four of which have been published in peer-reviewed journals, while one is currently under review. The PhD candidate is the first author in all the papers. Table 1 summarizes all the journal papers included in this thesis.

Five Chapters form the thesis body. The *first Chapter* introduces the research background, objectives and thesis structure and outlines the relationship and contribution of the journal papers to the thesis. The *second Chapter* presents a detailed literature review surrounding the works of this thesis, including discussions of the theoretical background, application and enhancement practice of foam-based fracturing fluids. *Chapters three, four, five, six and seven* are the novel research performed as part of this thesis.

Table 1: Chapter outlines

Chapter	Title	Status
Chapter 3	Study of the synergistic effects between different surfactant types and silica nanoparticles on the stability of liquid foams at elevated temperature	Published
Chapter 4	Effects of cationic and anionic surfactants on the stability, rheology and proppant suspension of nanoparticle-stabilized fracturing foams at elevated temperature	Published
Chapter 5	Simulation study of foam rheology and the effects on hydraulic fracture proppant placement	Submitted
Chapter 6	Experimental study of the effects of salinity on nanoparticle-surfactant foams for fracture stimulation application	Published
Chapter 7	Performance evaluation of synthetic and natural polymers in nitrogen foam-based fracturing fluids in the Cooper Basin, South Australia	Published

Chapter three presents the influences of three distinct surfactant groups on the surface characteristics of nanoparticles. This chapter also provides the synergistic effects between surfactants and nanoparticles (NP) on liquid foams' foaming capacity and drainage behaviour. *Chapter four* investigates the impacts of surfactant type and concentration on the key properties of NP-stabilized foams, including the foamability, foam stability, rheology and proppant suspension capacity. Both ambient and elevated temperatures are included in the experimental investigation. *Chapter five* incorporates the results of previous experiments and develops a 3-D fracture simulation model to evaluate and compare the fracturing performance of NP-surfactant-stabilized foams and slickwater on a tight gas reservoir. The key comparison metrics include the proppant distribution, fracture dimension, fracture conductivity and the cumulative gas production post-treatment. *Chapter six* studies the effects of salinity on the properties of fracturing foams stabilized by anionic surfactant and NP at both ambient and high temperatures. The influences of salt concentration on the surface characteristics of NP are included and supported by the colloidal dispersion stability's theory. *Chapter seven* presents the impacts of polymer as an alternative stabilizing agent on the rheological behaviour of liquid foams in reservoir conditions. By incorporating the experimental results and industry field data, this chapter provides a simulation study of the performance of fracturing foams on an actual gas field in Australia. *Chapter eight* summarises the main findings of this research and presents recommendations for future work.

1.4. How publications are related to the thesis

The paper "Study of the synergistic effects between different surfactant types and silica nanoparticles on the stability of liquid foams at elevated temperature" presents the influences of different surfactant types and concentrations on the zeta potential, aggregate size and wettability of silica nanoparticles (SNP). The interaction and adsorption mechanisms of surfactant molecules on SNP surface are thoroughly discussed. The effects of different SNP-surfactant mixtures on the drainage behaviour of foams are evaluated at both ambient and elevated temperatures, which helps determine whether the electrostatic attraction or electrostatic repulsion between SNP and surfactant molecules is more beneficial in stabilizing foams. The particle detachment energy theory is used to justify the enhanced stability of the SNP-surfactant foams. The study provides an insightful understanding of the synergistic interaction between surfactants and SNP, which contributes to establishing formulation guidelines to develop sustainable and optimal foam-based fluids used in hydraulic fracturing.

The next two papers entitled "Effects of cationic and anionic surfactants on the stability, rheology and proppant suspension of nanoparticle-stabilized fracturing foams at elevated temperature" and "Simulation study of foam rheology and the effects on hydraulic fracture proppant placement", an integrated approach is developed to investigate the impacts of cationic and anionic surfactants on the properties and fracturing performance of the SNP-stabilized foams. A comprehensive set of laboratory experiments is established to examine the foaming capacity, half-life, apparent viscosity and proppant settlement velocity of foam-based fracturing fluids at both ambient and elevated temperatures. The observed interrelationship among foam stability, foam rheology and proppant suspension capacity are elaborated in the study.

Besides that, a 3-D fracture simulation model on a tight gas reservoir is developed using the well logs, mini-frac, perforation design and reservoir properties data. The experimental viscosity results of SNP-cationic surfactant and SNP-anionic surfactant foams are characterized by the Power Law model and imported into the simulator, which allows for assessing and comparing the fracturing performance among the studied foams versus the industry benchmark frac slickwater fluid. The key assessment metrics include the proppant distribution, fracture dimension, fracture conductivity and the productivity of the stimulated well. Both papers provide practical guidelines for selecting the optimal surfactant type and concentration in the hydraulic fracturing application. The influences of SNP-surfactant interaction on the performance of liquid foams have been experimentally studied and then validated through simulation modelling. Clear linkages have been unveiled between the fracturing foams' properties and the reservoir productivity.

The paper "Experimental study of the effects of salinity on nanoparticle-surfactant foams for fracture stimulation application" presents a complete investigation of the influences of NaCl salt concentration on the foamability, stability, viscosity and proppant-carrying capacity of SNP-surfactant-stabilized fracturing foams at both ambient and elevated temperatures. DLVO (Derjaguin, Landau, Verwey & Overbeek) theory, which describes the electrostatic interaction between two substrates, is used to justify the impacts of salinity on the SNP colloidal stability and the foams' properties. At high salinity, the accumulation of SNP aggregates in the bulk dispersion is observed, causing a massive reduction in the properties of fracturing foams. This study contributes to developing practical guidelines for designing foam-

based fracturing fluids under high salinity conditions and understanding the impact of increased salinity conditions on the performance of a hydraulic fracture treatment.

In the final paper entitled "<u>Performance evaluation of synthetic and natural polymers in nitrogen foam-based fracturing fluids in the Cooper Basin, South Australia</u>", natural and synthetic polymers are studied as alternative agents to stabilize nitrogen foams at high-pressure high temperature (HPHT) conditions of 1000 psi and 110°C. Actual reservoir data, completion design and field production history from a local petroleum company are collected to build a fracture propagation model on a producing gas field in the Cooper Basin, Australia. The simulation model is used to investigate the fracturing effectiveness of the studied foam systems. Through simulation modelling, the paper emphasizes the significance of foam quality and thermal stability on the performance of fracturing foams in HPHT environments. The findings of the paper help formulate guidelines to develop the sustainable and optimal foam-based fluids used in hydraulic fracturing applications.

1.5. References

Abdelaal, A, Aljawad, MS, Alyousef, Z & Almajid, MM 2021, 'A review of foam-based fracturing fluids applications: From lab studies to field implementations', Journal of Natural Gas Science and Engineering, vol. 95.

Ahmed, S, Elraies, K, Hashmet, M & Alnarabiji, M 2018, 'Empirical Modeling of the Viscosity of Supercritical Carbon Dioxide Foam Fracturing Fluid under Different Downhole Conditions', Energies, vol. 11, no. 4.

Barati, R & Liang, JT 2014, 'A review of fracturing fluid systems used for hydraulic fracturing of oil and gas wells', Journal of Applied Polymer Science, vol. 131, no. 16.

Faroughi, SA, Pruvot, AJ-CJ & McAndrew, J 2018, 'The rheological behavior of energized fluids and foams with application to hydraulic fracturing: Review', Journal of Petroleum Science and Engineering, vol. 163, pp. 243-263.

Fei, Y, Johnson, RL, Gonzalez, M, Haghighi, M & Pokalai, K 2018, 'Experimental and numerical investigation into nano-stabilized foams in low permeability reservoir hydraulic fracturing applications', Fuel, vol. 213, pp. 133-143.

Fu, C & Liu, N 2019, 'Waterless fluids in hydraulic fracturing – A review', Journal of Natural Gas Science and Engineering, vol. 67, pp. 214-224.

Fu, C & Liu, N 2021, 'Rheology and stability of nanoparticle-stabilized CO2 foam under reservoir conditions', Journal of Petroleum Science and Engineering, vol. 196.

Gu, M & Mohanty, K 2014, 'Effect of foam quality on effectiveness of hydraulic fracturing in shales', International Journal of Rock Mechanics and Mining Science, vol. 70, pp. 273-285.

Gupta, D.V., 2009. 'Unconventional fracturing fluids for tight gas reservoirs', SPE Hydraulic Fracturing Technology Conference, Society of Petroleum Engineers, 119424-MS.

Harris, PC, Haynes, RJ & Egger, JP, 1984, 'The use of CO2-based fracturing fluids in the Red Fork formation in the Anadarko Basin, Oklahoma', Journal of Petroleum Technology, vol. 36.

Isah, A, Hiba, M, Al-Azani, K, Aljawad, MS & Mahmoud, M 2021, 'A comprehensive review of proppant transport in fractured reservoirs: Experimental, numerical, and field aspects', Journal of Natural Gas Science and Engineering, vol. 88.

Kapetas, L, Vincent Bonnieu, S, Danelis, S, Rossen, WR, Farajzadeh, R, Eftekhari, AA, Mohd Shafian, SR & Kamarul Bahrim, RZ 2016, 'Effect of temperature on foam flow in porous media', Journal of Industrial and Engineering Chemistry, vol. 36, pp. 229-237.

Kong, X, McAndrew, J & Cisternas, P 2016, 'CFD Study of Using Foam Fracturing Fluid for Proppant Transport in Hydraulic Fractures', in Abu Dhabi International Petroleum Exhibition & Conference, vol. Day 2 Tue, November 08, 2016.

Luo, X, Wang, S, Wang, Z, Jing, Z & Lv, M 2014, 'Experimental research on rheological properties and proppant transport performance of GRF–CO2 fracturing fluid', Journal of Petroleum Science and Engineering, vol. 120, pp. 154-162.

Lv, Q, Li, Z, Li, B, Li, S & Sun, Q 2015, 'Study of Nanoparticle–Surfactant-Stabilized Foam as a Fracturing Fluid', Industrial & Engineering Chemistry Research, vol. 54, no. 38, pp. 9468-9477.

Speight, JG 2016, Handbook of Hydraulic Fracturing, John Wiley & Sons.

Wang, L, Yao, B, Cha, M, Alqahtani, NB, Patterson, TW, Kneafsey, TJ, Miskimins, JL, Yin, X & Wu, Y-S 2016, 'Waterless fracturing technologies for unconventional reservoirs-opportunities for liquid nitrogen', Journal of Natural Gas Science and Engineering, vol. 35, pp. 160-174.

Wanniarachchi, WAM, Ranjith, PG, Perera, MSA, Lashin, A, Al Arifi, N & Li, JC 2015, 'Current opinions on foam-based hydro-fracturing in deep geological reservoirs', Geomechanics and Geophysics for Geo-Energy and Geo-Resources, vol. 1, no. 3-4, pp. 121-134.

Wanniarachchi, WAM, Ranjith, PG & Perera, MSA 2017, 'Shale gas fracturing using foam-based fracturing fluid: a review', Environmental Earth Sciences, vol. 76, no. 2.

Yekeen, N, Padmanabhan, E & Idris, AK 2018, 'A review of recent advances in foam-based fracturing fluid application in unconventional reservoirs', Journal of Industrial and Engineering Chemistry, vol. 66, pp. 45-71.

Zhou, J, Ranjith, PG & Wanniarachchi, WAM 2020, 'Different strategies of foam stabilization in the use of foam as a fracturing fluid', Advances in Colloid and Interface Science, vol. 276, Feb, p. 102104.

2. Literature Review

2.1. Hydraulic fracturing

Since first introduced in Texas, USA in the late 1940s, hydraulic fracturing has remained a fundamental engineering tool for extracting oil and gas from unconventional resources, which typically has low permeability of less than 1 milliDarcy (Smith and Montgomery, 2015; Yekeen et al., 2019). Some examples of unconventional resources are coalbed methane, shale gas, gas hydrates and tight gas reservoirs. A typical fracturing stimulation consists of five main stages: pre-pad, pad, slurry, displacement and shut-in (Guo et al., 2017). Each stage is illustrated in Figure 1, and is briefly described as follows:

1. Pre-pad: Involves injecting a small amount of fluid to initiate fractures and to obtain information about the characteristics of the reservoirs.
2. Pad: Involves injecting a large amount of more viscous fluids to break the formation and propagate the fracture network.
3. Slurry: In this stage, the proppant is mixed in with the fracturing fluid and pumped downhole to maintain a conductive pathway.
4. Displacement: Involves pumping fresh water to flush out the proppant slurry, which is left in the wellbore.
5. Shut-in: Involves shutting down the well to allow fractures to close on the proppant. The injected fracturing fluid then flows back, enabling hydrocarbon to be produced afterwards.
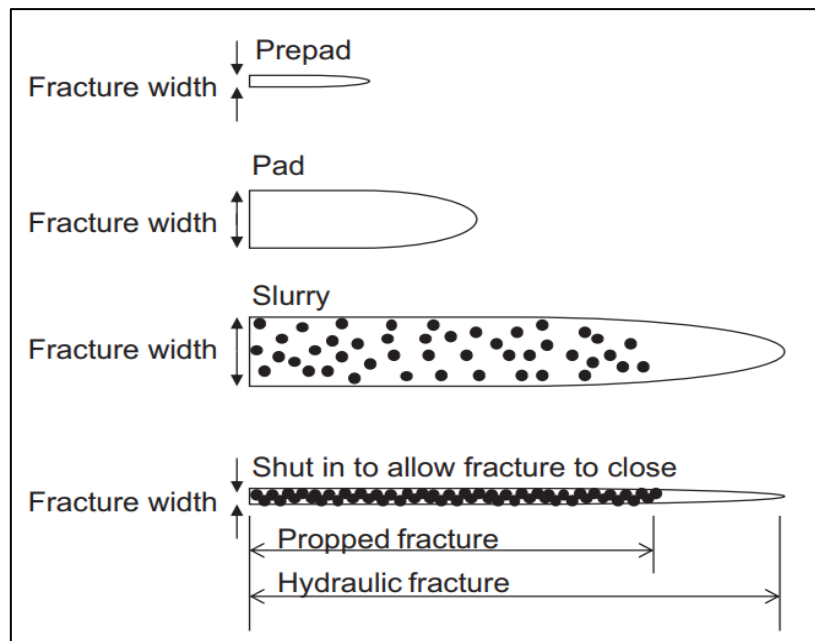
Figure 1: Fracture growth in width and length and proppant (black dots) placement (Guo et al., 2017)

2.1.1. Fracturing fluid

Fracturing fluids play a critical role in the success of the fracture treatment. Speight (2016) summarizes the key features of an ideal fracturing fluid, which should have:

- High viscosity to carry and place proppant into the fractures. As more proppants are transported and settled in a long distance, conductive pathways are created for oil and gas to flow.
- Compatibility with formation rock, reservoir fluid and the designed additives and proppant.
- Ability to generate a wide fracture by creating high-pressure drop along the fracture.
- Low viscosity after the main treatment to allow effective flowback.
- Cost-effective and environmentally friendly.

In order to achieve the above features, the fracturing fluid is designed with three main components: the base fluid, chemical additives and proppants. Base fluid accounts for the largest proportion of the total volume of the fracturing fluid mixture, typically 95 – 99% (Speight, 2016). Several types of base fluids have been introduced and applied throughout the history of hydraulic fracturing. Each base fluid type has its distinct properties, advantages and disadvantages. A summary of some common base fluid types is shown in Table 2.

Table 2: Comparisons of common types of fracturing fluids (Wanniarachchi et al., 2017)

Fluid type	Properties at ambient conditions	Advantages	Disadvantages
Slickwater	ρ =1000 kg/m^3 μ = 2 cP	+ Reduced well damage + Cost containment + Higher stimulated volume + Better fracture containment	- Poor proppant-carrying capacity - Large freshwater consumption - Large wastewater generation - Environmental issues - Cannot be used in water-sensitive formations
Cross-linked fluid	ρ = 950 kg/m^3 μ = 550 cP	+ Better proppant-carrying capacity + Reduced well damage + Cost containment + Higher stimulated volume + Better fracture containment	- Limited fracture network propagation - Large freshwater consumption - Large wastewater generation - Environmental issues
Oil-based fluid	ρ = 850 kg/m^3 μ = 100 cP	+ Reduced water usage + Reduced logistic work. + Higher recovery rates + Rapid well clean-up	- Unnecessarily induced high viscosity due to gelling - Higher capital cost - High flammability risk
Acid-based fluid	ρ = 1200 kg/m^3 μ = 2 cP	+ Reduced proppant usage + Reduced water usage	- Economically not efficient - Cannot be used in high-carbonate reservoirs
Foam-based fluid	ρ = 250 kg/m^3 μ = 150 cP	+ Reduced water usage and reduced wastewater generation + Reduced formation damage + Higher proppant-carrying capacity + Recyclable and reusable + Reduced environmental damage. + Suitable for water-sensitive formations	- Higher initial cost - Higher logistic requirements - Stability and viscosity reduction in high temperatures

2.1.2. Proppants

Proppants are small-sized round particles, which are typically made of natural sand or synthetic ceramic material. During fracturing operation, proppants are pumped in the slurry stage, preventing fracture closure from the downhole pressure. Therefore, the placement of fractures is critically important to the success of any fracture stimulation. Generally, proppants are characterized by their size and material. Guo et al. (2017) summarize some critical properties of proppants in Table 3.

Table 3: Common proppant properties (Guo et al., 2017)

Properties	Common types
Proppant sizes	12/20-mesh, 16/30-mesh, 20/40-mesh, 30/50 mesh, 40/70-mesh, 70/140-mesh
Common materials	Silica sands, artificial ceramics, resin-coated
Compressive strength	4000 – 12000 psi
Proppant porosity	0.35 – 0.43
Proppant specific gravity	For sand proppants: 2.62 – 2.65 For ceramic proppants: 2.55 – 3.9

2.2. Foam-based fracturing fluids

Foam is a dispersion of gas bubbles in the liquid. The schematic of the foam structure is demonstrated in Figure 2. The gas bubbles are separated by thin liquid films called lamella, while the junction point of three lamella is called the Plateau border. The behaviour of foams is heavily influenced by the foam quality, which is the ratio between gas volume and the total foam volume (Equation 1):

$$Q = \frac{V_{gas}}{V_{foam}} = \frac{V_{gas}}{V_{gas} + V_{liquid}} \tag{1}$$

where Q is the foam quality, V_{gas} is the gas volume, V_{liquid} is the liquid volume, and V_{foam} is the total foam volume. Liquid foams can be classified as wet foams with 52-74% quality, dry foams with 74-96% quality, and mist foams with >96% quality (Yekeen et al., 2018b). The optimal foam quality for hydraulic fracturing application has been suggested at between 70% and 80% (Kohshour et al., 2016; Anandan et al., 2017).
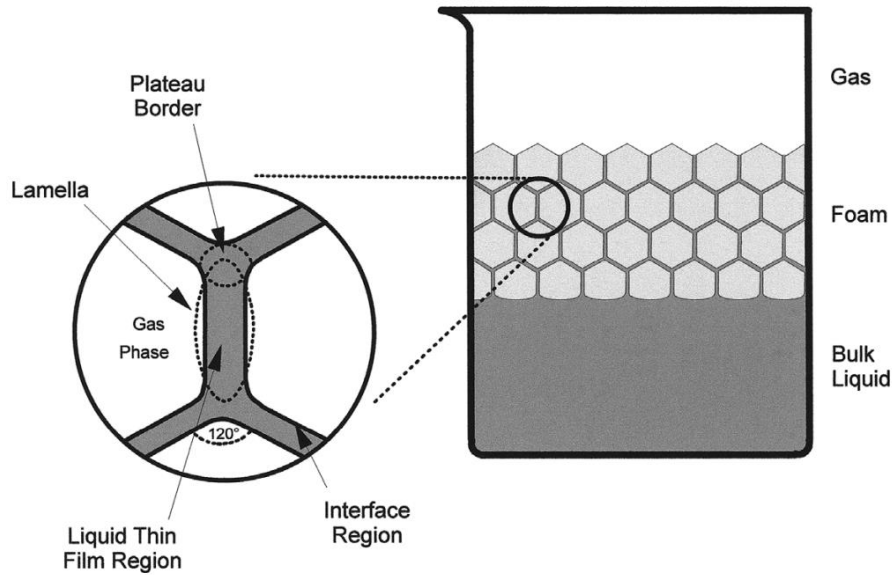

Figure 2: Schematic of foam structure in bubble scale (Schramm, 2005)

2.2.1. Surfactants

Surfactants, or surface-active agents, play an essential role in generating foams. The addition of surfactant helps reduce the surface tension of the liquid phase, allowing gas bubbles to be formed (Schramm, 1994). The increase in surfactant concentration gradually reduces the surface tension until reaching the critical micelle concentration (CMC). Beyond the CMC, surfactant molecules start to form organized aggregates called micelles, which have no further impacts on the surface tension or the foamability. The effects of surfactant concentration on the surface tension and the formation of surfactant micelles are illustrated in Figure 3.
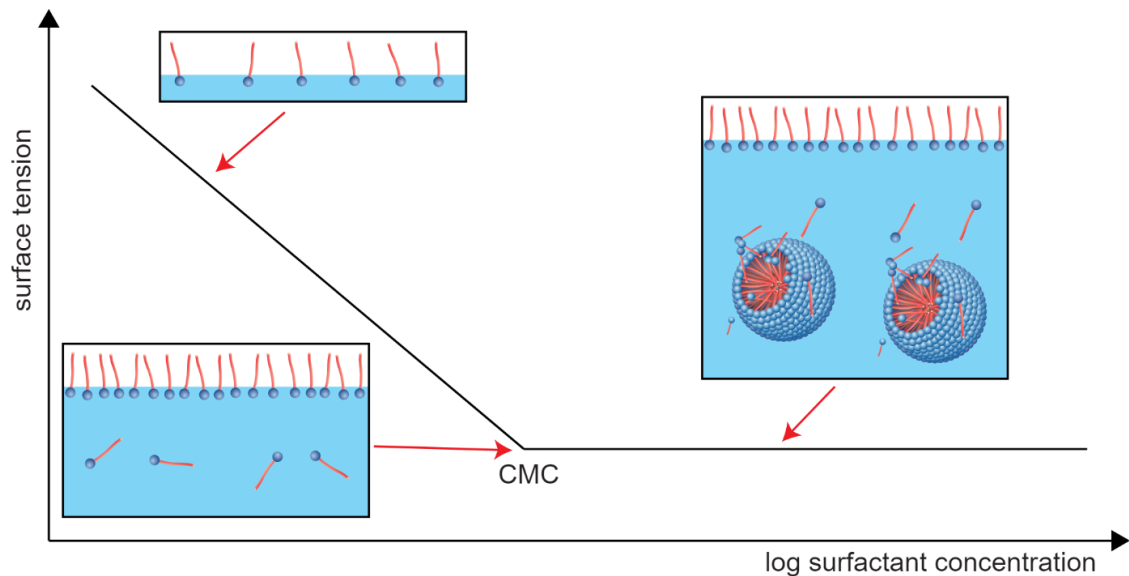
Figure 3: Effects of surfactant concentration on the surface tension

Surfactant molecules are amphiphilic, which contain a hydrophilic head attached to a long hydrophobic tail. Based on the different electric charges in the head groups, surfactants can be classified into four main categories as cationic surfactants (positively charged), anionic surfactants (negatively charged), non-ionic surfactants (uncharged) and zwitterionic surfactants (containing both positive and negative charges) (Negin et al., 2017). Figure 4 demonstrates four common surfactant types and their corresponding charges in the head groups.
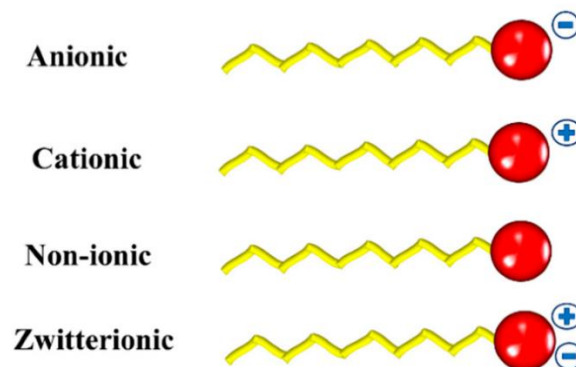
Figure 4: Common surfactant types and their charged head groups (Guerrero-Hernández et al., 2022)

2.2.2. Foam stability

Foams are thermodynamically unstable due to three main destabilization mechanisms: foam drainage, bubble coarsening and bubble coalescence (Schramm, 1994; Majeed et al., 2020). Figure 5 shows the simplified schematic of three destabilization mechanisms in foams. These phenomena are interdependent on each other. It is essential to understand these mechanisms to control and enhance the foams' properties. Among three mechanisms, liquid drainage has the greatest impacts on the foam instability due to the film thinning from reduced liquid content (Langevin, 2000; Kruglyakov et al., 2008; Li et al., 2017; Li et al., 2019). Therefore, foam drainage should be predominantly focused in the foam stabilization study.
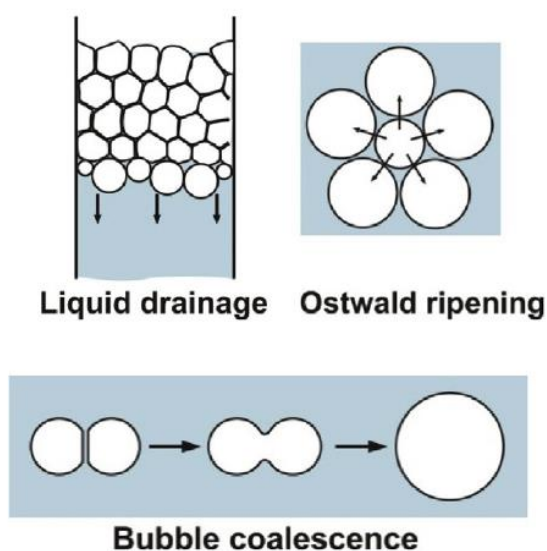
Figure 5: Simplified schematic of three main destabilization mechanisms in foams
(Denkov et al., 2020)

2.2.2.1. Foam drainage

In the foam drainage process, liquid flows downward and through the Plateau borders due to the combined gravitational and capillary forces (Sun et al., 2008). The drainage behaviour of different surfactant-foams over time can be shown in Figure 6.
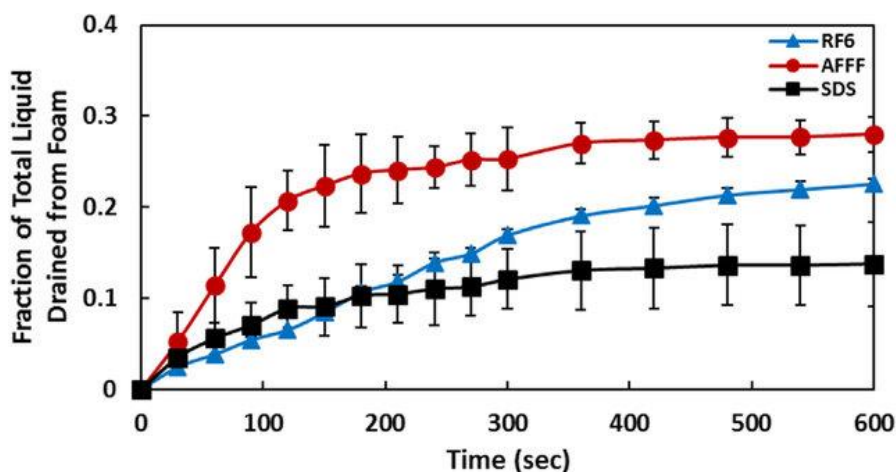
Figure 6: Liquid drainage from different surfactant-foams as a function of time (Hinnant et al., 2017)

The liquid drainage velocity of foams can be determined by Equation 2 (Yekeen et al., 2018a) as:

$$V_{drainage} = \frac{dh_f}{dt} = \frac{h_f^3}{3\mu_e R_b^2} \Delta P_f \tag{2}$$

where $V_{drainage}$ is the liquid drainage velocity, h_f is the film/lamellae thickness, μ_e is the effective viscosity of the aqueous phase, R_b is the foam film radius, and ΔP_f is the film pressure. The liquid drainage can be delayed by increasing the dispersion viscosity.

2.2.2.2.   Bubble coarsening

During the bubble coarsening or 'Ostwald ripening' process, gas diffuses from small bubbles to the larger ones. The bubble coarsening is driven by the pressure difference in bubbles, which is also known as the Laplace pressure. The Laplace pressure in a bubble (ΔP) can be determined from the Young-Laplace equation as:

$$\Delta P = P_{inside} - P_{outside} = P_{gas} - P_{liquid} = \frac{2\sigma}{R_b} \tag{3}$$

$$P_{gas} = P_{liquid} + \frac{2\sigma}{R_b} \tag{4}$$

where ΔP is the difference between the pressure inside the bubble (gas phase) and the pressure outside bubble (liquid phase), σ is the surface tension of the gas-liquid interface, and R_b is bubble radius.

It can be interpreted from Equation 4 that bubbles with smaller sizes have higher inside/gas pressure and vice versa. As a result, gas in smaller bubbles continuously breaks through the lamellae and diffuses to the larger bubbles, which can be demonstrated in Figure 7.

Figure 7: Schematic of the bubble growth caused by a driving force (Stevenson, 2010)

The foam drainage and bubble coarsening processes have simultaneous effects on each other. As liquid drains through the Plateau border, the lamellae become thinner, allowing easier

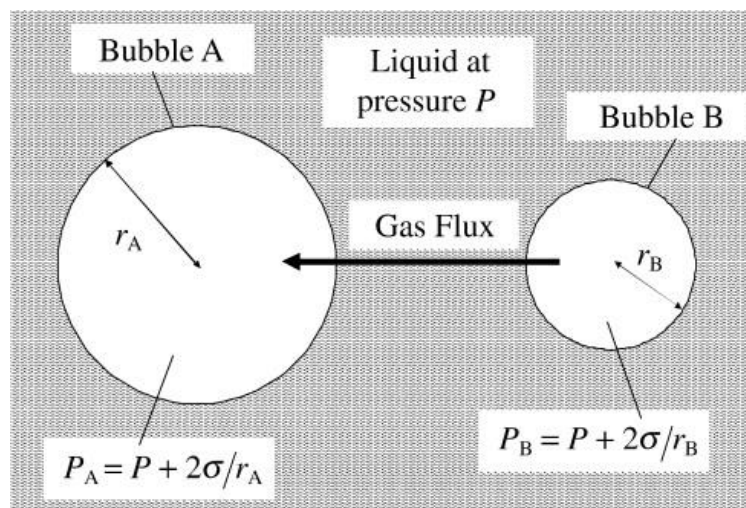diffusion of gas between the bubbles. On the other hand, bubble coarsening accelerates the liquid drainage rate due to gas expansion and increased bubble sizes (Hutzler et al., 2005).

2.2.2.3. Bubble coalescence

The influences of foam drainage and bubble coarsening cause film thinning and reduce the film stability. As the processes continue, the liquid films become ruptured, which merges small bubbles into the larger ones and eventually results in bubble collapse. This merging and breakage phenomenon is the bubble coalescence in foams, which can be illustrated in Figure 8.
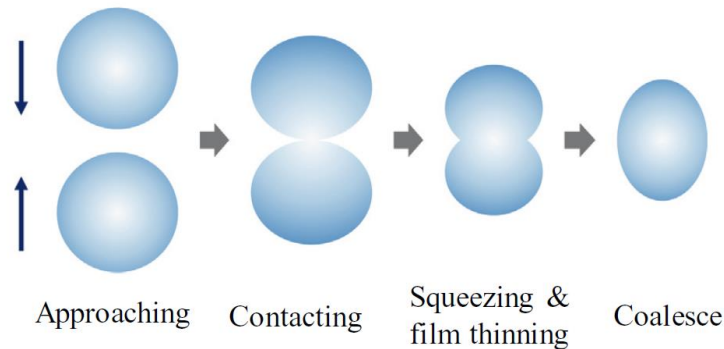
Figure 8: Schematic diagram of two bubbles coalescing (Zhou et al., 2020)

The stability of foam-based fracturing fluids can be affected by the operating conditions. The lifetime of foams is improved with increasing pressure. However, at higher operating temperatures, the rates of foam drainage, coarsening and coalescence increase, leading to faster foam decay (Faroughi et al., 2018).

2.2.3. Foam viscosity

The foam's viscosity is an essential property in the hydraulic fracturing application as it governs the fracture propagation patter and controls the proppant-carrying capacity. The foam viscosity depends on the foam texture, foam quality, dispersion viscosity and external conditions such as temperature, pressure and shear rate (Wanniarachchi et al., 2015). Foams with finer textures and smaller bubbles have higher resistance to deformation, leading to higher apparent viscosity (Fu and Liu, 2019). The relationship between foam viscosity and foam quality features the "mountain-shaped" trend, in which the optimal foam viscosities have been reported at between 60% and 80% (Pang, 2007; Mo et al., 2012; Worthen et al., 2013; Gu and Mohanty, 2014; Zhu et al., 2017).

As the pressure increases, the viscosity of foams is slightly improved due to the increased fluid density and fine foam texture (Gu and Mohanty, 2014; Gu and Mohanty, 2015). On the other hand, the increasing temperature considerably decreases the foam viscosity because of the gas expansion and reduced foam stability from surfactant degradation (Sun et al., 2014; Verma et al., 2017; Anandan et al., 2017). Figure 9 shows the effects of temperature and foam quality on the apparent viscosity of fracturing foams. The relationship between temperature and the apparent viscosity of liquid foam can be demonstrated by the Arrhenius law (Yekeen et al., 2018b), which is shown in Equation 5 as:

$$\mu_a = A_v \exp\left(\frac{E_f}{RT}\right) \tag{5}$$

where μ_a is the apparent viscosity of foam, A_v is an exponential constant, E_f is the activation energy, R is the university gas constant, and T is the absolute temperature.
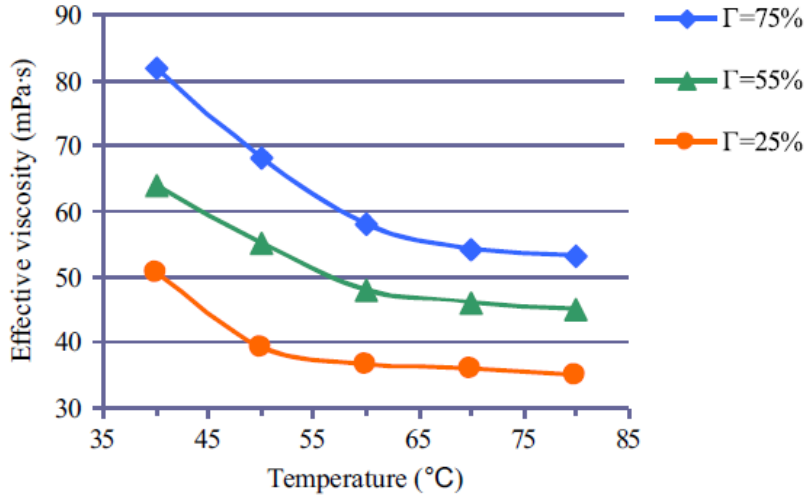
Figure 9: Effects of temperature on foam effective viscosity at different foam qualities
(Luo et al., 2014)

Foam-based fracturing fluids have non-Newtonian rheological characteristics (Sun et al., 2014, Du et al., 2020). Two common models have been used to characterize the foams' rheological properties: the power law model (Equation 6) and the Hershel Bulkley model (Equation 7). While many researchers prefer the power law model because its constants can be easily obtained, the Hershel Bulkley model can provide precise rheological modelling with sufficient experimental data.

$$Power\ law\ model: \quad \tau = k\dot{\gamma}^n \tag{6}$$

$$Hershel\ Bulkley\ model: \quad \tau = \tau_0 + k\dot{\gamma}^n \tag{7}$$

where τ is the shear stress, $\dot{\gamma}$ is the shear rate, k is the flow consistency index, n is the flow behavior index, and τ_0 is the yield stress, which is the stress required to start the flow (Beck et al., 2017).

Moreover, fracturing foams exhibit shear-thinning behaviour, in which the foam viscosity decreases with increasing shear rate. Figure 10 shows the typical shear-thinning behaviour of fracturing foams at ambient and elevated temperatures. The shear-thinning behaviour of foams is advantageous in the fracturing application. In the process of mixing and pumping fracturing fluids downhole, constant flow circulation and high pressure are typically required, leading to high shear rates. As foam has lower viscosity at a high shear rate, the friction loss and pumping requirements are reduced, helping bring down stimulation costs (Gu and Mohanty, 2015). On the other hand, low shear rates are usually observed in the porous media and the fracture flows. By having high viscosity at low shear rates, fracturing foams

have excellent capabilities of suspending and transporting proppants into the fractures, helping enhance the fracture dimensions and conductivity.
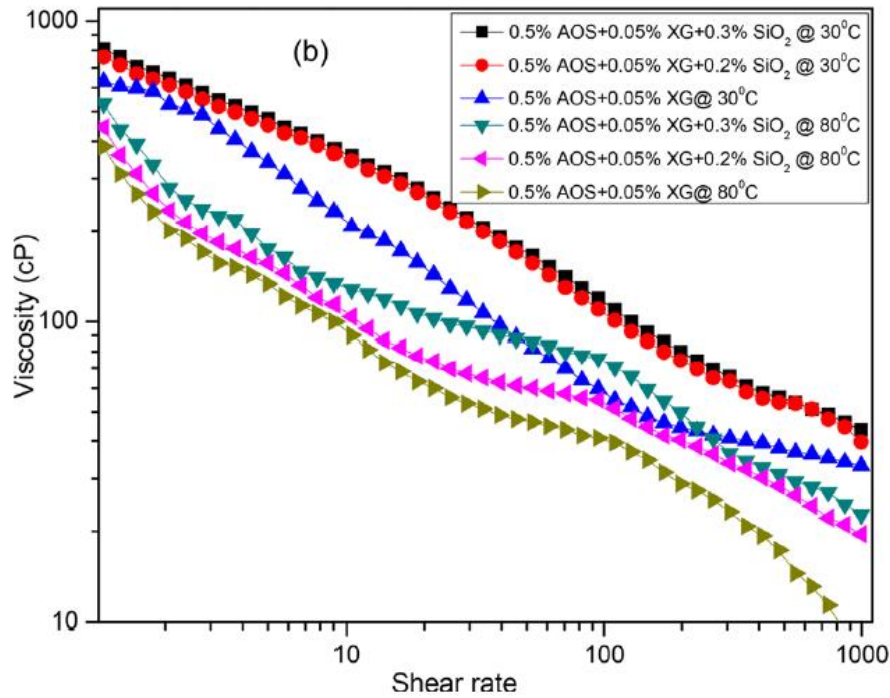
Figure 10: Effects of shear rates on foam viscosity at different temperatures (Verma et al., 2018)

2.2.4. Proppant suspension capacity

In addition to foam stability and foam rheology, the proppant-carrying capacity of foams plays an essential role in the effectiveness of the fracture treatment. Foams with higher proppant-carrying ability can transport and place more proppants from the near wellbore to the targeted fracture surfaces, resulting in higher fracture conductivity. The proppant suspension capacity of fracturing foams is mainly evaluated by the proppant settling velocity. Higher proppant setting velocity indicates lower proppant-carrying capacity, and vice versa. The classical Stokes' law model has been modified to capture the effects of the microstructure of foams on the static proppant settling (Stokes, 1851; Fei et al., 2017; Yekeen et al., 2018b).

Figure 11 demonstrates the main forces exerted on the settling proppant in the bubble scale. When settling through the foam structure, the proppant tends to squeeze or stretch the foam films, generating pressure force (from the pressure inside bubbles) and network force (from the lamellae) on the proppant (Tong et al., 2019). These two forces act as the drag forces against gravity, helping delay the settlement of proppants in fracturing foams. The total drag force (F_{drag}) of foam bubbles on a proppant can be described in Equation 8. While the pressure force is difficult to be characterized or measured, the network force has been commonly estimated by Equation 9 (Raufaste et al., 2007; Jing et al., 2016).

$$F_{drag} = F^p + F^n \tag{8}$$

$$F^n = \frac{0.516}{\left(1 - \phi_g\right)^{0.25}} \frac{\gamma d_p}{\sqrt{A_b}} \tag{9}$$

where F^p is the pressure force, F^n is the network force, ϕ_g is the foam quality, γ is the surface tension, d_p is the proppant particle diameter, and A_b is the bubble area.

Figure 11: Schematic of forces exerting on the settling proppant (reproduced from Zhu et al., 2019)

As the proppant-carrying capacity of fracturing foams heavily depends on the foam stability and foam viscosity, it is significantly influenced by the harsh reservoir conditions such as temperature, pressure, salinity an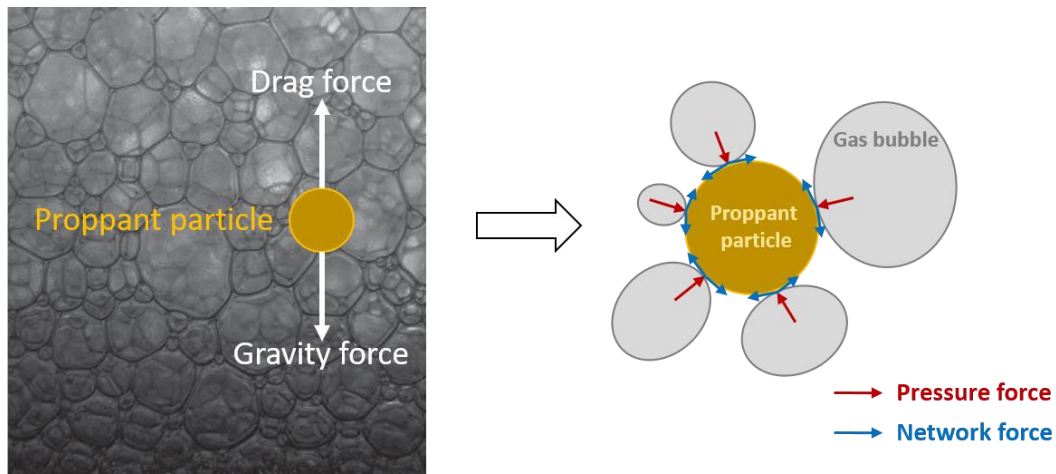d shear rate. Therefore, several stabilization methods have been introduced and implemented, and nanotechnology has been found to be one of the most effective solutions (Lv et al., 2015; AlYousef et al., 2017; Zhou et al., 2020; Zhang et al., 2021; Majeed et al., 2021).

2.2.5. Summary of foam-based fracturing fluids' properties

The characteristics and performance of foam-based fracturing fluids are greatly determined by four interconnected factors: foam quality, foam stability, foam viscosity and proppant suspension capacity. Understanding the linkages among these elements is essential as they collectively determine the success of hydraulic fracturing operations.

Foam quality represents the proportion of gas entrained within the fracturing fluid. The foam quality depends on the volume and size distribution of gas bubbles dispersed in the liquid phase. By achieving high-quality foam, fracture stimulation operations can generate fractures more efficiently and result in wider fracture lengths, which directly helps maximize contact area with the reservoir rock.

Proppant suspension capacity represents the fluid's ability to keep proppants suspended within the foam matrix during injection. The proppant suspension capacity of liquid foams is closely connected with foam viscosity and foam stability. With sufficient foam viscosity, foam-based fracturing fluids can effectively suspend and transport proppants into the fractures, and minimize the early settlement of proppants at the near wellbore region. Consequently, the generated fractures will have a uniform proppant distribution, effective propped area and fracture width, ultimately resulting in highly conductive pathways to enhance oil and gas production. However, foam viscosity tends to decrease over time due to the natural deformation in the structural integrity of foams. Therefore, it is extremely important to achieve and maintain high foam stability. Liquid foams with sufficient stability are less likely to break down prematurely, helping prevent inefficient proppant placement and fracture conductivity reduction.

2.3. Nanoparticle-surfactant-stabilized fracturing foams

Liquid foams are traditionally stabilized by surfactants and polymers, which have some practical limitations, such as surfactant adsorption on the rock surface, surfactant degradation at reservoir conditions, and increased formation damage from polymer residue (Yekeen et al., 2019; Emrani et al., 2017). As a result, nanoparticles (NP) have been studied and applied to improve the stability, rheological properties and proppant suspension capacity of foam-based fracturing fluids. The stabilization mechanisms and benefits of NP on liquid foams are discussed below

2.3.1. Stabilization mechanisms of NP on fracturing foams

The combination of NP and surfactant generates stable and effective fracturing foams in harsh environments. The adsorption of NP on the gas-liquid interface is fundamental to maintaining long-term stability and enhancing liquid foams' properties (Zhou et al., 2020). As NP adsorb on the bubble interface, they minimize the contact area between the fluids and increase the film strength and film elasticity. This significantly helps reduce gas diffusion, decrease liquid drainage, delay film thinning and directly improve the foam stability (Yekeen et al., 2017; Majeed et al., 2020). Figure 12 demonstrates the difference in bubble images between surfactant-foams and NP-surfactant-foams, on which smaller bubble sizes and narrower size ranges are observed with the addition of NP.
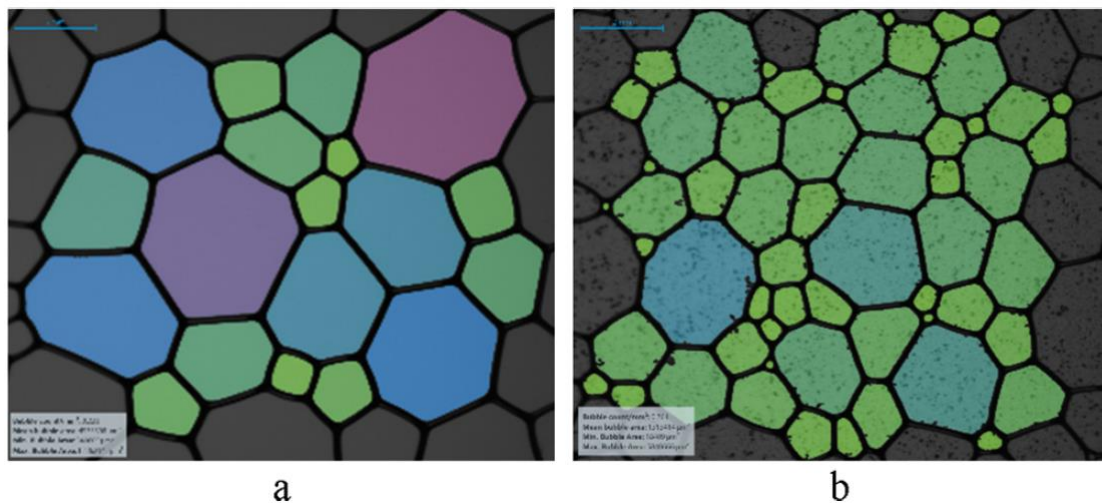
Figure 12: Bubble images of foams using (a) surfactant only and (b) surfactant with nanoparticles (Majeed et al., 2020)

The stabilization effects of NP on fracturing foams can be explained by three main mechanisms as 1) particle detachment energy, 2) maximum capillary pressure of coalescence, and 3) particle arrangement during film drainage (Zhou et al., 2020; Zhang et al., 2021; Rasid et al., 2022). The first two mechanisms are the interaction between NP and liquid film, while the last mechanism belongs to the particle-particle interaction among NP.

2.3.1.1. Particle detachment energy

Particle detachment energy is the energy required to remove the adsorbed particles from the gas-liquid interface (Hunter et al., 2008; Zhou et al., 2020). The detachment energy of a spherical particle can be calculated by Equation 10 as:

$$E = \pi R_p^2 \gamma (1 - cos\theta)^2 \qquad (10)$$

where E is the particle detachment energy, R_p is the particle radius, γ is the surface tension, and θ is the contact angle of the particle at the interface.

The detachment energy of NP is of the order 10^3 kT, which is several times greater than that of the surfactant molecule of the order 1 kT (Binks et al., 2008; Sun et al., 2014). As a result, NP tend to have irreversible adsorption on the gas-liquid interface to stabilize foams, while surfactant molecules can desorb easily after some time or under extreme conditions. In addition, the detachment energy of NP increases with increasing hydrophobicity and reaches the maximum at the contact angle of 90° (Zhang et al., 2016; Emrani et al., 2017).

2.3.1.2. Maximum capillary pressure of coalescence

Maximum capillary pressure of coalescence (P_c^{max}) is the pressure required to decrease the gap between bubbles to zero, resulting in film rupture (Yekeen et al., 2018a; Rasid et al., 2022). As the maximum capillary pressure increases, the bubble coalescence rate reduces, causing higher foam stability. The relationship between P_c^{max} and its parameters were developed by Kaptay (2006) and can be expressed in Equation 11 as:

$$P_c^{max} = \beta \frac{2\gamma_{aw}}{R_p} cos\theta \qquad (11)$$

where β is the theoretical packing parameter, γ_{aw} is the air-water interfacial tension, R_p is the particle radius, and θ is the contact angle of the particle at the interface.

According to Equation 11, P_c^{max} is greatly affected by the packing parameter at the interface (β). The adsorption of NP tends to form a network of particle aggregates at the interface, which increases the packing parameter to prevent bubble coalescence and enhance the stability of foams. Besides that, NP with moderate hydrophobicity has been commonly reported as the ideal for the maximum foam stability, while extremely hydrophobic or hydrophilic NP can have very limited effects on enhancing the properties of foams (AlYousef et al., 2017; AlYousef et al., 2018).

2.3.1.3. Particle arrangement during film drainage

As NP adsorb and aggregate at the liquid film and Plateau border, they can form three possible structures, which are a monolayer of bridging particles, a thick bilayer of close-packed particles, and a network of particle aggregates (Fameau and Salonen, 2014). Figure 13 shows the schematic of three structures of NP adsorption at the interface.
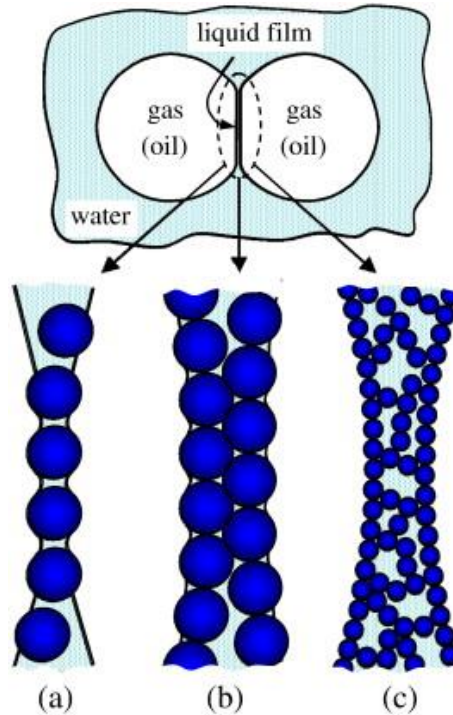
Figure 13: Possible mechanisms of liquid film stabilization by: (a) a monolayer of bridging particles; (b) a bilayer of close-packed particles, and (c) a network of particle aggregates (Horozov, 2008)

The structure of NP depends on the NP concentration and affects the foam stability differently. While the single layer of NP generates a steric interfacial barrier to prevent foam coarsening and coalescence, the bilayer of close-packed particles effectively reduces liquid drainage in foams (Singh and Mohanty, 2015; Kumar and Mandal, 2017). Besides that, a network of particle aggregates has been acknowledged as the most effective mechanism for foam stabilization (AlYousef et al., 2017). The aggregate network at the gas-liquid interface has several benefits, which help generate thick solid films to reduce gas diffusion, slow down gravitational drainage, delay film thinning and prevent film rupture in liquid foams (Yekeen et al., 2018a). However, suppose the aggregation of NP takes place in the bulk dispersion rather than at the gas-liquid interface, they are very likely to result in negative impacts on the properties of the NP-stabilized foams.

2.3.2. DLVO theory on the stability of NP colloidal dispersion

The properties of NP-stabilized foams greatly depend on the stability of the NP dispersion. At low colloidal stability, NP aggregates tend to be formed in the dispersion, which reduces the foam stabilization effects of NP. According to DLVO theory (Derjaguin and Landau, 1941; Verwey and Overbeek, 1949), the stability of a colloidal system is determined by the sum of the Van der Waals (VdW) attractive and the electric double layer (EDL) repulsive forces exerted on the particles. The VdW attractive and EDL repulsive interaction energy between two spherical particles of same radius can be simplified and expressed in Equations 12 & 13 (Adair et al., 2001). The combined interaction energy between two particles $W(D)$ is the total of the VdW interaction energy $W_{VdW}(D)$ and EDL interaction energy $W_{EDL}(D)$ (Equation 14).

$$W_{VdW}(D) = -\frac{AR_p}{12D} \qquad (12)$$

where A is the Hamaker constant, R_p is the particle radius, and D is the separation distance.

$$W_{EDL}(D) = 2\pi\varepsilon\varepsilon_0 R_p \psi_s^2 \ \exp(-\kappa D) \qquad (13)$$

where ε is the relative dielectric constant of the liquid, ε_0 is the permittivity of vacuum, R_p is the particle radius, ψ_s is the Stern potential, κ^{-1} is the Debye length, and D is the separation distance.

$$W(D) = W_{VdW}(D) + W_{EDL}(D) \qquad (14)$$

Figure 14 demonstrates the relationship between separation distance and the interaction energy from VdW and EDL forces. While the Van der Waals attractive force is significant at a very small separation distance, the effect of Electric Double Layer repulsive force is generally stronger and in a wider range (Adair et al., 2001). At a considerable separation distance, the EDL repulsion is the predominant force to prevent particles from approaching each other due to the Brownian motion. Stern potential and zeta potential are used to explain the repulsion mechanism between the particles. However, under extreme conditions such as high temperature and high salinity, the attractive force on the particles may overcome the repulsion and result in irreversible particle aggregation. At a significant level of aggregation, particle flocculates are formed within the dispersions, which decreases the stability of the colloidal system (Freitas and Muller, 1998).
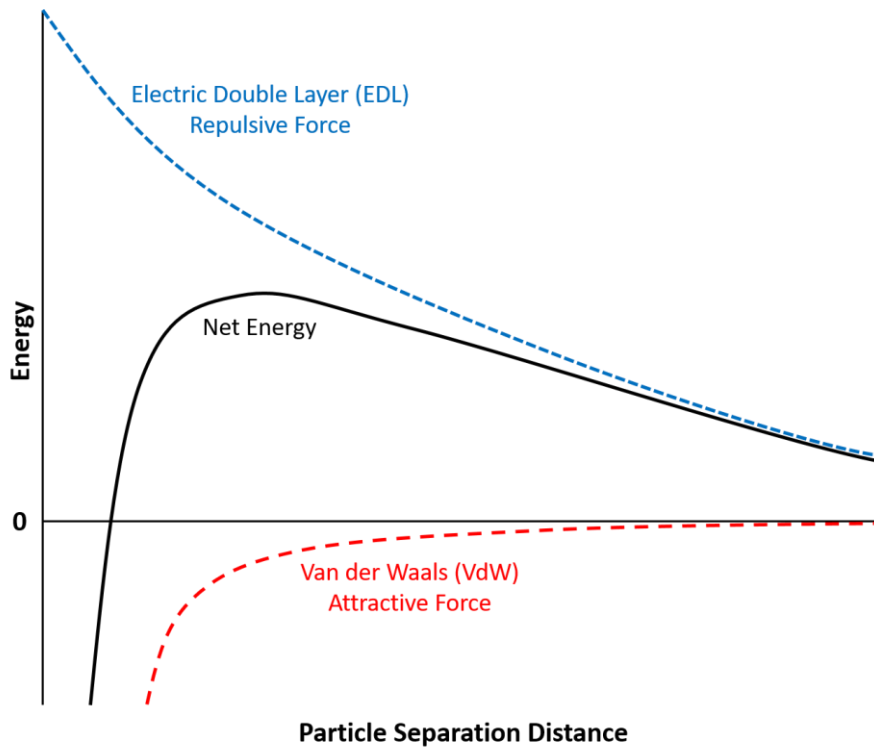
Figure 14: Schematic of repulsive and attractive energy on particles in dispersion (Cardellini et al., 2016)

2.4. Summary

In this chapter, the introduction of hydraulic fracturing and foam-based fracturing fluids are first discussed. After that, the key properties of fracturing foams, including foam stability, viscosity and proppant suspension capacity, and the three main destabilization mechanisms of foams are reviewed. Furthermore, the literature on current research of NP-surfactant-stabilized foams are presented. Finally, the stabilization mechanisms of NP on liquid foams are reviewed, followed by the DLVO theory to explain and emphasize the importance of the NP colloidal dispersion stability.

2.5. References

Adair, JH, Suvaci, E & Sindel, J 2001, 'Surface and Colloid Chemistry', Encyclopedia of Materials: Science and Technology, Elsevier, Oxford, pp. 1-10.

AlYousef, ZA, Almobarky, MA & Schechter, DS 2017, 'Enhancing the stability of foam by the use of nanoparticles', Energy & Fuels, vol. 31, p. 10620 – 10627.

AlYousef, ZA, Almobarky, MA & Schechter, DS 2018, 'The effect of nanoparticle aggregation on surfactant foam stability', Journal of Colloid and Interface Science, vol. 511, pp. 365-373.

Anandan, R, Johnson, S & Barati, R 2017, 'Polyelectrolyte complex stabilized CO2 foam systems for hydraulic fracturing application', SPE Liquids-Rich Basin Conference – North America, Texas, USA, September 2017, SPE-187489-MS.

Beck, G, Nolen, C, Hoopes, K, Krouse, C, Poerner, M, Phatak, A & Verma, S 2017, 'Laboratory evaluation of a natural gas–based foamed fracturing fluid', SPE Annual Technical Conference and Exhibition, Texas, USA, October 2017, SPE-187199-MS.

Binks, B, Kirkland, M & Rodrigues, JA 2008, 'Origin of stabilization of aqueous foams in nanoparticle–surfactant mixtures', Soft Matter, vol. 4, pp. 2373-2382.

Cardellini, A, Fasano, M, Bozorg Bigdeli, M, Chiavazzo, E & Asinari, P 2016, 'Thermal transport phenomena in nanoparticle suspensions', Journal of Physics: Condensed Matter, vol. 28, no. 48, p. 483003.

Denkov, N, Tcholakova, S & Politova-Brinkova, N 2020, 'Physicochemical control of foam properties', Current Opinion in Colloid & Interface Science, vol. 50.

Derjaguin, B & Landau, L 1941, 'Theory of the stability of strongly charged lyophobic sols and of the adhesion of strongly charged particles in solutions of electrolytes', Progress in Surface Science, vol. 43, pp. 30-59.

Du, D, Zhang, X, Li, Y, Zhao, D, Wang, F & Sun, Z 2020, 'Experimental study on rheological properties of nanoparticle-stabilized carbon dioxide foam', Journal of Natural Gas Science and Engineering, vol. 75.

Emrani, A & Nasr-El-Din, H 2017, 'Stabilizing CO2 foam by use of nanoparticles', SPE Journal, vol. 22, no. 2, pp. 494-504.

Fameau, A-L & Salonen, A 2014, 'Effect of particles and aggregated structures on the foam stability and aging', Comptes Rendus Physique, vol. 15, no. 8-9, pp. 748-760.

Faroughi, SA, Pruvot, AJ-CJ & McAndrew, J 2018, 'The rheological behavior of energized fluids and foams with application to hydraulic fracturing: Review', Journal of Petroleum Science and Engineering, vol. 163, pp. 243-263.

Fei, Y, Zhu, J, Xu, B, Li, X, Gonzalez, M & Haghighi, M 2017, 'Experimental investigation of nanotechnology on worm-like micelles for high-temperature foam stimulation', Journal of Industrial and Engineering Chemistry, vol. 50, pp. 190-198.

Freitas, C & Müller, RH 1998, 'Effect of light and temperature on zeta potential and physical stability in solid lipid nanoparticle (SLN™) dispersions', International Journal of Pharmaceutics, vol. 168, no. 2, pp. 221-229.

Fu, C & Liu, N 2019, 'Waterless fluids in hydraulic fracturing – a review', Journal of Natural Gas Science and Engineering, vol. 67, pp. 214-224.

Gu, M & Mohanty K 2014, 'Effect of foam quality on effectiveness of hydraulic fracturing in shales', International Journal of Rock Mechanics and Mining Sciences, vol. 70, pp. 273-285.

Gu, M & Mohanty, KK 2015, 'Rheology of polymer-free foam fracturing fluids', Journal of Petroleum Science and Engineering, vol. 134, pp. 87-96.

Guerrero-Hernández, L, Meléndez-Ortiz, H, Cortez-Mazatan, G, Vaillant-Sánchez, S & Peralta-Rodríguezm R 2022, 'Gemini and bicephalous surfactants: a review on their synthesis, micelle formation, and uses', International Journal of Molecular Sciences, vol. 23, no. 3.

Guo, B, Liu, X & Tan, X 2017, 'Hydraulic Fracturing', in Petroleum Production Engineering, pp. 389-501.

Hinnant, K, Conroy, M & Ananth, R 2017, 'Influence of fuel on foam degradation for fluorinated and fluorine-free foams', Colloids and Surfaces A: Physicochemical and Engineering Aspects, vol. 522, p. 1-17.

Horozov, T 2008, 'Foams and foam films stabilized by solid particles', Current Opinion in Colloid & Interface Science, vol. 13, no. 3, pp. 134-140.

Hunter, T, Pugh, R, Franks, G & Jameson, G 2008, 'The role of particles in stabilizing foams and emulsions', Advances in Colloid and Interface Science, vol. 137, pp. 57-81.

Hutzler, S, Weaire, D, Saugey, A, Cox, S & Peron, N 2005, 'The physics of foam drainage', European Detergent Conference.

Jing, Z, Wang, S & Wang, Z 2016, 'Detailed Structural and Mechanical Response of Wet Foam to the Settling Particle', Langmuir, vol. 32, no. 10, pp. 2419-2427.

Kaptay, G 2006, 'On the equation of the maximum capillary pressure induced by solid particles to stabilize emulsions and foams and on the emulsion stability diagrams', Colloids and Surfaces A: Physicochemical and Engineering Aspects, vol. 282, pp. 387-401.

Kohshour, I, Leshchyshyn, T, Munro, J, Yorro, M, Adejumo, A, Ahmed, U, Barati, R, Kugler, I, Reynods, M, Cullen, M, McAndrew, J & Wedel, D 2016, 'Examination of water management challenges and solutions in shaleresource development- could waterless fracturing technologies work?', Unconventional Resources Technology Conference, San Antonio, USA, August 2016.

Kruglyakov, PM, Karakashev, SI, Nguyen, AV & Vilkova, NG 2008, 'Foam drainage', Current Opinion in Colloid & Interface Science, vol. 13, no. 3, pp. 163-170.

Kumar, S & Mandal, A 2017, 'Investigation on stabilization of CO 2 foam by ionic and non-ionic surfactants in presence of different additives for application in enhanced oil recovery', Applied Surface Science, vol. 420, pp. 9-20.

Langevin, D 2000, 'Influence of interfacial rheology on foam and emulsion properties', Advances in Colloid and Interface Science, vol. 88, pp. 209-222.

Li, S, Qiao, C, Li, Z & Wanambwa, S 2017, 'Properties of Carbon Dioxide Foam Stabilized by Hydrophilic Nanoparticles and Hexadecyltrimethylammonium Bromide', Energy & Fuels, vol. 31, no. 2, pp. 1478-1488.

Li, S, Yang, K, Li, Z, Zhang, K & Jia, N 2019, 'Properties of CO2 Foam Stabilized by Hydrophilic Nanoparticles and Non-ionic Surfactants', Energy & Fuels, vol. 33, no. 6, pp. 5043-5054.

Luo, X, Wang, S, Wang, Z, Jing, Z & Lv, M 2014, 'Experimental research on rheological properties and proppant transport performance of GRF–CO2 fracturing fluid', Journal of Petroleum Science and Engineering, vol. 120, pp. 154-162.

Lv, Q, Li, Z, Li, B, Li, S & Sun, Q 2015, 'Study of Nanoparticle–Surfactant-Stabilized Foam as a Fracturing Fluid', Industrial & Engineering Chemistry Research, vol. 54, no. 38, pp. 9468-9477.

Majeed, T, Kamal, MS, Zhou, X & Solling, T 2021, 'A Review on Foam Stabilizers for Enhanced Oil Recovery', Energy & Fuels, vol. 35, no. 7, pp. 5594-5612.

Majeed, T, Sølling, TI & Kamal, MS 2020, 'Foamstability: The interplay between salt-, surfactant- and critical micelle concentration', Journal of Petroleum Science and Engineering, vol. 187.

Mo, D, Yu, J, Liu, N & Lee, R 2012, 'Study of the effect of different factors on nanoparticle-stabilized CO2 foam for mobility control', SPE Annual Technical Conference and Exhibition, San Antonio, Texas, USA, October 2012, SPE-159282-MS.

Negin, C, Ali, S & Xie, Q 2017, 'Most common surfactants employed in chemical enhanced oil recovery', Petroleum, vol. 3, no. 2, pp. 197-211.

Pang ZX, Cheng, LS & Li, CL 2007, 'Enhanced heavy oil recovery with thermal foam flooding', Journal of Southwest Petroleum University, vol. 29, no. 6, pp. 71-74.

Rasid, SA, Mahmood, SM, Kechut, NI & Akbari, S 2022, 'A review on parameters affecting nanoparticles stabilized foam performance based on recent analyses', Journal of Petroleum Science and Engineering, vol. 208.

Raufaste, C, Dollet, B, Cox, Jiang, Y & Graner, F 2007, 'Yield drag in a two-dimensional foam flow around a circular obstacle: Effect of liquid fraction', The European Physical Journal E, vol. 23, pp. 217-228.

Schramm, LL 1994, Foams: Fundamentals and Applications in the Petroleum Industry, American Chemical Industry, Washington DC, USA.

Schramm, LL 2005, Emulsions, Foams, and Suspensions: Fundamentals and Applications, Wiley-VCH.

Singh, R & Mohanty, KK 2015, 'Synergy between Nanoparticles and Surfactants in Stabilizing Foams for Oil Recovery', Energy & Fuels, vol. 29, no. 2, pp. 467-479.

Smith, MB & Montgomery, C 2015, Hydraulic Fracturing, 1st edition, Boca Raton: CRC Press.

Speight, JG 2016, Handbook of Hydraulic Fracturing, John Wiley & Sons.

Stevenson, P 2010, 'Inter-bubble gas diffusion in liquid foam', Current Opinion in Colloid & Interface Science, vol. 15, no. 5, pp. 374-381.

Stokes, GG 1851, 'On the Effect of the Internal Friction of Fluids on the Motion of Pendulums', Transactions of the Cambridge Philosophical Society, vol. 9, pp. 8-106.

Sun, Q, Tan, L & Wang, G 2008, 'Liquid foam drainage: an overview', International Journal of Modern Physics B, vol. 22, no. 15, pp. 2333-2354.

Sun, X, Liang, X, Wang, S & Lu, Y 2014, 'Experimental study on the rheology of CO2 viscoelastic surfactant foam fracturing fluid', Journal of Petroleum Science and Engineering, vol. 119, pp. 104-111.

Tong, S, Gu, M, Singh, R & Mohanty, K 2019, 'Proppant transport in foam fracturing fluid during hydraulic fracturing', Journal of Petroleum Science and Engineering, vol. 182.

Verma, A, Chauhan, G & Ojha, K 2017, 'Synergistic effects of polymer and bentonite clay on rheology and thermal stability of foam fluid developed for hydraulic fracturing', Asia-Pacific Journal of Chemical Engineering, vol. 12, pp. 872-883.

Verma, A, Chauhan, G, Baruah, PP & Ojha, K 2018, 'Morphology, Rheology, and Kinetics of Nanosilica Stabilized Gelled Foam Fluid for Hydraulic Fracturing Application', Industrial & Engineering Chemistry Research, vol. 57, no. 40, pp. 13449-13462.

Verwey, EJW & Overbeek, JTG 1948, 'Theory of the Stability of Lyophobic Colloids: The Interaction of Sol Particles Having an Electric Double Layer', Elsevier.

Wanniarachchi, WAM, Ranjith, PG & Perera, MSA 2017, 'Shale gas fracturing using foam-based fracturing fluid: a review', Environmental Earth Sciences, vol. 76, no. 2.

Wanniarachchi, WAM, Ranjith, PG, Perera, MSA, Lashin, A, Al Arifi, N & Li, JC 2015, 'Current opinions on foam-based hydro-fracturing in deep geological reservoirs', Geomechanics and Geophysics for Geo-Energy and Geo-Resources, vol. 1, no. 3-4, pp. 121-134.

Worthen, AJ, Bagaria, HG, Chen, Y, Bryant, SL, Huh, C & Johnston, KP 2013, 'Nanoparticle-stabilized carbon dioxide-in-water foams with fine texture', Journal of Colloid and Interface Science, vol. 391, pp. 142-151.

Yekeen, N, Manan, MA, Idris, AK & Samin, AM 2017, 'Influence of surfactant and electrolyte concentrations on surfactant adsorption and foaming characteristics', Journal of Petroleum Science and Engineering, vol. 149, pp. 612-622.

Yekeen, N, Manan, MA, Idris, AK, Padmanabhan, E, Junin, R, Samin, AM, Gbadamosi, AO & Oguamah, I 2018a, 'A comprehensive review of experimental studies of

nanoparticles-stabilized foam for enhanced oil recovery', Journal of Petroleum Science and Engineering, vol. 164, pp. 43-74.

Yekeen, N, Padmanabhan, E & Idris, AK 2018b, 'A review of recent advances in foam-based fracturing fluid application in unconventional reservoirs', Journal of Industrial and Engineering Chemistry, vol. 66, pp. 45-71.

Yekeen, N, Padmanabhan, E, Idris, AK & Chauhan, PS 2019, 'Nanoparticles applications for hydraulic fracturing of unconventional reservoirs: A comprehensive review of recent advances and prospects', Journal of Petroleum Science and Engineering, vol. 178, pp. 41-73.

Zhang, C, Li, Z, Sun, Q, Wang, P, Wang, S & Liu, W 2016, 'CO2 foam properties and the stabilizing mechanism of sodium bis(2-ethylhexyl)sulfosuccinate and hydrophobic nanoparticle mixtures', Soft Matter, vol. 12, pp. 946-956.

Zhang, Y, Liu, Q, Ye, H, Yang, L, Luo, D & Peng, B 2021, 'Nanoparticles as foam stabilizer: Mechanism, control parameters and application in foam flooding for enhanced oil recovery', Journal of Petroleum Science and Engineering, vol. 202.

Zhou, J, Ranjith, PG & Wanniarachchi, WAM 2020, 'Different strategies of foam stabilization in the use of foam as a fracturing fluid', Advances in Colloid and Interface Science, vol. 276, p. 102104.

Zhu, J, Yang, Z, Li, X, Song, Z, Liu, Z & Xie, S 2019, 'Settling behavior of the proppants in viscoelastic foams on the bubble scale', Journal of Petroleum Science and Engineering, vol. 181.

Zhu, Y, Tian, J, Hou, Q, Luo, Y & Fan, J 2017, 'Studies on nanoparticle-stabilized foam flooding EOR for a high temperature and high salinity reservoir', Abu Dhabi International Petroleum Exhibition & Conference, Abu Dhabi, UAE, November 2017, SPE-188964-MS.

3. Study of the synergistic effects between different surfactant types and silica nanoparticles on the stability of liquid foams at elevated temperature

The application of foam-based fluids has gained increasing interests in the field of hydraulic fracturing. A critical aspect of optimizing foam-based fluids for practical use lies in understanding the interplay between nanoparticles (NP) and surfactants, particularly in the context of elevated temperatures found in reservoir conditions. This paper investigates how three types of surfactants, each at varying concentrations, impact both the properties of silica nanoparticles (SNP) and the stability of nano-stabilized foams under different temperature conditions. The research presents insightful findings, including the unique ability of cationic surfactants to convert SNP surface charges, promote particle aggregation, and enhance hydrophobicity. Furthermore, it highlights the distinct behaviours of NP in surfactant dispersions at elevated temperatures, with significant implications for foam stability. These insights deepen our understanding of surfactant-NP interactions and help develop more stable foams in hydraulic fracturing and other applications, ultimately contributing to more effective hydrocarbon recovery practices in reservoir conditions.

Statement of Authorship

Title of Paper	Study of the synergistic effects between different surfactant types and silica nanoparticles on the stability of liquid foams at elevated temperature
Publication Status	☑ Published ☐ Accepted for Publication ☐ Submitted for Publication ☐ Unpublished and Unsubmitted work written in manuscript style
Publication Details	Tran, T, Gonzalez Perdomo, ME, Haghighi, M & Amrouch, K 2022, 'Study of the synergistic effects between different surfactant types and silica nanoparticles on the stability of liquid foams at elevated temperature', Fuel, vol. 315.

Principal Author

Name of Principal Author (Candidate)	Tuan Huynh Minh Tran		
Contribution to the Paper	Literature review, Data collection, Result analysis and interpretation, Writing the manuscript		
Overall percentage (%)	70%		
Certification:	This paper reports on original research I conducted during the period of my Higher Degree by Research candidature and is not subject to any obligations or contractual agreements with a third party that would constrain its inclusion in this thesis. I am the primary author of this paper.		
Signature		Date	14/03/2023

Co-Author Contributions

By signing the Statement of Authorship, each author certifies that:

 i. the candidate's stated contribution to the publication is accurate (as detailed above);

 ii. permission is granted for the candidate in include the publication in the thesis; and

 iii. the sum of all co-author contributions is equal to 100% less the candidate's stated contribution.

Name of Co-Author	Maria Gonzalez Perdomo		
Contribution to the Paper	Support in result analysis, Reviewing the manuscript (15%)		
Signature		Date	14/03/2023

Name of Co-Author	Manouchehr Haghighi		
Contribution to the Paper	Support in result analysis, Reviewing the manuscript (10%)		
Signature		Date	16/03/2023

Name of Co-Author	Khalid Amrouch		
Contribution to the Paper	Support in result analysis, Reviewing the manuscript (5%)		
Signature		Date	17/03/2023

Full Length Article

Study of the synergistic effects between different surfactant types and silica nanoparticles on the stability of liquid foams at elevated temperature

Tuan Tran [a],[*], Maria Elena Gonzalez Perdomo [a], Manouchehr Haghighi [a], Khalid Amrouch [a],[b]

[a] Australian School of Petroleum and Energy Resources, University of Adelaide, South Australia 5000, Australia
[b] Geology & Sustainable Mining, Mohammed VI Polytechnic University, Lot-660, Benguerir 43150, Morocco

ABSTRACT

In recent years, there has been an increasing interest in the application of foam-based fluids in the field of hydrocarbon recovery. The combination of nanoparticles (NP) and surfactant has been intensively studied to improve the thermal stability and optimize the performance of foams. However, the synergistic interactions between NP and surfactants, and their impacts on foam stabilization at elevated temperature have yet to be clearly understood. This paper studies the effects of three types of surfactants with varied concentrations on the properties of silica nanoparticles (SNP) and on the stability of nano-stabilized foams at ambient and elevated temperatures. The experiments involved the zeta potential, particle size and contact angle measurements of SNP in surfactant solutions as well as the foamability and bulk static stability tests. The results showed that among three surfactant types, cationic surfactant had some unique impacts on SNP such as converting the surface charge, promoting particle aggregation and increasing the hydrophobicity of SNP. The aggregation behaviour and hydrophobization of SNP were found to delay liquid drainage and affect the foam stability positively. At elevated temperature, SNP in surfactant dispersions were observed to have lower magnitude of zeta potential and larger particle sizes. In comparison with ionic surfactants, non-ionic surfactant demonstrated considerably smaller effects on generating and stabilizing nano-foams. At sufficient surfactant concentration, the electrostatic attraction between cationic surfactant and SNP promoted higher foam stability than the electrostatic repulsion between anionic surfactant and SNP. This research provides a better insight into the synergistic interactions between surfactants and SNP, and their influences on the stability of foams at reservoir temperature.

1. Introduction

In the past few years, foam fluids have been increasingly studied and employed in the oil and gas industry for their applications in enhanced oil recovery (EOR), drilling and fracture stimulation. Liquid foams are dispersions of gas in liquid, which are typically generated and stabilized by surface-active agents or surfactants. In general, foam fluids have several advantages such as high mobility, excellent rheological properties, low water consumption and reduced formation damage [1–5]. However, foams are thermodynamically unstable due to their decay mechanisms of liquid drainage, coarsening and bubble coalescence [6]. At elevated reservoir temperature, surfactant-stabilized foams are not able to maintain their long-term stability, which eliminates the superior benefits and negatively affects the performance of foams in petroleum applications [7,8].

In order to address this limitation, nanotechnology has been recently implemented to stabilize liquid foams at elevated reservoir temperature [7,9–19].The adsorption of nanoparticles (NP) on the gas–liquid interface acts as a steric barrier to enhance the film strength, improve the interface viscoelasticity and increase the maximum capillary pressure, leading to the reduced drainage rate and the prevention of gas diffusion and bubble coalescence [20–22]. As a result, foams become more stable and have higher thermal tolerance with the presence of NP.

The synergy between surfactants and NP plays a critical role in foam stabilization. Every surfactant molecule has a hydrophobic tail and a hydrophilic head, which contains either positive electric charge (cationic surfactant), negative charge (anionic surfactant), or neutral charge (non-ionic surfactant). When absorbing on NP surface, different surfactant types tend to affect the properties of NP differently. In previous literature, Wang et al. (2005) investigated the influences of cationic, anionic and non-ionic surfactants at low concentration on the formation and surface properties of silica nanoparticles (SNP) at

ambient conditions [23]. Recently, Yekeen et al. (2019) studied the impacts of different surfactant types on the stability of various NP systems at room temperature. In their work, the surfactant concentration was maintained fixed and above the critical micelle concentration (CMC) [24]. While many insightful findings on the interaction between surfactants and NP have been presented, very few to none research have been conducted to study the effects of surfactants on the properties of NP at elevated temperature and in varied surfactant concentrations.

Moreover, in the current literature, the relationship between the surfactant-nanoparticle interaction and the stability of liquid foams remains quite controversial and poorly understood especially at reservoir temperature. Some researchers concluded that the electrostatic repulsion between oppositely charged NP and surfactant is most effective at stabilizing foams since the repulsion can prevent particle aggregation and increase the strength of the liquid films [20,25–28]. On the other hand, some argued that the electrostatic attraction between the same charged NP and surfactant promotes better foam stability due to the modified surface properties and the increased surface activity of NP [24,29–31].

Due to the presented research gaps, our paper studied the effects of surfactant type and concentration on the stability and surface properties of SNP at ambient and elevated temperature conditions. Three surfactants namely SDBS (anionic), CTAB (cationic) and TX-100 (non-ionic) were studied at below and above CMC. The impacts of different surfactant types on the foamability, drainage behaviour and stability of nanoparticle-stabilized foams were investigated to clarify some contradictory findings in the literature. The paper is expected to establish a comprehensive study of the synergistic interactions between surfactants and nanoparticles at ambient and elevated reservoir temperature, and to enhance understanding of how those interactions influence the stability of foams used in petroleum applications.

2. Experimental

2.1. Materials

Sodium dodecylbenzene sulfonate (SDBS), hexadecyl-trimethylammonium bromide (CTAB) and Triton X-100 (TX-100) were used as anionic, cationic, and non-ionic surfactants, respectively. All surfactants were obtained from Sigma Aldrich. Hydrophilic silica nanoparticles (SNP) in colloidal form were purchased from Sigma Aldrich with a concentration of 34 wt% suspension in H_2O. The SNP has an average diameter of 22 nm, a molecular weight of 60.08 g/mol and a surface area of 110–150 m^2/g. All surfactants and SNP were used without any modification. Deionized distilled water with the resistivity of 18.2 mΩ was used as a base fluid in all experiments.

2.2. Nanoparticle-surfactant mixtures preparation

Firstly, a defined amount of surfactant was added into deionized distilled water and stirred continuously for 2 h. SNP were then added into the mixture and stirred for another 2 h. After that, the mixture was sonicated at a frequency of 40 Hz for 30 min to reach adsorption equilibrium. The dispersion appeared slightly hazy and was sealed for use in experiments. All dispersions were prepared at ambient conditions with the adjusted pH of 7. Several SNP concentrations were analyzed, and the optimal point was found at 1.0 wt%. This SNP concentration has been previously found optimal for foam stabilization and rheology improvement in previous studies [32,33].

The critical micelle concentrations (CMC) of the surfactants were provided by the supplier, which are 0.021 wt% for SDBS, 0.029 wt% for CTAB and 0.014 wt% for TX-100 surfactants. Each surfactant was prepared in three concentrations: 0.01 wt% (below CMC), 0.1 wt% (above CMC) and 0.5 wt% (excessively high concentration).

2.3. Zeta-potential & particle size measurement

There are two electrical layers associated with any particle exposed in a charged fluid called electric double layer. The first layer (Stern layer) contains strongly bounded ions due to the electrostatic interaction, while the second layer (diffuse layer) contains loosely attached ions (Fig. 1). Zeta potential is defined as the electrical potential at the boundary of the diffuse layer [34], and it is an excellent correlation to the surface potential of the particle as well as a direct indicator for the stability of the colloidal dispersion.

The zeta potential and particle size of SNP in surfactant solutions were measured at room temperature of 25° C and at an elevated temperature of 65° C using a Zetasizer Nano Series (Malvern Instrument, UK). The instrument is operated based on the dynamic light scattering principle and is capable of measuring particles in the size range from 1 nm up to 6μ m. Each experiment was repeated at least 3 times and averaged to ensure the reliability and accuracy of the results. By determining the zeta potential values and particle sizes, the electrostatic interaction between SNP and surfactants, and the aggregation behavior can be investigated and discussed.

2.4. Contact angle measurement

To study the effect of different surfactant types on the wettability of SNP, contact angles of unmodified and modified SNP were measured by the OCA 15EC device (Dataphysics Instrument, Germany). The instrument applies the sessile drop method to measure the contact angle of the particles. Firstly, the prepared dispersion was centrifuged at 4500 RPM for 10 min using a Sigma 2-16P centrifuge. Solid SNP were then collected, dried at room temperature, and pressed into a thin sheet on the glass slide [35]. Finally, a drop of distilled water was slowly placed onto the glass slide. The shape of the droplet was immediately recorded by a digital camera with multiple-fold zoom lens. The droplet profile was interpreted and analyzed by using SCA 20 – an integrated software from Dataphysics Instrument to estimate the contact angle of the modified SNP. All contact angle measurements were conducted at room temperature. Each experiment was repeated at least 3 times and averaged to ensure the reliability and accuracy of the results.

2.5. Foamability and bulk static stability tests

The prepared dispersion was stirred at 2000 RPM for 3 min to produce fine foams. After the foam was generated, the initial total foam volume was immediately recorded as a measure for foamability. The foam was then transferred into a glass cylinder, which was pre-heated using a water bath system. The top of the cylinder was sealed to prevent contamination and disturbance from the environment. During the experiment, the drained ratio as a function of time was recorded by a digital camera, and was used as a standard measure for foam stability. The drained ratio is defined as the ratio between the total liquid drained volume at time t and the initial suspension volume before foam is generated. The drainage half-life is the time taken to separate 50% of the initial liquid from the foam [11,36,37]. All stability measurements were conducted at atmospheric pressure and the temperature of 25 °C and 90 °C.

3. Results and discussion

3.1. Zeta potential measurement

Fig. 2 shows the zeta potential values of the ten different SNP dispersions. Without the presence of surfactants, the zeta potential of SNP was measured at −42.9 mV at room temperature, confirming the high negative charge on the surface of SNP [23]. The effects of temperature, surfactant types and surfactant concentrations on the zeta potentials of SNP were observed and discussed below.
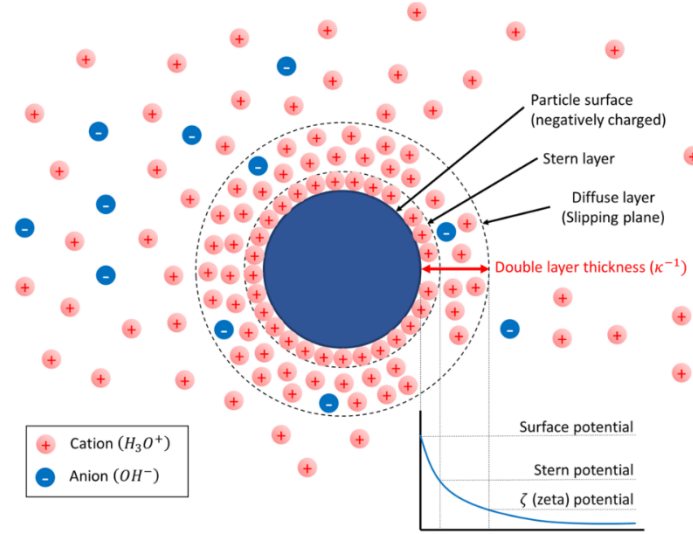
2

Fig. 1. A schematic of two electrical layers and ion adsorption of a negatively charged particle.
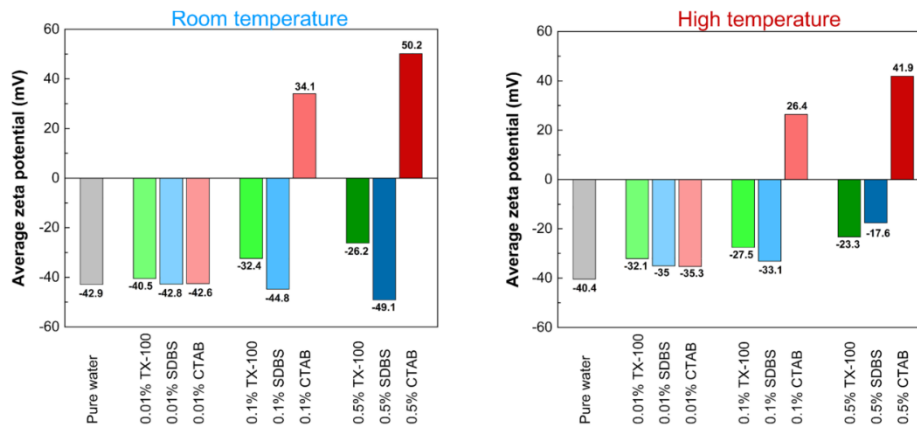
Fig. 2. Influence of surfactant type and concentration on the zeta potential of SNP dispersion at room temperature and at high temperature.

3.1.1. Effect of temperature on the zeta potential of silica nanoparticles

In general, the absolute zeta potential of SNP decreased with the increasing temperature (Fig. 2). In other words, the SNP colloidal dispersions became less stable at elevated temperature. This observation can be explained by the self-ionization reaction of water:

$$2H_2O \rightleftharpoons H_3O^+ + OH^-$$
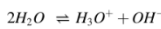
As water self-ionises, the hydronium ions (H_3O^+) and hydroxide ions (OH^-) are generated and released in the solution. As SNP are negatively charged, the H_3O^+ cations are strongly attracted to the particle surface, forming an ion structure in the Stern and diffuse layers (Fig. 1). When the temperature increases, water molecules vibrate faster and generate more amount of H_3O^+ and OH^- ions at the same rate. Consequently, the concentration of H_3O^+ cations in the electric double layer increases

significantly, which reduces the negativity of particle charge and decreases the absolute zeta potential. Al Mahrouqi et al. (2016) presented a similar observation when studying the zeta potential of natural carbonate samples at up to 120 °C [38]. Furthermore, the decrease in absolute zeta potential of SNP might also be attributed by the increased kinetic energy of surfactant molecules at high temperature, which reduces the adsorption density and results in degradation and precipitation of surfactants [39,40].

3.1.2. Effect of surfactant type and concentration on the zeta potential of silica nanoparticles

Due to the distinct characteristics, different surfactant types tend to have different electrostatic interactions and adsorption mechanisms on NPs. It was observed that the absolute value of SNP zeta potential

reduced with the increasing concentration of TX-100 surfactant. This is possibly because non-ionic surfactant molecules have zero electric charge in their head groups, therefore, when attaching to the SNP surface, they tend to neutralize and decrease the negative surface charge of SNP. At higher surfactant concentration, a greater number of TX-100 molecules were attracted to the SNP surface and further decreased the absolute surface charge of SNP.

On the other hand, cationic CTAB surfactant contains positive charge in their head groups, which is opposite to the negative charge of SNP. The significant charge difference results in a very strong electrostatic attraction between the CTAB molecules and the SNP surface. By increasing the CTAB concentration, more positively charged heads are likely to attach to the surface of SNP, which reduces the negativity and enhances the positivity of the SNP surface charge. Fig. 2 shows that at a low CTAB concentration of 0.01 wt%, the surface charge of SNP was slightly reduced, while at higher concentrations of 0.1 wt% and 0.5 wt%, CTAB was capable of converting the SNP surface charge from negative to highly positive. Similar phenomenon was reported in previous literature [24,41].

As anionic surfactants and SNP are both negatively charged, there exists a significant electrostatic repulsive force to prevent direct surfactant attachment on the SNP surface. Therefore, the anionic surfactant adsorption is promoted by another mechanism, which is via ion association with the H_3O^+ cations existing on the surface of the SNP [42]. The addition of anionic surfactant molecules is likely to reduce the neutralization effect of H_3O^+ cations (Fig. 1), therefore, increases the negative charge of the SNP surface. This explains the increase in the absolute zeta potential of SNP with increasing SDBS concentration at room temperature (Fig. 2). However, an opposite observation was found at elevated temperature where the magnitude of SNP zeta potential decreased with increasing SDBS concentration. While the strong degradation of SDBS molecules at elevated temperature is suspected to be one of the possible reasons, future investigation should be conducted to study the effect of temperature on the NP's surface properties in anionic surfactant dispersions.

3.2. Particle size measurement

Besides zeta potential, the aggregation behaviour of NP plays an important role in foam stabilisation. According to DLVO theory, the total interaction energy between charged particles is a summation of the Van der Waals attraction and the Electric Double Layer repulsion [43,44]. While the Van der Waals attractive force is significant at a very small separation distance, the effect of Electric Double Layer repulsive force is generally stronger and in a wider range [45]. Aggregation is prevented when the electrostatic repulsion between particles is dominant over the Van der Waals attraction. In order to form aggregates, particles have to closely approach each other at high velocity or with high kinetic energy to overcome the barrier of electrostatic repulsion.

Fig. 3 shows the average sizes of SNP dispersed in distilled water and in different surfactant fluids at room temperature and at elevated temperature.

At room temperature, the measured size of SNP in distilled water was 20.3 nm, which is similar to the particle diameter data from the supplier. At elevated temperature, the SNP in all studied dispersions became larger in size. The increase in SNP size is mainly due to the surfactant precipitates on SNP surface and/or the aggregation of SNP. While the surfactant degradation and precipitation at reservoir temperature have been observed and reported previously [40], the aggregation of SNP largely depends on the stability of the colloidal dispersion. Fig. 2 shows the reduction in the absolute zeta potential of SNP dispersions at elevated temperature. With the decreased absolute zeta potential, the electrostatic repulsion among SNP is weaker and the colloidal dispersions become less stable, which eventually promotes the aggregation of NP [46].

At the same surfactant concentration, the SNP size in TX-100 dispersion were smaller than that in SDBS or CTAB dispersion due to the low adsorption capability of non-ionic surfactant molecules on the NP surface. It was previously reported that ionic surfactant molecules had stronger electrostatic interaction with the SNP than non-ionic surfactants, leading to their easily adsorbing as a monolayer on the NP surface [28].

Fig. 3 also shows that the SNP had larger size with increasing surfactant concentration. In TX-100 and SDBS dispersions, the increased SNP size is mainly because of the increased adsorption of surfactant molecules and surfactant micelles on the surface of each individual SNP, forming a partial or full monolayer [47]. Due to the strong electrostatic repulsion between SNP and the anionic surfactant molecules, the chance of SNP aggregation in SDSB dispersions is relatively low [48].

On the other hand, CTAB cationic surfactant has a very strong electrostatic attraction with the negatively charged SNP surface, which can generate multilayer structure of surfactant molecules on the SNP surface. As the CTAB concentration increased, the surface potential of SNP became less negative and passed the isoelectric point of 0 mV (Fig. 2). At around this point, the stability of the NP colloidal system is extremely low with very weak repulsive force among the NP [37].
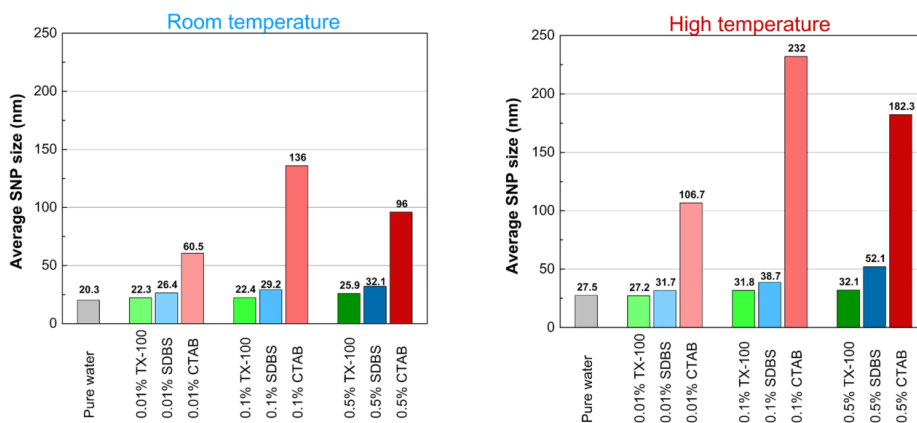

Fig. 3. Influence of surfactant type and concentration on the measured particle/aggregate size of SNP dispersion at room temperature and high temperature.

Consequently, SNP could aggregate easily in CTAB dispersions, resulting in the large aggregate sizes of 132 nm at room temperature and 232 nm at elevated temperature.

It is interesting to note from Fig. 3 that at both ambient and elevated temperature conditions, the SNP aggregate size in 0.5 wt% CTAB dispersion was smaller than that in 0.1 wt% CTAB dispersion. Excessively high zeta potential is believed to be the main reason for this phenomenon [41]. According to Fig. 2, as the CTAB concentration increased from 0.1 wt% to 0.5 wt%, the zeta potential of SNP increased from 34.1 mV to 50.2 mV at room temperature, and from 26.4 mV to 41.9 mV at elevated temperature. When the absolute zeta potential of SNP is excessively high, the electrostatic repulsion among SNP becomes significant to diminish the aggregation and reduce the SNP aggregate size.

3.3. Contact angle measurement

The wettability of SNP was determined by measuring the particles' contact angle at the water–air interface. Fig. 4 shows the measured contact angle of 16.20° for unmodified SNP, confirming the hydrophilic characteristic of SNP due to the presence of the silanol ($SiOH^-$) groups on their surface.

Fig. 5 shows the contact angles of the modified SNP mixed in different surfactant dispersions. The measurements at 0.01 wt% surfactant concentration were not displayed as they had negligible influence on the contact angle results.

With the presence of surfactants, the contact angles of modified SNP were higher than 16.20° of unmodified SNP. As mentioned previously, every surfactant has a hydrophilic head containing an electric charge and a hydrophobic tail. When interacting with SNP, the charged hydrophilic heads tend to attach to the SNP surface due to the electrostatic interaction or ion bridging [42]. As a result, the hydrophobic tails will expose outwards the environment, which increases the overall hydrophobicity of the SNP [49]. Highest contact angles of SNP were observed in CTAB dispersions due to the strong electrostatic attraction and high adsorption capability of CTAB molecules on the SNP surface. On the other hand, SDBS has an electrostatic repulsion with SNP due to their opposite charges. Therefore, it is expected that the adsorption capability of SDBS heads on SNP surface is significantly lower than that of CTAB or TX-100 surfactants. Fig. 5 shows that the contact angle of SNP increased 33–53% in TX-100 dispersions, but was barely improved in SDBS dispersions.

When increasing the surfactant concentration, it is expected that the contact angle of SNP increases due to the incremental exposure of hydrophobic tails from the increased adsorption of surfactant molecules. While SNP in TX-100 and SDBS dispersions followed the expectation, the contact angle of SNP decreased from 40.65° to 27.93° when increasing the CTAB concentration from 0.1 wt% to 0.5 wt%. This observation can be explained by the formation of the second adsorption layer, which is demonstrated in Fig. 6. At low concentration, few CTA^+ ions adsorb on SNP surface by electrostatic interaction between the opposite electric charges (Fig. 6a). However, the zeta potential of SNP remains at high negative values (Fig. 2), and particle aggregation is not likely to occur as the electrostatic repulsion between SNP is still relatively strong. As the CTAB concentration increases, the CTAB surfactant molecules start to form a monolayer on the SNP surface (Fig. 6b), and the negative zeta potential of SNP gradually increases to zero then to positive values. To a certain point, the positive surface charge of SNP is similar to that of CTAB surfactants, preventing the continued formation of the monolayer. Beyond this point, CTAB molecules adsorb on SNP surface by the hydrophobic interaction and a second adsorption layer starts to be formed [42]. In the hydrophobic interaction, the newly adsorbed CTAB are oppositely orientated, where the hydrophobic tails attach to the NP surface and the hydrophilic heads expose outwards the environment (Fig. 6c). Eventually, the exposure of the hydrophilic heads in the second layer diminishes the hydrophobization effects of the first layer, reducing the contact angle of SNP.

3.4. Foamability & foam stability

3.4.1. Foamability

Fig. 7 shows the foaming ability of SNP dispersions in different surfactant systems. All foams were generated from a same dispersion volume of 100 mL with the same SNP concentration of 1.0 wt%. Without surfactant, SNP alone had a very low foamability of only 105 mL due to its limited capability of reducing surface tension [50]. In contrast, surfactant molecules can greatly reduce the surface tension at the gas–liquid interface and produce a large number of foam bubbles [51]. With the presence of surfactants, the foamability of SNP dispersions increased significantly, and it was also directly proportional to the surfactant concentration.

It is observed that foams generated from the SDBS/SNP mixtures had the highest initial volume compared to other dispersion systems. The outstanding foamability of SDBS foams can be attributed to the effects of SNP on enhancing the surface activity and interfacial properties of the anionic surfactant molecules [27]. It was found that the mixture of SNP with non-ionic TX-100 surfactant had lower foamability than SNP with ionic surfactants, and the difference became more obvious at higher surfactant concentration. This is possibly because non-ionic surfactants have lower interaction with SNP than ionic surfactants.
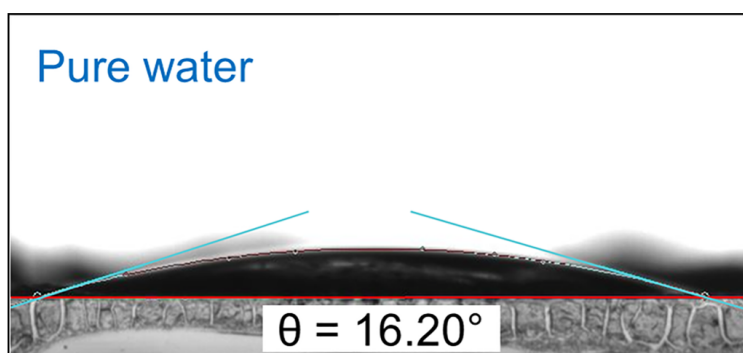

Fig. 4. Measured contact angle of SNP mixed in pure water on the glass slide surface.
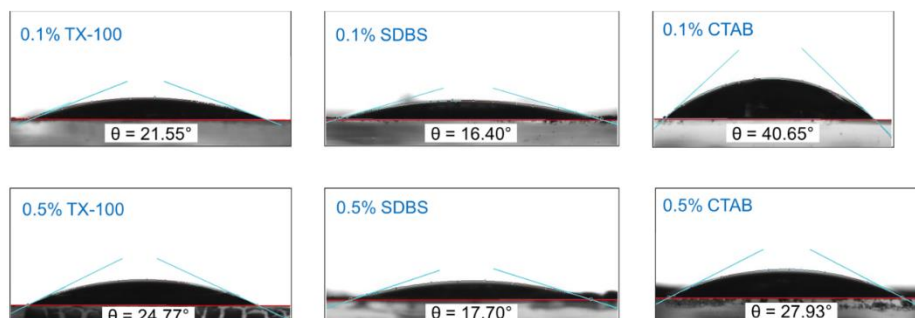
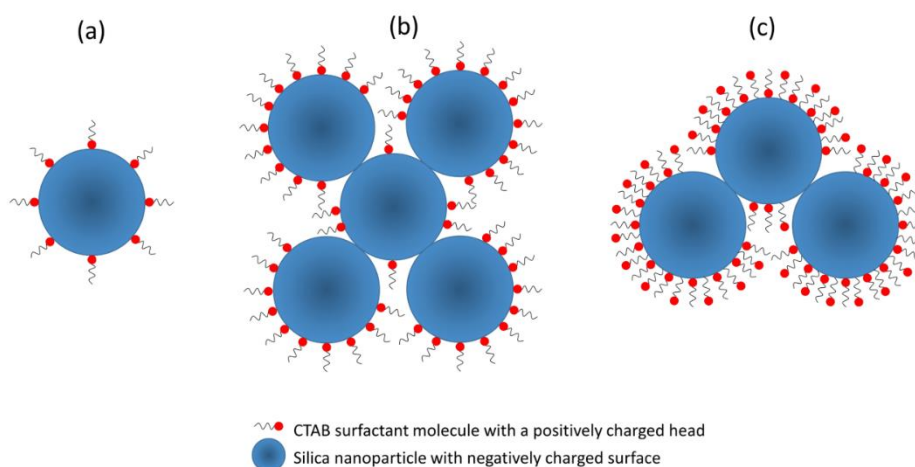Fig. 5. Influence of surfactant type and concentration on the contact angle of SNP on glass slide surface.

Fig. 6. A schematic of aggregation and CTAB adsorption on SNP surface at a) low CTAB concentration; b) medium CTAB concentration; c) excessively high CTAB concentration.

3.4.2. Foam stability at below critical micelle concentration

Liquid foams must have a good foaming capacity but more importantly, they must remain stable at both ambient and reservoir conditions. Foam stability has been widely considered the key factor determining the performance of foams in EOR and fracturing treatment [52]. Fig. 8 shows the stability of SNP-surfactant stabilized foams with the surfactant concentration of 0.01 wt%, which is below the CMC.

As the temperature increased from 25 °C to 90 °C, the liquid drainage in all foams occurred more rapidly, indicating a dramatic decline in the foam stability. It is believed that as temperature increases, the kinetic energy of the surfactant molecules increases, preventing them from effectively adsorbing and accumulating at the gas–liquid interface [53]. Moreover, surfactant molecules are very likely to degrade at elevated temperature, therefore, losing their superior properties of reducing surface tension and stabilising foams [48,54]. In addition, the increase in temperature can reduce the surface elasticity of the gas–liquid interface and accelerate gas diffusion through lamellae [7,55]. This results in the significant increase in the liquid drainage and film thinning rates, which eventually reduces the overall foam stability.

It was found that at below CMC, the stability of TX-100/SNP and CTAB/SNP foams was extremely low. At room temperature, it took only 30 s for TX-100/SNP and 60 s for CTAB/SNP foams to drain 80% of their original liquid volume. On the other hand, SDBS/SNP system was relatively good at stabilising foams, where nearly 400 s was required to reach the same drainage ratio at room temperature. The stability difference between the SDBS/SNP foam and the two other foams became more significant at higher temperature of 90 °C. It is clear that at below CMC, the electrostatic repulsion between surfactants and SNP results in better foam stability than the electrostatic attraction at both ambient and elevated temperature.

3.4.3. Foam stability at above critical micelle & high concentration

Fig. 9 and Fig. 10 show the stability of SNP-stabilized foams at 0.1 wt % and 0.5 wt% surfactant concentration, respectively. At above CMC, the effect of temperature on foam stability remained very significant. The increase in temperature promoted higher rates of liquid drainage, gas diffusion and film thinning, contributing to the foam destabilisation [53]. At above CMC, the stability of CTAB/SNP and TX-100/SNP foams were noticeably improved compared to their results at below CMC.

The results show that TX-100/SNP foams had lower stability than the CTAB/SNP and SDBS/SNP foams at both temperature conditions. This can be explained by the difference in electrostriction interaction between the surfactants and SNP. When NPs adsorb on the gas–liquid interface, the electrostatic repulsion among the charged NPs generate a
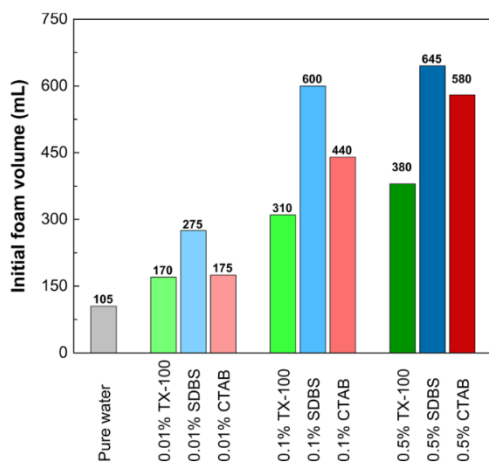
37

Fig. 7. Influence of surfactant type and concentration on the foamability of the 1.0 wt% SNP-stabilised foams.
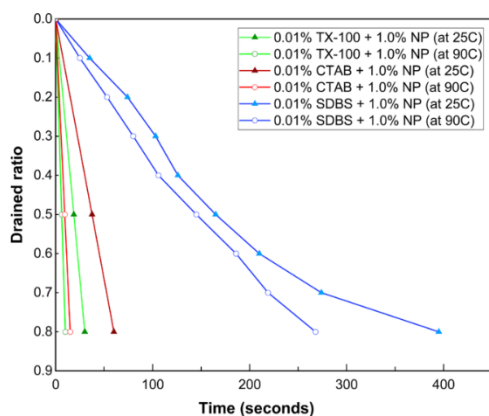

Fig. 8. Influence of surfactant type at 0.01 wt% concentration (below CMC) on the stability of the 1.0 wt% SNP-stabilized foams at the temperature of 25 °C and 90 °C.

repulsive force between the interface sides to separate the liquid films and prevent foam decay [56,57]. As non-ionic surfactant has zero electric charge on its head group, they tend to neutralize the absolute surface potential and decrease the interaction energy of SNP (Fig. 2). This lowers the repulsive force between SNP on each side of the liquid film and lessens the SNP's effects of reducing drainage and stabilising foams. Kumar and Mandal (2017) also reported that the ionic surfactants can stabilize NP-foams better than non-ionic surfactants due to the high disjoining pressure among the foam bubbles [28]. White et al. (2007) claimed that the mixtures of NP and non-ionic surfactant stabilized foams mainly by steric stabilisation rather than electrostatic stabilisation [58].

Between the ionic surfactants, CTAB was better than SDBS in enhancing foam stability and reducing drainage rate. At 1.0 wt% surfactant concentration, the stability of CTAB foam was dominant over that of the SDBS foam as the half-lives of CTAB and SDBS foams were

1631 and 383 s at room temperature; and 484 and 272 s at 90 °C, respectively. At 0.5 wt% concentration, higher foam stability was also achieved in the CTAB foam but with a smaller difference. It can be concluded that at above CMC, the electrostatic attraction between the oppositely charged cationic surfactant and SNP promoted higher foam stability than the electrostatic repulsion between like-charged anionic surfactants and SNP. The dominance in the stability of CTAB/SNP foams can be attributed to the in-situ hydrophobization and the aggregation behavior of SNP.

3.4.3.1. Effect of hydrophobization of NP on foam stability. It is undeniable that the wettability of NP plays an important role in stabilising foams. The relationship between the wettability of NP and foam stability is linked to the particle detachment energy theory [59]. In definition, particle detachment energy is the minimum energy required to remove the adsorbed particles from the gas–liquid interface. With higher detachment energy, the particle adsorbs stronger on the gas–liquid interface and results in more stable foam films and bubbles. The foam drainage behavior largely depends on the detachment energy. In comparison, the detachment energy of surfactant molecules on the gas–liquid interface is much smaller than that of NP [16,60]. This explains why surfactant molecules are easy to detach from the interface and attach to the reservoir rocks, while NP can adsorb firmly and irreversibly on the interface to provide robust foam stability. For NP, the buoyancy and gravity effects are negligible due to their tiny size, thereby, the detachment energy of NP can be expressed in Eq. (1) [59]:

$$E = \pi R^2 \gamma (1 - cos\theta)^2 \qquad (1)$$

where E is the detachment energy, R is the radius of the NP, γ is the interfacial tension and θ is the contact angle of the NP at the gas–liquid interface. According to the Eq. (1), the particle detachment energy reaches the maximum when the contact angle is close to 90°, referring to the moderate hydrophobic NP. It was previously found that extremely hydrophilic or extremely hydrophobic NP cannot stabilize foams due to the increased film thinning and rupture [31,61]. At below 90°, a higher contact angle indicates higher hydrophobicity of NP, resulting in a decrease in the drainage rate and a more stable foam [11,62–64].

As discussed previously, the adsorption of CTAB surfactant molecules was able to considerably increase the hydrophobicity of SNP; and SNP in CTAB dispersions had the highest contact angles compared to that in SDBS and TX-100 dispersions (Fig. 5). Therefore, SNP/CTAB is expected to have the highest detachment energy and tend to adsorb stronger on the gas–liquid interface. The significant accumulation of SNP helps increase the film strength and reduce direct contact between the fluids, leading to the observed delay in liquid drainage and the highest stability in the CTAB foams.

3.4.3.2. Effect of particle aggregation on foam stability. Besides the high detachment energy, one of the main advantages of NPs over chemical surfactants in foam stabilisation is their multiple arrangements at the bubble interface [52]. As NPs adsorb on the gas–liquid interface, they increase the liquid film strength by three possible mechanisms: a bridging monolayer, a bridging bilayer, and a network of particle aggregates [61]. The aggregation network was found to be the most effective mechanism in stabilising foams since the particle aggregates act as a thick solid barrier on foam bubbles to reduce direct contact between the fluids and keep the bubbles well separated. As a result, they help increase the film viscosity, delay gravity drainage, reduce the gas diffusion rate, and prevent bubble coalescence [51,65,66]. Therefore, the aggregation behavior of SNP in CTAB dispersions is believed to be the main factor contributing to the slow drainage and the high stability of the CTAB foams.

According to the previous experimental results, larger NP aggregate size tends to form more stable foams. The SNP had the largest aggregate size in 0.1 wt% CTAB dispersion, followed by 0.5 wt% CTAB then
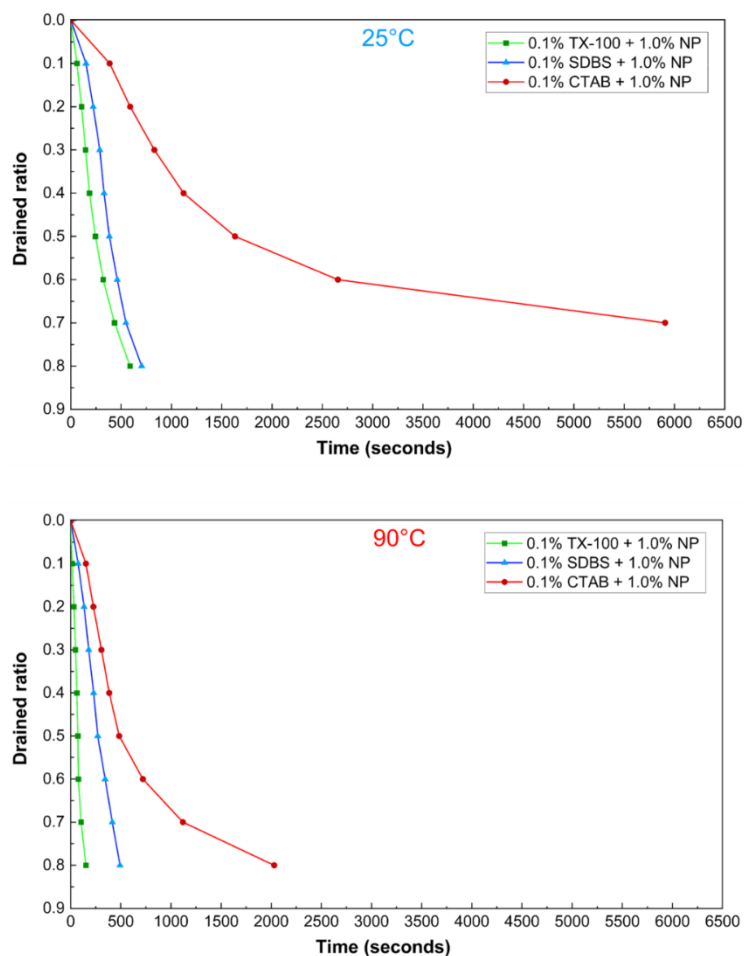
38

Fig. 9. Influence of surfactant type at 0.1 wt% concentration on the stability of the 1.0 wt% SNP-stabilized foams at the temperature of 25 °C and 90 °C.

0.01 wt% CTAB dispersion (Fig. 3). Consequently, the 0.1 wt% CTAB foam was most stable with the half-life of 1631 s at room temperature, compared to 412 s of 0.5 wt% CTAB foam and around 60 s of 0.01 wt% CTAB foam (Fig. 9). Similar observation was seen at higher temperature of 90 °C (Fig. 10). However, the correlation only remains true when comparing at the same temperature. As temperature increased, even though the aggregate size increased, the foam stability decreased. This is probably because the effects of temperature on destabilising and increasing the decay rate of foams are much more significant than the effect of particle aggregation on enhancing foam stability.

While the effect of the hydrophobicity of NP on foam stability is widely acknowledged, there have been some opposite arguments on the effect of the aggregate size. In theory, the foam generation energy should exceed the particle detachment energy to efficiently place NP onto the gas–liquid interface. According to Eq. (1), the detachment energy is directly proportional to the square of the particle size, which means larger NP require higher mixing energy to be placed on the liquid films. In previous literature, some claimed that smaller NP can easily migrate

and adsorb on the interface to provide a barrier around the foam bubbles [67–69], and particle aggregates and very large particles are not suitable for foam stabilization as they can hardly move into the interface [21,48,49]. For large-sized particles in micron-scale or higher, the mixing energy is unlikely to overcome the high detachment energy, which causes particles to stay in the bulk solution and have no impact on stabilising foams. However, since NP aggregates have the size of few hundreds of nanometres, they can adsorb into the interface with intermediate mixing energy to effectively stabilise foams. In this study, it was proven that the stability of CTAB foams was successfully improved with the NP aggregate size of up to 232 nm.

In addition, the foam generation method plays an important role in the adsorption capability of NP. Mechanical stirring and gas injection are the most popular methods to generate foams. As mechanical stirring provides higher shear force and greater mixing energy than gas injection, it is expected to be more effective in placing NP and NP aggregates onto the gas–liquid interface to stabilize foams. Future work requires further investigation into the influence of different mixing methods on

8

39
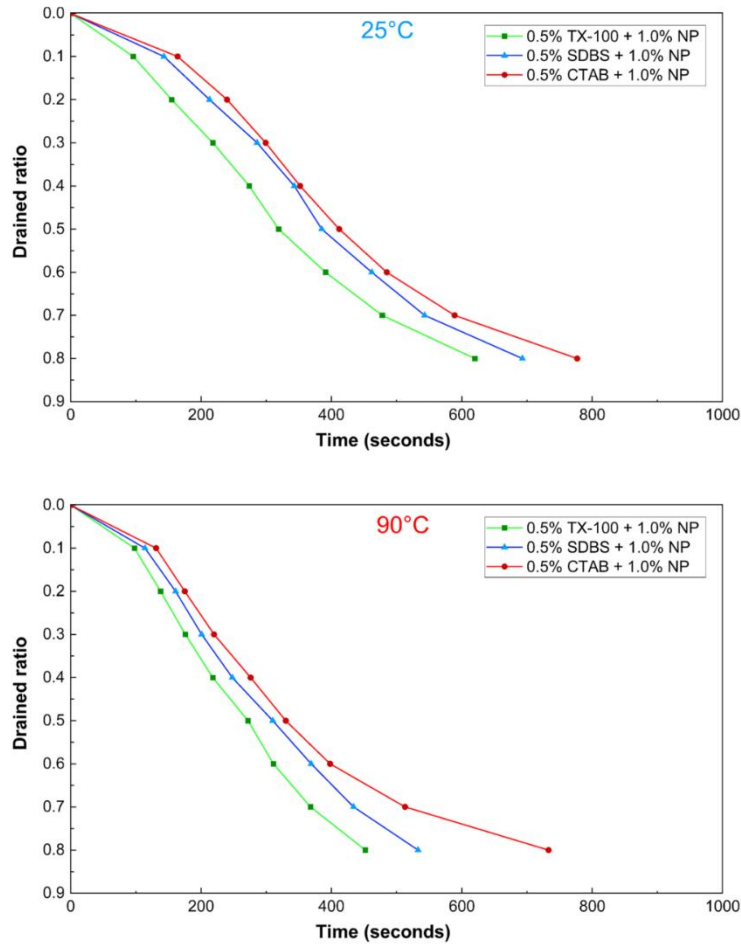
Fig. 10. Influence of surfactant type at 0.5 wt% concentration on the stability of the 1.0 wt% SNP-stabilized foams at the temperature of 25 °C and 90 °C.

the foam stability, in which the impacts of the gas injection rate, dispersion injection rate and stirring speed can be comprehensively studied.

4. Conclusions

The purpose of this work is to study the effects of anionic, cationic and non-ionic surfactants on the stability and surface properties of SNP, and on the stability of surfactant-nanoparticle-stabilized foams at ambient and elevated temperatures. Through the improved understanding, liquid foams can be better optimized with high stability to work effectively in reservoir conditions for EOR, drilling and fracturing applications. The key conclusions can be summarized as follows:

1. At above CMC, the cationic CTAB surfactant had some unique capabilities of converting the surface charge of SNP from negative to positive, forming particle aggregates and significantly increasing the

hydrophobicity of SNP. Similar interactions were not observed by either non-ionic TX-100 or anionic SDBS surfactants.

2. At elevated temperature, SNP in surfactant dispersions had lower absolute zeta potential and larger average size. The increased sizes of SNP are resulted from the particle aggregation in the cationic CTAB dispersion and due to the surfactant precipitation and layer adsorption in non-ionic TX-100 and anionic SDBS dispersions.

3. At both ambient and elevated temperatures, the combination of SNP and ionic surfactants resulted in higher foam stability and foamability than that of SNP and non-ionic surfactants. It was found that SNP had the best synergy with SDBS surfactant in producing the highest initial volume of foams.

4. At below CMC, TX-100/SNP and CTAB/SNP foams were extremely unstable while the stability of SDSB/SNP foam was relatively high. At above CMC, the stability of TX-100/SNP foams was considerably improved and the CTAB/SNP foams outperformed others with their lowest drainage rate and highest foam stability. The dominant stability of CTAB foams was attributed to the hydrophobization and

40

particle aggregation behavior of SNP, both of which were promoted by the electrostatic attraction between the oppositely charged SNP and CTAB surfactants.

CRediT authorship contribution statement

Tuan Tran: Investigation, Methodology, Data curation, Formal analysis, Writing – original draft. **Maria Elena Gonzalez Perdomo:** Conceptualization, Supervision, Writing – review & editing, Validation, Resources. **Manouchehr Haghighi:** Conceptualization, Supervision, Writing – review & editing, Validation, Resources. **Khalid Amrouch:** Supervision, Writing – review & editing.

Declaration of Competing Interest

The authors declare that they have no known competing financial interests or personal relationships that could have appeared to influence the work reported in this paper.

References

[1] Yekeen N, Padmanabhan E, Idris AK. A review of recent advances in foam-based fracturing fluid application in unconventional reservoirs. J Ind Eng Chem 2018;66: 45–71.

[2] Wang L, Yao B, Cha M, Alqahtani NB, Patterson TW, Kneafsey TJ, et al. Waterless fracturing technologies for unconventional reservoirs-opportunities for liquid nitrogen. J Nat Gas Sci Eng 2016;35:160–74.

[3] Wanniarachchi WAM, Ranjith PG, Perera MSA, Lashin A, Al Arifi N, Li JC. Current opinions on foam-based hydro-fracturing in deep geological reservoirs. Geomechanics and Geophysics for Geo-Energy and Geo-Resources 2015;1(3-4): 121–34.

[4] Speight JG. Handbook of Hydraulic Fracturing. John Wiley & Sons; 2016.

[5] Tran T, Gonzalez Perdomo ME, Wilk K, Kasza P, Amrouch K. Performance evaluation of synthetic and natural polymers in nitrogen foam-based fracturing fluids in the Cooper Basin, South Australia. The APPEA Journal 2020;60(1):227. https://doi.org/10.1071/AJ19062.

[6] Schramm LL. Foams: Fundamentals and Applications in the Petroleum Industry. Washington DC, USA: American Chemical Industry; 1994.

[7] Yang K, Li S, Zhang K, Wang Y. Synergy of hydrophilic nanoparticle and nonionic surfactant on stabilization of carbon dioxide-in-brine foams at elevated temperatures and extreme salinities. Fuel 2021;288:119624. https://doi.org/10.1016/j.fuel.2020.119624.

[8] Faroughi SA, Pruvot A-C, McAndrew J. The rheological behavior of energized fluids and foams with application to hydraulic fracturing: Review. J Petrol Sci Eng 2018;163:243–63.

[9] Worthen AJ, Bagaria HG, Chen Y, Bryant SL, Huh C, Johnston KP. Nanoparticle-stabilized carbon dioxide-in-water foams with fine texture. J Colloid Interface Sci 2013;391:142–51.

[10] Verma A, Chauhan G, Baruah PP, Ojha K. Morphology, Rheology, and Kinetics of Nanosilica Stabilized Gelled Foam Fluid for Hydraulic Fracturing Application. Ind Eng Chem Res 2018;57(40):13449–62.

[11] Verma A, Chauhan G, Ojha K, Padmanabhan E. Characterization of Nano-Fe2O3-Stabilized Polymer-Free Foam Fracturing Fluids for Unconventional Gas Reservoirs. Energy Fuels 2019;33(11):10570–82.

[12] Fei Y, Johnson RL, Gonzalez M, Haghighi M, Pokalai K. Experimental and numerical investigation into nano-stabilized foams in low permeability reservoir hydraulic fracturing applications. Fuel 2018;213:133–43.

[13] Fei Y, Pokalai K, Johnson R, Gonzalez M, Haghighi M. Experimental and simulation study of foam stability and the effects on hydraulic fracture proppant placement. J Nat Gas Sci Eng 2017;46:544–54.

[14] Fei Y, Zhu J, Xu B, Li X, Gonzalez M, Haghighi M. Experimental investigation of nanotechnology on worm-like micelles for high-temperature foam stimulation. J Ind Eng Chem 2017;50:190–8.

[15] Da C, Alzobaidi S, Jian G, Zhang L, Biswal SL, Hirasaki GJ, et al. Carbon dioxide/water foams stabilized with a zwitterionic surfactant at temperatures up to 150 °C in high salinity brine. J Petrol Sci Eng 2018;166:880–90.

[16] Singh R, Mohanty KK. Synergy between Nanoparticles and Surfactants in Stabilizing Foams for Oil Recovery. Energy Fuels 2015;29(2):467–79.

[17] Singh, R & Mohanty, KK 2017, 'Nanoparticle-Stabilized Foams for High-Temperature, High-Salinity Oil Reservoirs', in SPE Annual Technical Conference and Exhibition, vol. Day 2 Tue, October 10, 2017, <https://doi.org/10.2118/187165-MS>.

[18] Singh R, Mohanty KK. Study of Nanoparticle-Stabilized Foams in Harsh Reservoir Conditions. Transp Porous Media 2020;131(1):135–55.

[19] Wang Y, Zhang Y, Liu Y, Zhang L, Ren S, Lu J, et al. The stability study of CO 2 foams at high pressure and high temperature. J Petrol Sci Eng 2017;154:234–43.

[20] Lv Q, Li Z, Li B, Li S, Sun Q. Study of Nanoparticle–Surfactant-Stabilized Foam as a Fracturing Fluid. Ind Eng Chem Res 2015;54(38):9468–77.

[21] Zhang Y, Liu Qi, Ye H, Yang LeiLei, Luo D, Peng Bo. Nanoparticles as foam stabilizer: Mechanism, control parameters and application in foam flooding for enhanced oil recovery. J Petrol Sci Eng 2021;202:108561. https://doi.org/10.1016/j.petrol.2021.108561.

[22] Wang P, You Q, Han Li, Deng W, Liu Y, Fang J, et al. Experimental Study on the Stabilization Mechanisms of CO2 Foams by Hydrophilic Silica Nanoparticles. Energy Fuels 2018;32(3):3709–15.

[23] Wang W, Gu B, Liang L. Effect of Surfactants on the Formation, Morphology, and Surface Property of Synthesized SiO2Nanoparticles. J Dispersion Sci Technol 2005; 25(5):593–601.

[24] Yekeen N, Padmanabhan E, Idris AK. Synergistic effects of nanoparticles and surfactants on n-decane-water interfacial tension and bulk foam stability at high temperature. J Petrol Sci Eng 2019;179:814–30.

[25] Sun Q, Li Z, Li S, Jiang L, Wang J, Wang P. Utilization of Surfactant-Stabilized Foam for Enhanced Oil Recovery by Adding Nanoparticles. Energy Fuels 2014;28 (4):2384–94.

[26] Xiao C, Balasubramanian SN, Clapp LW. Rheology of Viscous CO2 Foams Stabilized by Nanoparticles under High Pressure. Ind Eng Chem Res 2017;56(29):8340–8.

[27] Vatanparast H, Samiee A, Bahramian A, Javadi A. 'Surface behavior of hydrophilic silica nanoparticle-SDS surfactant solutions: I. Effect of nanoparticle concentration on foamability and foam stability', Colloids and Surfaces A: Physicochemical and Engineering Aspects 2017;513:430–41.

[28] Kumar S, Mandal A. Investigation on stabilization of CO 2 foam by ionic and nonionic surfactants in presence of different additives for application in enhanced oil recovery. Appl Surf Sci 2017;420:9–20.

[29] Cui Z-G, Cui Y-Z, Cui C-F, Chen Z, Binks BP. Aqueous foams stabilized by in situ surface activation of CaCO3 nanoparticles via adsorption of anionic surfactant. Langmuir 2010;26(15):12567–74.

[30] Maestro A, Guzmán E, Santini E, Ravera F, Liggieri L, Ortega F, et al. Wettability of silicananoparticle–surfactant nanocomposite interfacial layers. Soft Matter 2012;8 (3):837–43.

[31] Veyskarami M, Ghazanfari MH. Synergistic effect of like and opposite charged nanoparticle and surfactant on foam stability and mobility in the absence and presence of hydrocarbon: A comparative study. J Petrol Sci Eng 2018;166:433–44.

[32] Yekeen N, Idris AK, Manan MA, Samin AM, Risal AR, Kun TX. Bulk and bubble-scale experimental studies of influence of nanoparticles on foam stability. Chin J Chem Eng 2017;25(3):347–57.

[33] Sun Q, Li Z, Wang J, Li S, Li B, Jiang L, et al. Aqueous foam stabilized by partially hydrophobic nanoparticles in the presence of surfactant. Colloids Surf, A 2015;471: 54–64.

[34] Barhoum A, García-Betancourt ML, Rahier H, Van Assche G. In: Emerging Applications of Nanoparticles and Architecture Nanostructures. Elsevier; 2018. p. 255–78. https://doi.org/10.1016/B978-0-323-51254-1.00009-9.

[35] Sonn JS, Lee JY, Jo SH, Yoon I-H, Jung C-H, Lim JC. Effect of surface modification of silica nanoparticles by silane coupling agent on decontamination foam stability. Ann Nucl Energy 2018;114:11–8.

[36] Li S, Yang K, Li Z, Zhang K, Jia Na. Properties of CO2 Foam Stabilized by Hydrophilic Nanoparticles and Nonionic Surfactants. Energy Fuels 2019;33(6): 5043–54.

[37] Li S, Qiao C, Li Z, Wanambwa S. Properties of Carbon Dioxide Foam Stabilized by Hydrophilic Nanoparticles and Hexadecyltrimethylammonium Bromide. Energy Fuels 2017;31(2):1478–88.

[38] Al Mahrouqi D, Vinogradov J, Jackson MD. Temperature dependence of the zeta potential in intact natural carbonates. Geophys Res Lett 2016;43(22). https://doi.org/10.1002/grl.v43.2210.1002/2016GL071151.

[39] Kamal MS, Hussein IA, Sultan AS. Review on Surfactant Flooding: Phase Behavior, Retention, IFT, and Field Applications. Energy Fuels 2017;31(8):7701–20.

[40] Belhaj AF, Elraies KA, Mahmood SM, Zulkifli NN, Akbari S, Hussien OS. The effect of surfactant concentration, salinity, temperature, and pH on surfactant adsorption for chemical enhanced oil recovery: a review. J Pet Explor Prod Technol 2020;10 (1):125–37.

[41] Yang W, Wang T, Fan Z, Miao Q, Deng Z, Zhu Y. Foams Stabilized by In Situ-Modified Nanoparticles and Anionic Surfactants for Enhanced Oil Recovery. Energy Fuels 2017;31(5):4721–30.

[42] Liu Z, Hedayati P, Sudhölter EJR, Haaring R, Shaik AR, Kumar N. Adsorption behavior of anionic surfactants to silica surfaces in the presence of calcium ion and polystyrene sulfonate. Colloids Surf, A 2020;602:125074. https://doi.org/10.1016/j.colsurfa.2020.125074.

[43] Derjaguin B, Landau L. Theory of the stability of strongly charged lyophobic sols and of the adhesion of strongly charged particles in solutions of electrolytes. Prog Surf Sci 1993;43(1-4):30–59.

[44] Verwey EJW, Overbeek JTG. Theory of the Stability of Lyophobic Colloids: The Interaction of Sol Particles Having an Electric Double Layer. Elsevier; 1948.

[45] Adair JH, Suvaci E, Sindel J. Surface and Colloid Chemistry. In: Buschow KHJ, Cahn RW, Flemings MC, Ilschner B, Kramer EJ, Mahajan S, Veyssière P, editors.

Encyclopedia of Materials: Science and Technology. Oxford: Elsevier; 2001. p. 1–10.

[46] Freitas C, Müller RH. Effect of light and temperature on zeta potential and physical stability in solid lipid nanoparticle (SLN™) dispersions. Int J Pharm 1998;168(2).

[47] Wang W, Gu B, Liang L. Effect of anionic surfactants on synthesis and self-assembly of silica colloidal nanoparticles. J Colloid Interface Sci 2007;vol. 313, no. 1, Sep 1: 169–73.

[48] Fu C, Liu N. Study of the Synergistic Effect of the Nanoparticle-Surfactant-Polymer System on CO2 Foam Apparent Viscosity and Stability at High Pressure and Temperature. Energy Fuels 2020;34(11):13707–16.

[49] Majeed T, Kamal MS, Zhou X, Solling T. A Review on Foam Stabilizers for Enhanced Oil Recovery. Energy Fuels 2021;35(7):5594–612.

[50] Karakashev SI, Ozdemir O, Hampton MA, Nguyen AV. Formation and stability of foams stabilized by fine particles with similar size, contact angle and different shapes. Colloids Surf, A 2011;382(1–3):132–8.

[51] Yekeen N, Manan MA, Idris AK, Padmanabhan E, Junin R, Samin AM, et al. A comprehensive review of experimental studies of nanoparticles-stabilized foam for enhanced oil recovery. J Petrol Sci Eng 2018;164.

[52] Zhou J, Ranjith PG, Wanniarachchi WAM. Different strategies of foam stabilization in the use of foam as a fracturing fluid. Adv Colloid Interface Sci 2020;276.

[53] Hanamertani AS, Pilus RM, Manan NA, Mutalib MIA. The use of ionic liquids as additive to stabilize surfactant foam for mobility control application. J Petrol Sci Eng 2018;167.

[54] Emrani, AS, Ibrahim, AF & Nasr-El-Din, HA 2017, 'Evaluation of Mobility Control with Nanoparticle-Stabilized CO2 Foam', in SPE Latin America and Caribbean Petroleum Engineering Conference, vol. Day 2 Thu, May 18, 2017, <https://doi.org/10.2118/185551-MS>.

[55] Yekeen N, Padmanabhan E, Idris AK, Chauhan PS. Nanoparticles applications for hydraulic fracturing of unconventional reservoirs: A comprehensive review of recent advances and prospects. J Petrol Sci Eng 2019;178.

[56] Espinosa D, Caldelas F, Johnston K, Bryant SL, Huh C. 'Nanoparticle-Stabilized Supercritical CO2 Foams for Potential Mobility Control Applications', in SPE Improved Oil Recovery Symposium, vol. All Days, <https:// 2010. https://doi.org/10.2118/129925-MS>.

[57] Bayat AE, Rajaei K, Junin R. Assessing the effects of nanoparticle type and concentration on the stability of CO 2 foams and the performance in enhanced oil recovery. Colloids Surf, A 2016;511:222–31.

[58] White, B, Banerjee, S, O'Brien, S, Turro, NJ & Herman, IP 2007, 'Zeta-Potential Measurements of Surfactant-Wrapped Individual Single-Walled Carbon Nanotubes', The Journal of Physical Chemistry C, vol. 111, no. 37, 2007/09/01, pp. 13684-13690.

[59] Binks, B 2002, 'Binks, B. P. Particles as surfactants-similarities and differences. Curr. Opin. Colloid Interface Sci. 7, 21-41', Current Opinion in Colloid & Interface Science, vol. 7, 03/01, pp. 21-41.

[60] Eftekhari AA, Krastev R, Farajzadeh R. Foam Stabilized by Fly Ash Nanoparticles for Enhancing Oil Recovery. Ind Eng Chem Res 2015;54(50):12482–91.

[61] Horozov T. Foams and foam films stabilised by solid particles. Curr Opin Colloid Interface Sci 2008;13(3):134–40.

[62] Binks, BP, Duncumb, B & Murakami, R 2007, 'Effect of pH and Salt Concentration on the Phase Inversion of Particle-Stabilized Foams', Langmuir, vol. 23, no. 18, 2007/08/01, pp. 9143-9146.

[63] Yu J, Khalil M, Liu N, Lee R. Effect of particle hydrophobicity on CO2 foam generation and foam flow behavior in porous media. Fuel 2014;126:104–8.

[64] Ravera F, Ferrari M, Liggieri L, Loglio G, Santini E, Zanobini A. Liquid–liquid interfacial properties of mixed nanoparticle–surfactant systems. Colloids Surf, A 2008;323(1–3):99–108.

[65] Carn F, Colin A, Pitois O, Vignes-Adler M, Backov R. Foam drainage in the presence of nanoparticle-surfactant mixtures. Langmuir 2009;vol. 25, no. 14, Jul 21: 7847–56.

[66] AlYousef ZA, Almobarky MA, Schechter DS. The effect of nanoparticle aggregation on surfactant foam stability. J Colloid Interface Sci 2018;vol. 511, Feb 1:365–73.

[67] Tang F-Q, Xiao Z, Tang J-A, Jiang L. The effect of SiO2 particles upon stabilization of foam. J Colloid Interface Sci 1989;131(2).

[68] Kim I, Taghavy A, DiCarlo D, Huh C. Aggregation of silica nanoparticles and its impact on particle mobility under high-salinity conditions. J Petrol Sci Eng 2015; 133:376–83.

[69] Stocco A, Rio E, Binks BP, Langevin D. Aqueous foams stabilized solely by particles. Soft Matter 2011;7:no. 4.

4. Effects of cationic and anionic surfactants on the stability, rheology and proppant suspension of nanoparticle-stabilized fracturing foams at elevated temperature

In recent years, the application of liquid foams in hydraulic fracturing has gained significant attention due to their potential to reduce formation damage, offering a more environmentally sustainable approach. While the combination of anionic surfactants and nanoparticles (NP) has been extensively explored to enhance the properties of foam-based fracturing fluids, a critical knowledge gap existed concerning the synergy between cationic surfactants and NP, particularly at the elevated temperatures encountered in reservoirs. This paper addresses this gap by investigating and comparing the effects of cationic and anionic surfactants in combination with silica nanoparticles (SNP) on the stability, rheology, and proppant-carrying capacity of fracturing foams under varying temperature conditions. The study highlights the superior performance of foams stabilized by cationic surfactants and SNP, particularly at medium cationic surfactant concentrations. This finding directly contributes to the development of more effective and thermally stable foam systems, which helps advance hydraulic fracturing practices to be both efficient and environmentally responsible.

Statement of Authorship

Title of Paper	Effects of cationic and anionic surfactants on the stability, rheology and proppant suspension of nanoparticle-stabilized fracturing foams at elevated temperature
Publication Status	☑ Published ☐ Accepted for Publication ☐ Submitted for Publication ☐ Unpublished and Unsubmitted work written in manuscript style
Publication Details	Tran, T, Gonzalez Perdomo, ME, Haghighi, M & Amrouch, K 2023, 'Effects of cationic and anionic surfactants on the stability, rheology and proppant suspension of nanoparticle-stabilized fracturing foams at elevated temperature', Journal of Geoenergy Science and Engineering.

Principal Author

Name of Principal Author (Candidate)	Tuan Huynh Minh Tran		
Contribution to the Paper	Literature review, Data collection, Result analysis and interpretation, Writing the manuscript		
Overall percentage (%)	70%		
Certification:	This paper reports on original research I conducted during the period of my Higher Degree by Research candidature and is not subject to any obligations or contractual agreements with a third party that would constrain its inclusion in this thesis. I am the primary author of this paper.		
Signature		Date	14/03/2023

Co-Author Contributions

By signing the Statement of Authorship, each author certifies that:

    i.   the candidate's stated contribution to the publication is accurate (as detailed above);

    ii.   permission is granted for the candidate in include the publication in the thesis; and

    iii.   the sum of all co-author contributions is equal to 100% less the candidate's stated contribution.

Name of Co-Author	Maria Gonzalez Perdomo		
Contribution to the Paper	Support in result analysis, Reviewing the manuscript (15%)		
Signature		Date	14/03/2023

Name of Co-Author	Manouchehr Haghighi		
Contribution to the Paper	Support in result analysis, Reviewing the manuscript (10%)		
Signature		Date	16/03/2023

44

Name of Co-Author	Khalid Amrouch		
Contribution to the Paper	Support in result analysis, Reviewing the manuscript (5%)		
Signature		Date	17/03/2023

Contents lists available at ScienceDirect

Geoenergy Science and Engineering

Effects of cationic and anionic surfactants on the stability, rheology and proppant suspension of nanoparticle-stabilized fracturing foams at elevated temperature

Tuan Tran [a,*], Maria Elena Gonzalez Perdomo [a], Manouchehr Haghighi [a], Khalid Amrouch [a,b]

[a] *Australian School of Petroleum and Energy Resources, University of Adelaide, South Australia, 5000, Australia*
[b] *Geology & Sustainable Mining, University Mohammed VI Polytechnic, Lot-660, Benguerir, 43150, Morocco*

A B S T R A C T

Much attention has been paid to applying liquid foams in hydraulic fracturing in the past few years due to their significant benefits, including minimal formation damage. In the current literature, the combination of anionic surfactants and nanoparticles (NP) has been thoroughly studied to improve foam-based fracturing fluids' thermal stability and viscosity. However, very little research has focused on the synergy between cationic surfactants and NP, which results in a limited understanding of the effects of this mixture on enhancing the properties of fracturing foams, especially at reservoir temperature. This paper investigates and compares the synergy between cationic/anionic surfactant and silica nanoparticles (SNP) in improving the fracturing foams' stability, rheology and proppant-carrying capacity under ambient and elevated temperature conditions. The experiments involved foamability, bulk static stability, viscosity measurement and proppant settling tests at fixed NP concentration and varied surfactant concentrations. The results showed that the foams' properties were gradually enhanced with increasing surfactant concentration until reaching a peak at around 0.05–0.1 wt%. At ambient and elevated temperatures, the foams stabilized by SNP and cationic hexadecyltrimethylammonium bromide (CTAB) surfactant had higher half-life, apparent viscosity, and better proppant-carrying ability than those stabilized by SNP and anionic sodium dodecyl benzene sulfonate (SDBS) surfactant. The properties of CTAB/SNP foams were found most outstanding at medium CTAB concentration; however, they declined dramatically at very low or very high surfactant concentration. This study enhances our understanding of the influences of surfactant type and concentration on the stability, rheology and proppant suspension behaviour of nanoparticle-stabilized foams, which directly contributes to developing an effective foam system for high-temperature fracturing application.

1. Introduction

Fracture stimulation has been widely acknowledged as the most effective technique to extract hydrocarbon from tight and unconventional reservoirs in the last few decades. The conventional water-based fracturing fluid is safe and straightforward to use; however, it consumes an enormous amount of water and can result in water blocking and clay swelling when interacting with water-sensitive formations (Wanniarachchi et al., 2017; Yekeen et al., 2018; Abdelaal et al., 2021). Furthermore, clay swelling can lead to serious consequences such as fracture conductivity decline, wellbore collapse and casing damage (Fu and Liu, 2021). Therefore, fracturing fluids with low water content have been introduced to reduce water consumption and prevent shale

swelling, such as foam-based fluids (Wang et al., 2016).

Foams are gas dispersions in liquid, typically generated and stabilized by surface-active agents or surfactants. Compared to conventional water-based fracturing fluids, foams have several advantages: lower water and chemical additives consumption, lower fluid loss, better clean-up, and minimal formation damage (Yekeen et al., 2018; Wanniarachchi et al., 2015; Speight, 2016; Abdelaal et al., 2021). For any foam-based fracturing fluid, foam's stability, rheology, and proppant-carrying ability are essential properties that determine the fracture treatment's success. Generally, foams have relatively high viscosity, making them very efficient in suspending, transporting and uniformly placing proppants into the fractures (Isah et al., 2021). Previous simulation results have shown that foam fracturing can prevent

* Corresponding author.
E-mail address: tuan.tran@adelaide.edu.au (T. Tran).

46

the early settlement of proppants (Kong et al., 2016); and fractures generated by foams have larger reservoir contact area, higher proppant distribution and higher conductivity than those generated by slickwater (Fei et al., 2018; Tran et al., 2020). However, foams are thermodynamically unstable due to their decay mechanisms of liquid drainage, coarsening and bubble coalescence (Schramm, 1994). Under high-temperature conditions, surfactants are likely to degrade and lose their desired functions (Kapetas et al., 2016; Abdelaal et al., 2021), which negatively affects the long-term stability, rheological properties and proppant-carrying ability of foams (Ahmed et al., 2018; Lv et al., 2015; Luo et al., 2014). This thermal instability remains the major limitation of foam fracturing fluids in field application.

In order to address this limitation, nanotechnology has been recently implemented to increase the stability and rheology of fracturing foams at elevated temperatures (Faroughi et al., 2018; Li et al., 2017a; Fu and Liu, 2020; Lv et al., 2015, 2017; Verma et al., 2018, 2019; Fei et al., 2017, 2018). As solid nanoparticles (NP) absorb onto the gas-liquid interface, they act as a steric barrier to enhance the film strength and viscoelasticity, preventing gas diffusion and reducing the rates of coarsening and coalescence (Ab Rasid et al., 2022; Lv et al., 2015; Zhang et al., 2021). In addition, NP also increases the bulk viscosity of the surfactant-NP dispersions, leading to higher foam viscosity and a slower drainage process. Results from Lv et al. (2015) showed that with the presence of silica nanoparticles (SNP), the proppant settling velocity of SDBS foams could reduce by nearly ten times, indicating a significant improvement in the proppant-carrying capacity.

The synergy between surfactant and NP plays a critical role in the properties of foams. Among all types of nanoparticles, silica nanoparticles (SNP) have been most commonly applied for foam stabilization due to their high availability and low costs (Yekeen et al., 2019b; Zhang et al., 2021; Majeed et al., 2021). Conversely, a wide range of surfactants has been used in foam studies. The most popular surfactant groups are anionic surfactants (SDBS, SDS, AOS) and cationic surfactants (CTAB, DTAB) (Yekeen et al., 2019a). In the field of EOR foam flooding, both anionic and cationic surfactants have been commonly combined with SNP to enhance the thermal tolerance and increase the oil displacement efficiency of foams (Singh and Mohanty, 2015; Bayat et al., 2016; Harati et al., 2020; Yekeen et al., 2019a, 2019b; Veyskarami and Ghazanfari, 2018; Li et al., 2017b; Sun et al., 2014a; Wu et al., 2018; Farhadi et al., 2016; Kumar and Mandal, 2017). On the other hand, in the field of foam fracturing, current literature mainly focuses on the synergy between NP and anionic surfactants to improve thermal stability, reduce proppant settling velocity (Lv et al., 2015; Verma et al., 2018), and increase the viscosity of foams (Xiao et al., 2017; Li et al., 2017a; Fu and Liu, 2020). The synergistic effects of NP and cationic surfactants on the properties of fracturing foams, conversely, have yet to be covered or thoroughly investigated. The influence of the SNP-cationic surfactant system on the stability, rheology and proppant suspension of fracturing foams remains ambiguous, especially at elevated reservoir temperatures. In addition, it is still questionable whether the SNP/cationic surfactant system would promote higher foam viscosity and better proppant suspension than the SNP/anionic surfactant system for foam fracturing application or vice versa.

Therefore, this paper aims to comprehensively study the synergy between anionic/cationic surfactant and SNP in improving the stability, rheology and proppant-carrying capacity of the fracturing foams under ambient and elevated temperature conditions. The foam static stability, viscosity measurement and proppant settling tests were conducted with anionic SDBS and cationic CTAB surfactants in varied concentrations and with SNP at fixed concentration. The research is expected to improve our understanding of the surfactants' effects on the behaviours of NP-stabilized fracturing foams and provide reference guidelines for selecting the suitable surfactant type and concentration for the foam fracturing application.

2. Methodology

2.1. Materials

The anionic surfactant used in our experiments was sodium dodecylbenzene sulfonate (SDBS, >99% purity), and the cationic surfactant was hexadecyltrimethylammonium bromide (CTAB, >98% purity). Both surfactants were obtained from Sigma Aldrich. The critical micelle concentrations (CMC) of the surfactants were provided by the supplier, which is 0.61 mM for SDBS and 0.92 mM for CTAB at 25 °C. In addition, hydrophilic silica nanoparticles (SNP) in colloidal form were purchased from Sigma Aldrich with a concentration of 34 wt% suspensions in water. The SNP has an average diameter of 22 nm, a molecular weight of 60.08 g/mol and a surface area of 110–150 m^2/g. Both surfactants and SNP were used without any modification. Deionized distilled water with a resistivity of 18.2 mΩ was used as a base fluid in all experiments (Li et al., 2017b).

2.2. Sample preparation

Firstly, a certain amount of surfactant (from 0.025 wt% to 0.5 wt%) was added into distilled water and continuously stirred at a low speed of 50 RPM for 2 h without interruption. After that, 1.0 wt% SNP were added to the mixture and stirred for another 2 h. The surfactant-nanoparticle dispersion was then ultra-sonicated at a frequency of 40 Hz for 30 min to reach adsorption equilibrium. The dispersion appeared slightly hazy and was sealed for use in experiments. Finally, the prepared dispersion was stirred at 2000 RPM for 2 min to produce fine foams.

2.3. Foam static stability measurement

After foam generation, the initial foam volume was immediately recorded as a measure of foamability. The foam was then transferred into a glass cylinder, which was pre-heated using a water bath system. The top of the cylinder was sealed to prevent contamination and disturbance from the environment. Foam half-life, the total time taken to drain 50% of liquid from the foam (Verma et al., 2019; Li et al., 2019), was recorded and used as a standard measure for foam stability. All stability measurements were conducted at atmospheric pressure and temperatures of 25 °C and 90 °C.

2.4. Apparent viscosity measurement

The apparent viscosity measurement of foams was conducted by a SR5 Rheometer (Rheometric Scientific, USA) using a smooth-surfaced cylindrical couette geometry (Fei et al., 2017; Verma et al., 2019). The influence of surfactant type, concentration, and shear rate on the foam viscosity was studied at 25 °C and 90 °C. Atmospheric pressure was applied in this experiment to match the testing conditions of the foam stability and proppant settling experiments.

In the future work, it is recommended to measure the foam viscosity with a grooved coutee, instead of the smooth-surfaced one. It has been shown that using a grooved couette significantly reduces macroscopic shrinkage at the geometry walls, allowing higher measurement accuracy, especially at low shear rates (Abeli et al., 2021).

2.5. Static proppant settling measurement

In static proppant settling tests, 1 g of sand proppants (20/40 mesh size) was evenly added to the foam column in the pre-heated glass cylinder (Zhang et al., 2020). The proppant settling velocity was determined by measuring the height of the initial foam column and the time taken for the proppants to settle on the bottom of the cylinder. The proppant settling measurements were performed at atmospheric pressure and temperatures of 25 °C and 90 °C. The diameter of the

2

47

measuring cylinder was more than 25 times larger than that of the proppants to minimize the effect of confining walls on the proppant-settling velocity (Goel et al., 2002).

3. Results & discussions

3.1. Foamability

Surfactants have a prominent role in generating and stabilizing foams. The adsorption of surfactant molecules on the gas-liquid interface helps reduce surface tension and surface energy to create colloidal structures (Langevin, 2000). Fig. 1 shows the foaming ability of different surfactant systems with varied surfactant concentrations from 0.025 wt % to 0.5 wt%. All foams were generated from the same dispersion volume of 100 mL. As surfactant concentration increased, the foamability increased gradually until reaching a plateau point. The foamability of CTAB and CTAB/SNP foams increased very slightly after reaching the plateau point at 0.1 wt% CTAB. SDBS and SDBS/SNP foams' initial volumes increased steadily until starting to decrease beyond 0.25 wt% SDBS.

The addition of SNP has a negative effect on foamability. The initial volumes of CTAB and SDBS foams with SNP were 5–15% lower than those without SNP. Previous studies have reported similar observations (Verma et al., 2019; Hu et al., 2018; Binks et al., 2015; Sun et al., 2015). In addition, as SNP is added to the solutions, the dispersion viscosity increases, leading to increased interfacial tension on the gas-liquid interface. Consequently, gas becomes more difficult to dissolve in the dispersion, obstructing bubble formation and lowering foamability.

At the same concentration, SDBS surfactant has a much better foaming ability than CTAB surfactant. Without SNP, the initial volumes of SDBS foams were approximately 1.5 times higher than those of CTAB foams, and the difference was nearly two times in the presence of SNP. This behaviour can be explained by the foam texture difference. Fu and Liu (2021) observed that both surfactants could generate fine foams; however, CTAB foams tend to have thicker liquid films than SDBS foams, which significantly reduces air entrainment and results in lower foam quality and lower foamability of CTAB foams.

Additionally, the foaming capacity of foams largely depends on the electrostatic interaction between surfactants and SNP. It is commonly known that SNP has a high negative charge on its surface (Wang et al., 2005; Tran et al., 2022). As anionic SDBS surfactants and SNP are both negatively charged, the electrostatic repulsive force between the two

elements reduces the attachment of SDBS molecules on the SNP surface and promotes more adsorption of SDBS molecules on the gas-liquid interface. As a result, the surfactant molecules adsorbed on the gas-liquid interface are considered 'active molecules' (Fu and Liu, 2020), which help to further reduce the surface tension and increase the foamability. On the other hand, as cationic CTAB surfactants contain positive charges in their head groups, a strong electrostatic attraction exists between CTAB molecules and the SNP surface due to the opposition of their electric charges. As a result, CTAB molecules are more likely to adsorb on the SNP surface than on the gas-liquid interface (Briceño-Ahumada et al., 2021). Eventually, the concentration of active CTAB molecules is significantly reduced, leading to the low foamability behaviour observed in Fig. 1.

By definition, foam quality (Q) is the ratio between the gas volume (V_{gas}) and the total foam volume (V_{foam}) (Schramm, 1994). The equation for foam quality can be expressed in Eq. (1). Using the foamability results and the fixed mixture volume of 100 mL, the quality of the studied foams can be calculated and presented in Table 1:

$$Q\ (\%) = \frac{V_{gas}}{V_{foam}} = \frac{V_{foam} - V_{liquid}}{V_{foam}} \tag{1}$$

3.2. Foam stability

In foam fracturing application, foam stability is one of the critical factors to the success of the treatment. Fig. 2 shows the drainage half-lives of the studied foam systems with varied surfactant concentrations at 25 °C and 90 °C. The effects of temperature, SNP, surfactant type and concentration on foam stability are observed and discussed.

As the temperature increased from 25 °C to 90 °C, all foams became less stable with lower drainage half-lives. The stability impairment is mainly due to surfactant degradation at high temperatures. As temperature increases, the kinetic energy of the surfactant molecules increases rapidly, preventing their adsorption on the gas-liquid interface and reducing their ability to stabilize foams (Verma et al., 2018; Hanamertani et al., 2018; Fu and Liu, 2020; Emrani et al., 2017). The rise in temperature also reduces the surface elasticity of the gas-liquid interface and promotes gas diffusion through lamellae (Yang et al., 2021). Consequently, the drainage, coarsening, and coalescence rates are accelerated with increasing temperature. This leads to an increase in bubble size and a decrease in film thickness, resulting in early film rupture (Lv et al., 2015).

According to Fig. 2, adding SNP considerably increased the stability of both CTAB and SDBS foams. Naturally, when the distance between two bubble surfaces gets closer, the van der Waals attractive force between the surfaces becomes significant in causing a disturbance and film rupture (Fei et al., 2018; Verma et al., 2019). As SNP is added, they adsorb on the gas-liquid interface to form monolayers, bilayers or a multi-layer network around the foam bubbles (Hunter et al., 2008; Zhou et al.,2020). These layers help enhance film strength, maintain film thickness, reduce the coarsening rate and significantly decrease the probability of film rupture (Fei et al., 2017). Moreover, adding SNP increases the viscosity of foam solutions and dispersions. This enhances the foams' ability to hold water content in the liquid films and decelerates the drainage rate (Hu et al., 2018; Fei et al., 2017).

In the absence of SNP, CTAB foams generally had higher stability
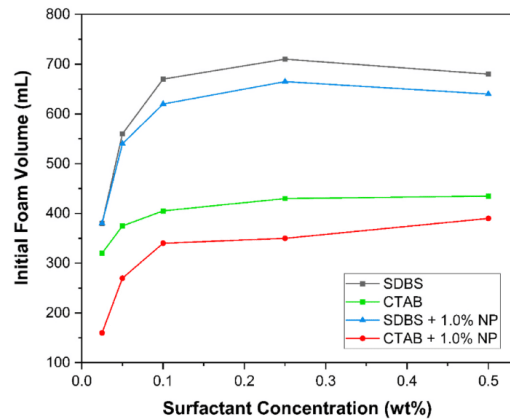
Fig. 1. Influence of surfactant concentration on the foamability of foams with and without 1.0 wt% SNP.

Table 1
Foam quality results.

Surfactant concentration (wt%)	SDBS foam	CTAB foam	SDBS + 1.0% NP foam	CTAB + 1.0% NP foam
0.025	73.7%	68.8%	73.7%	37.5%
0.05	82.1%	73.3%	81.5%	63.0%
0.10	85.1%	75.3%	83.9%	70.6%
0.25	85.9%	76.7%	85.0%	71.4%
0.50	85.3%	77.0%	84.4%	74.4%
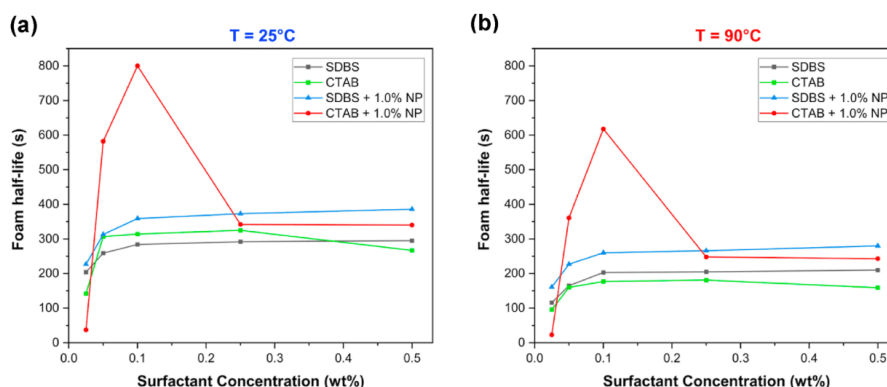
Fig. 2. Influence of surfactant concentration on the stability of foams at the temperature of (a) 25 °C and (b) 90 °C.

than SDBS foams at ambient temperature. The observation can be attributed to the self-aggregation characteristics of CTAB molecules in solutions. According to Yekeen et al. (2019c), due to the self-aggregation behaviour, a higher number of active CTAB molecules are generated and quickly migrated from bulk solution into the gas-liquid interface to better stabilize foams. However, at the higher temperature of 90 °C, SDBS foams were more stable than CTAB foams. From the observed stability difference, SDBS foams are believed to have higher thermal resistance than CTAB foams.

The effects of surfactant concentration on foam stability are quite different among the foam systems. For SDBS and SDBS/SNP foams, the measured half-lives increased dramatically when SDBS concentration increased from 0.025 wt% to 0.1 wt%, then improved very slightly after 0.1 wt%. The 0.1 wt% point is considered the critical value, beyond which the foam stability is independent of the surfactant concentration (Wang et al., 2018). Similarly, the stability of CTAB foams increased consistently with CTAB concentration from 0.025 wt% to 0.25%. However, after reaching a peak half-life at 0.25 wt%, the stability of CTAB foams started to reduce considerably. This observation is possibly related to the self-aggregation of CTAB molecules in solutions. At high surfactant concentrations, the self-aggregation behaviour of CTAB can become redundant and form excessively large CTAB aggregates. As a result, these aggregates have minimal adsorption on the gas-liquid interface, reducing their capability of stabilizing foams.

Last but not least, Fig. 2 shows very interesting results in the stability of CTAB/SNP foams. At 0.025 wt% surfactant concentration, CTAB/SNP foams had the lowest drainage half-life compared to the other foam systems. It is believed that there is a minimum threshold of CTAB concentration, below which the synergy between SNP and CTAB is not possible for foam stabilization. As CTAB concentration increased to 0.05 wt% and 0.1 wt%, the stability of CTAB/SNP foams increased sharply and dominated other foams. At 0.1 wt% CTAB, the drainage half-lives of CTAB/SNP foams were 800s at 25 °C and 620s at 90 °C, both of which are 2.2–2.4 times higher than those of SDBS/SNP foams. However, as CTAB concentration further increased to 0.25% and 0.5%, the stability of CTAB/SNP foams dropped significantly by approximately 250% - even lower than the SDBS/SNP foams. The same behaviours were observed at both ambient and elevated temperatures.

3.2.1. Stability of CTAB/SNP foams at medium CTAB concentration

Two main mechanisms can explain the stability dominance of CTAB/SNP foams at medium CTAB concentrations: 1) high detachment energy of SNP and 2) cork formation at the bubble interface. Firstly, particle detachment energy is the minimum energy required to remove adsorbed particles from the gas-liquid interface. The detachment energy (*E*) of

nanoparticles is shown in Eq. (2) (Binks, 2002):

$$E = \pi R^2 \gamma (1 - \cos\theta)^2 \qquad (2)$$

Where R is the radius of the NP, γ is the interfacial tension, and θ is the contact angle of the NP at the gas-liquid interface. The higher the detachment energy is, the stronger particles adsorb on the gas-liquid interface to stabilize foams. When interacting with SNP, cationic CTAB molecules tend to attach to the SNP surface due to the electrostatic attractive force between them. As the CTAB concentration increases from low to medium, more CTAB molecules will adsorb on the SNP surface, reducing the absolute zeta potential to the isoelectric point, enhancing the hydrophobicity and promoting particle aggregation of the SNP (Tran et al., 2022). This directly results in a higher contact angle and larger aggregate size of SNP with increasing CTAB concentration. According to Eq. (2), the detachment energy of NP largely depends on the NP size and contact angle. Therefore, with increasing CTAB concentration from low to medium, SNP is expected to have higher detachment energy, allowing them to adsorb stronger on the gas-liquid interface and stabilize liquid films and foam bubbles more effectively.

The second stabilization mechanism is the cork formation in the plateau border. As SNP interact with cationic surfactant molecules, they are likely to generate SNP aggregates, which act as solid barriers on the foam bubbles to constrain film thinning and maintain film thickness (AlYousef et al., 2018; Zhou et al., 2020). In addition, SNP aggregates are also very effective in delaying foam drainage. As SNP aggregates collide with each other in short ranges, they form large accumulations known as 'corks' in the lamellae (Fei et al., 2017). Fig. 3 demonstrates the formation of corks from surfactant-nanoparticle aggregates in the plateau border. As the corks grow progressively, they block the liquid flow and reduce the number of drainage channels (Fameau and Salonen, 2014; Carn et al., 2009). This results in particle jamming in the plateau border, thereby decreasing the drainage rate and improving overall foam stability.

Both stabilization mechanisms are only possible due to the interaction between the oppositely charged SNP and cationic surfactants. The unique synergistic effects explain why CTAB/SNP foams were much more stable than anionic SDBS/SNP foams at 0.05 wt% and 0.1 wt% surfactant concentration.

3.2.2. Stability of CTAB/SNP foams at high CTAB concentration

Even though CTAB/SNP foam had outstanding stability at medium surfactant concentrations, its drainage half-life declined dramatically at 0.25 and 0.5 wt% CTAB (Fig. 2). The stability impairment is most likely due to the negative effects of the excessive CTAB concentration on the

49
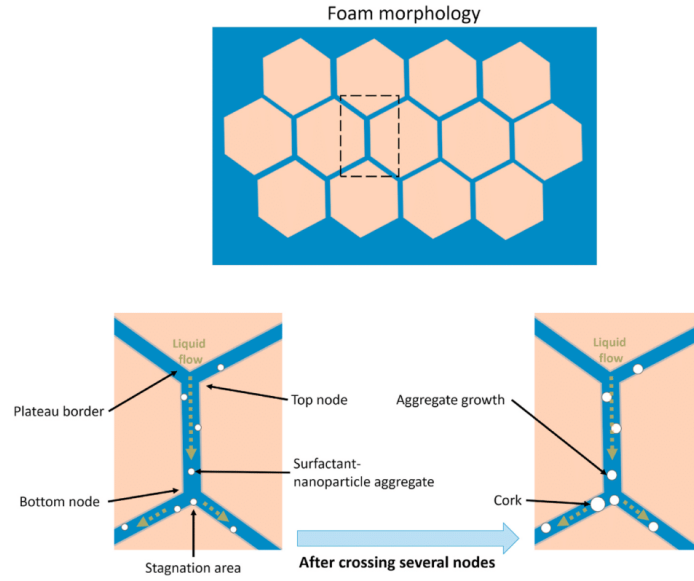
Fig. 3. Schematic diagram of cork formation and particle jamming from SNP-surfactant aggregates in the plateau border (Carn et al., 2009).

behaviour of CTAB/SNP dispersions. At high concentrations, CTAB molecules tend to attach to the SNP surface in bilayers, which results in the increased hydrophilicity of the SNP and makes SNP more difficult to adsorb on the gas-liquid interface (Liu et al., 2010; Hu et al., 2018; Tran et al., 2022).

However, SNP aggregation and flocculation can stabilize foams only when they are on a micro-scale (Wang et al., 2018). When mixing a high concentration of CTAB surfactant in SNP dispersions, it was observed that very large SNP aggregates and flocculates were formed; they have white colour and are visible to the naked eye. Due to their large sizes, these structures require very high mixing energy to be placed on the gas-liquid interface. Therefore, they tend to settle and precipitate in bulk solutions rather than adsorb on the plateau borders (Tran et al., 2022).

It can be concluded that at high CTAB concentration, the increased hydrophilicity of SNP and the formation of large SNP flocculates result in the low adsorption of SNP and the destruction of the SNP network on the lamellae (Wang et al., 2018; AlYousef et al., 2018). These behaviours considerably reduce the film strength, decline the film elasticity, and eventually decrease the stability of CTAB/SNP foams at high CTAB concentrations (Fig. 2).

3.3. Foam rheology

The viscosity behaviour is crucial for any fracturing fluid as it determines the proppant-carrying capacity and filtration property. Foam viscosity generally is relatively high; however, it is susceptible to bubble and lamellae deformation. Fig. 4 shows the apparent viscosity of the studied foam systems at ambient and elevated temperatures. The viscosity results were measured at the fixed shear rate of $100 \ s^{-1}$.

According to Fig. 4, the foam viscosity decreased considerably when

Fig. 4. Influence of surfactant concentration on the apparent viscosity of foams at (a) 25 °C and (b) 90 °C.

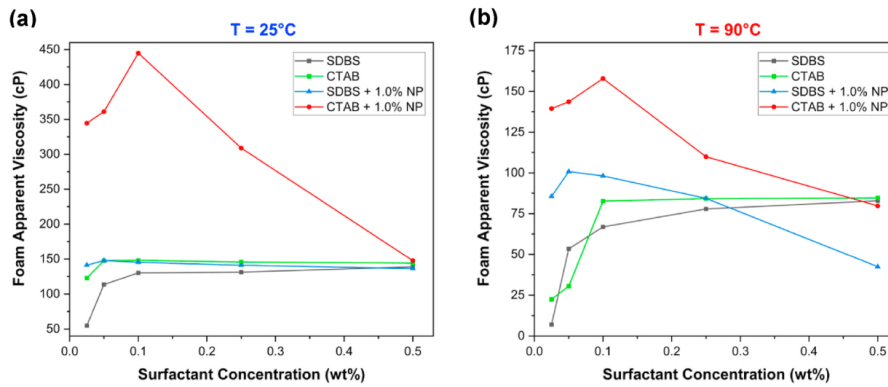the temperature increased from 25 °C to 90 °C. A similar observation has been reported in previous studies. The foam viscosity reduction at a high temperature can be attributed to the decreased viscosity of the surfactant solutions and the NP-surfactant dispersions (Fu and Liu, 2020); the increased film loss rate from the increased surfactant molecular activity (Langevin, 2000); and the increased coarsening rate and film rupture from the gas expansion (Lv et al., 2015). The inverse relationship between foam viscosity and temperature is related to the flow activation energy by the Arrhenius' law (Gidley et al., 1995; Pozrikidis, 2001), which can be expressed in Eq. (3):

$$\eta_a = A_v \exp\left(\frac{E_f}{RT}\right) \tag{3}$$

where η_a is the foam's apparent viscosity, A_v is the exponential constant, E_f is the activation energy, R is the university gas constant, and T is the absolute temperature. During fracturing at reservoir temperature, foam viscosity is expected to decline; however, the reduced viscosity should be high enough to carry and transport proppants effectively.

CTAB foams had higher apparent viscosity at ambient and elevated temperatures than SDBS foams. This observation is most likely because of the foam quality of CTAB and SDBS foams. According to Table 1, CTAB foams had 68–74% quality while the quality of SDBS foams was relatively higher, around 82–85%. This is because SDBS foams have higher gas volume and lower liquid content in the lamellae by having higher foam quality. As a result, the liquid films in SDBS foams are thinner and have less deformation resistance than those in CTAB foams. This explains why SDBS foams had lower apparent viscosity than CTAB foams at 25 °C and 90 °C. In some previous studies, the optimal foam quality for peak viscosity was found to be between 70 and 75% (Fu and Liu, 2021; Worthen et al., 2013; Zhu et al., 2017), which is very close to the quality of CTAB foams in this study.

The effects of surfactant concentration on the foam viscosity can also be observed in Fig. 4. With increasing surfactant concentration, the apparent viscosity of CTAB and SDBS foams increased gradually, then started to slow down after reaching the critical point at 0.1 wt% surfactants. Again, the foam morphology can explain this observation. As the surfactant concentration increases, foams have a finer texture with smaller bubble size, a higher number of bubbles and more stable lamellae (Fu and Liu, 2021; Worthen et al., 2013; Gu and Mohanty, 2015). Due to the improved texture and increased lamellae stability, foams have higher flow resistance. As a result, they are more difficult to deform, which leads to improved foam viscosity at higher surfactant concentrations.

In the presence of SNP, on the other hand, the relationship between surfactant concentration and foam viscosity is much more complicated. Generally, as SNP adsorb on the gas-liquid interface, they help to improve the foam texture and enhance the viscoelasticity of the liquid films (Lv et al., 2015; Georgieva et al., 2009; Fu and Liu, 2021). Consequently, foams have higher interfacial strength and increased structural integrity, which significantly reduces interactions among foam bubbles, resists disturbances, and eventually increases the foam viscosity (Georgieva et al., 2009). According to Fig. 4, the apparent viscosity of CTAB and SDBS foams increased remarkably with the inclusion of 1.0 wt% SNP. Furthermore, CTAB/SNP foams had a higher viscosity than SDBS/SNP foams at ambient and elevated temperatures. This observation claims that the combination of SNP and cationic surfactants is more effective in enhancing foam viscosity than the SNP/anionic surfactant mixtures.

Moreover, it is observed that the effects of SNP on the foam viscosity could be reduced at high surfactant concentrations. For example, at low CTAB concentrations between 0.025 wt% and 0.1 wt%, CTAB/SNP foams had excellent rheological properties where the foam viscosity could reach nearly 450 cP at ambient temperature and 160 cP at high temperature. At higher CTAB concentrations, on the other hand, the apparent viscosity of CTAB/SNP foams dropped massively. For instance,

at 0.5 wt% CTAB, the viscosity of CTAB/SNP foams was not much different or even lower than that of the CTAB and SDBS foams. Similar behaviour was observed in the viscosity of SDBS/SNP foams.

Given that the optimal SDBS concentration was found at 0.05 wt%, the foam viscosity started to decrease at higher surfactant concentrations. While the decline rate was relatively slight at 25 °C, it became very significant at a higher temperature. At 90 °C, the apparent viscosity of SDBS/SNP foams at 0.5 wt% SDBS was only 42 cP - the lowest in the four foam systems. Li et al. (2017a) claimed that the reduction of the CTAB/SNP and SDBS/SNP foam viscosity at high surfactant concentrations could be attributed to the decreased dispersion viscosity. As the surfactant concentration is too high, the excessive amount of surfactant molecules may form micelles in the solution and solubilize SNP, which potentially reduces the flow resistance of the liquid phase and thereby lowers the macroscopic viscosity of the dispersions (Lv et al., 2017). Future work is strongly suggested further investigate and explain the viscosity behaviour of NP-stabilized foams at high surfactant concentrations.

Fig. 5 shows the effects of shear rate on the apparent viscosity of SNP-stabilized foams at 0.1 wt% surfactant concentration. It can be observed that the foam viscosity decreased when increasing shear rates from 50 to 1000 s^{-1}. As shear rates increase, foam bubbles will likely organize themselves in an ordered arrangement. Because of that, foams become easier to flow and deform, leading to their reduced viscosity. Nevertheless, it has been found that the interaction between the gas-liquid interfaces becomes weaker at a higher shear rate, which also results in the foam viscosity decline (Sun et al., 2014b).

The observed relationship between the shear rate and apparent viscosity confirms the non-Newtonian characteristics and the shear-thinning behaviour of the foamed fluids. The shear-thinning behaviour of foams has many advantages in the fracturing application. In the process of mixing and pumping fracturing fluids downhole, constant flow circulation and high pressure are typically required, leading to high shear rates. Foam has lower viscosity at a high shear rate, so it helps decrease friction loss and reduce the pumping requirements, bringing down stimulation costs (Gu and Mohanty, 2015). On the other hand, low shear rates are usually observed in the porous media, and the fracture flows. By having high viscosity at low shear rates, fracturing foams have excellent capabilities of suspending and transporting proppants into the fractures (Gu and Mohanty, 2015). This benefit significantly helps enhance the fracture dimensions and conductivity (Tran et al., 2020; Fei et al., 2018).
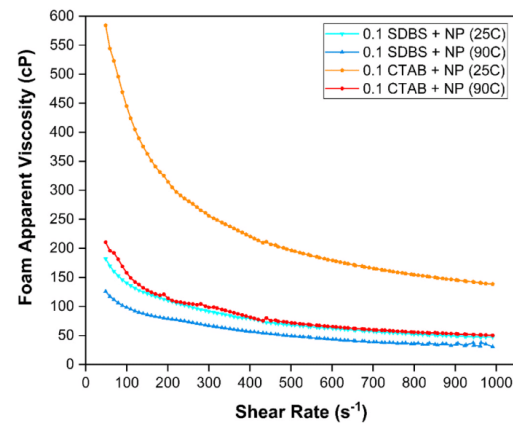

Fig. 5. Influence of shear rate on the apparent viscosity of foams at the temperature of 25 °C and 90 °C.

As shown in Fig. 5, the negative impacts of elevated temperature on the foam viscosity are quite clear. At the same 0.1 wt% surfactant concentration, CTAB/SNP foams had higher apparent viscosity than SDBS/SNP foams, and the viscosity difference was more significant at ambient temperature.

3.4. Proppant suspension of foams

Proppant-carrying ability plays an essential role in the performance of the fracturing fluid, and settling velocity is the critical measure for the proppant suspension. With lower settling velocity, fluids can transport more proppants from the wellbore to fractures and effectively distribute proppants into the main and small-sized fractures (Gu and Mohanty, 2015). Fig. 6 shows the proppant settling velocity of the studied foams at the temperature of 25 °C and 90 °C.

Generally, foams have excellent proppant-carrying capacity with low settling velocity compared to other fracturing fluid systems. The exceptional proppant-carrying ability of foams is mainly due to the foam structure. Zhu et al. (2019) illustrated the forces exerted on the settling proppant in the bubble scale (Fig. 7). When settling through the foam, the proppant tends to squeeze or stretch the foam films, generating bubble pressure and network force on the proppant. These two forces in the vertical direction act as drag forces against gravity, slowing down the proppant settlement in the foam.

It is widely believed the proppant suspension depends mainly on the stability and viscosity of foams (Abdelaal et al., 2021; Yekeen et al., 2018). Therefore, most proppant settling behaviours in foams can be related and explained by the foam stability and rheology observations. For example, in Fig. 6, the proppant settling velocity of all studied foams increased by a magnitude when increasing temperature from 25 °C to 90 °C. This is because the foam becomes less stable with reduced viscosity and increased liquid drainage and film rupture rates as the temperature rises. These consequences heavily decrease the interactions between the gas bubbles and the proppants, leading to the early proppant settlement at elevated temperatures.

Under both temperature conditions, CTAB foams had lower proppant settling velocity than SDBS foams. The observation is most likely because of CTAB foams obsessing greater rheological properties (Fig. 4). By having higher apparent viscosity, CTAB foams are better at holding proppants and other particles in the bubbles. Moreover, as previously presented, the liquid films in CTAB foams tend to be thicker with higher liquid content than those in SDBS foams. This potentially increases the vertical drag forces exerting on the proppants, thereby delaying the proppant settlement.

Fig. 6 shows that the proppant settling velocity of CTAB and SDBS foams was further reduced with the addition of 1.0 wt% SNP. There are three main reasons contributing to the positive effects of SNP on the proppant settling behaviour. First, the foam half-lives with SNP were significantly higher than those without SNP (Fig. 2). This directly allows CTAB/SNP and SDBS/SNP foams much more time to support and delay the settlement of proppants. Additionally, as CTAB and SDBS foams have higher viscosity in the presence of SNP (Fig. 4), their bubbles tend to have more resistance against the liquid flow and proppant settlement (Lv et al., 2015). Lastly, as SNP adsorb on the gas-liquid interface, the surfaces of the foam bubbles become rougher (Verma et al., 2018). This considerably prevents proppants from easily slipping on the surface, thereby lowering their settling velocity.

Overall, the proppant settling rate of foams decreased with increasing surfactant concentration. However, CTAB/SNP foam is an exceptional case where the effect of surfactant concentration is not consistent. Between 0.025 wt% and 0.1 wt%, CTAB/SNP foams had the lowest proppant settling velocity compared to other foam systems, and these settling rates were observed to decrease with increasing surfactant concentration. For example, at 0.1 wt% CTAB, the settling velocity of proppants could reach down to 0.017 mm/s at ambient temperature and 0.23 mm/s at elevated temperature. On the other hand, when increasing the CTAB concentration beyond 0.1 wt%, the proppant settling velocity of CTAB/SNP foams increased sharply – even higher than that of CTAB and SDBS foams without SNP. This behaviour can be attributed to the reduced stability and viscosity of CTAB/SNP foams at high CTAB concentrations (Figs. 2 and 4) and the excessive SNP aggregation. At high CTAB concentrations, SNP aggregates tend to form large-sized corks in the gas-liquid interface. While corks are beneficial in blocking the liquid channels and reducing gravitational drainage, they can cause negative impacts on the proppant settlement. When interacting or colliding with proppants in the plateau border, these large-sized corks are very likely to result in additional gravity force on the proppants. Moreover, in that case, the bubble pressure force and network force would exert not only on the proppants but also on the corks. This directly decreases the vertical drag force on the proppants, thereby accelerating the settlement of proppants in the CTAB/SNP foams.

3.5. Advantages & limitations of CTAB/SNP foams

CTAB/SNP foams were observed to have the highest stability, highest viscosity and lowest proppant settling velocity among the four studied foam systems. With the mentioned advantages, CTAB/SNP foam is expected to have a very high capacity for transporting and distributing
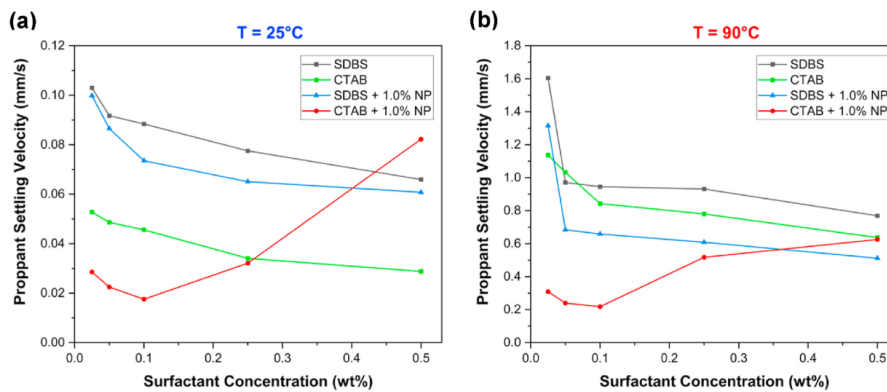

Fig. 6. Influence of surfactant concentration on the proppant settling velocity of foams (a) 25 °C and (b) 90 °C.
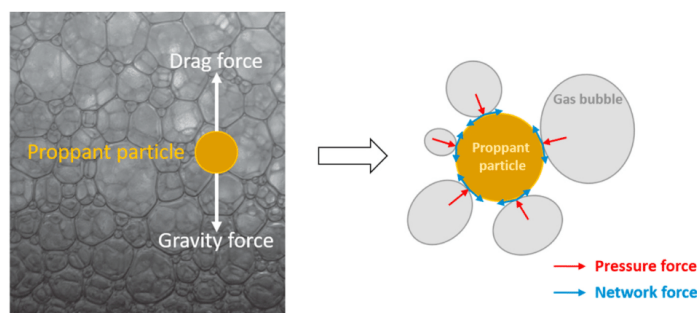
Fig. 7. Schematic diagram of the forces exerting on the settling proppant in the foam structure (Zhu et al., 2019).

proppants to the target reservoir area, preventing early proppant settlement and enhancing the fracture dimensions and conductivity.

On the other hand, CTAB/SNP foams have a few limitations in the fracturing application. First of all, the properties of CTAB/SNP foams are susceptible to surfactant concentration. In this study's optimal concentration range, for example, 0.05 wt% and 0.1 wt% CTAB, we achieved excellent stability, rheology, and outstanding proppant settling behaviour of CTAB/SNP foams at both ambient and elevated temperatures. However, at too low or too high CTAB concentration, the properties of CTAB/SNP foams are severely impacted, which may be even worse than the foams without SNP. Secondly, at high CTAB concentrations, excessive SNP-surfactant aggregates tend to form corks in the gas-liquid interface and flocculate in the bulk solution. Due to the large sizes, these structures might block pore throats and pore bodies, which potentially causes formation damage and decreases fracture conductivity and well productivity. Lastly, cationic CTAB surfactant molecules have high adsorption capacity on negatively-charged formation rocks such as sandstone and clay with high quartz content. Therefore, the presence of SNP could reduce the adsorption of CTAB on reservoir rocks by up to 50% (Yekeen et al., 2019c); however, the surfactant loss might still be considerable for foam fracturing treatment.

Despite the presented drawbacks in field application, at the appropriate concentration, CTAB/SNP foams have several promising benefits in foam fracturing at reservoir temperature. They are superior to the SDBS/SNP foams used in recent foam studies. More studies are required to investigate further the practical use of the CTAB/SNP fracturing foams and address their limitations by chemical tuning and introducing new additives to the dispersion mixtures. In addition, future work is strongly encouraged to study the damage of the nanoparticle-surfactant fracturing foam systems to the properties and performance of different reservoir types.

4. Conclusions

In this paper, the effects of anionic and cationic surfactants on the properties of nanoparticle-stabilized fracturing foams were investigated and compared. The foams' foamability, stability, rheology and proppant settling behaviour were studied in a wide range of surfactant concentrations at ambient and elevated temperatures. The study provides significant insights into the influences of surfactant type and concentration on the properties of nano-foams. This significantly contributes to developing a stable, high-performance foam system that works effectively at reservoir temperature. The key conclusions can be summarized as follows.

1. As the surfactant concentration increased from 0.025 wt% to 0.5 wt %, the properties of foams were enhanced enormously until reaching

a plateau/peak point. These critical points were mainly found between 0.05 wt% and 0.1 wt% of surfactant concentration.

2. Without SNP, CTAB foams had lower foamability, less thermal resistance, higher apparent viscosity and better proppant-carrying ability than SDBS foams. In the presence of 1.0 wt% SNP, the adsorption of SNP on the gas-liquid interface noticeably delayed the gravitational drainage and considerably improved the viscosity and proppant suspension behaviour of both CTAB and SDBS foams.

3. At both ambient and elevated temperatures, the synergy between cationic CTAB surfactant and SNP resulted in higher foam stability, foam viscosity and lower proppant settling velocity than the anionic SDBS surfactant and SNP.

4. CTAB/SNP foam is strongly considered a promising fracturing fluid which can be applied under reservoir conditions. Their properties were observed to depend massively on the surfactant concentration. At medium CTAB concentrations such as 0.05 wt% and 0.1 wt%, CTAB/SNP foams had superior features with the highest stability, apparent viscosity and lowest proppant settling velocity compared to other foams. However, these excellent features were significantly diminished at higher CTAB concentrations. At redundant surfactant concentration, the excessive amount of SNP-CTAB aggregates tend to form large-sized corks in the gas-liquid interface and flocculates in the bulk solution, both of which can cause negative impacts on the properties of CTAB/SNP foams.

This study suggests further research focused on applying high pressure conditions and/or other gas types, such as CO_2 and N_2 to observe the impacts of these external factors on the foams' properties. In addition, microscopic experiments, including scanning electron microscope (SEM) are recommended to visualise the size, shape, and distribution of the bubbles and SNP aggregates at the bubble scale. Besides that, oscillatory measurements of the yield stress, yield strain, storage moduli and loss moduli should be incorporated to study the elastic properties of liquid foams. All these measurements are believed to provide significant insights to justify and support the discussions.

Credit authors statement

Tuan Tran: Investigation, Methodology, Data curation, Formal analysis, Writing – original draft.; **M.E Gonzalez Perdomo**: Conceptualization, Supervision, Writing – review & editing, Validation, Resources.; **Manouchehr Haghighi**: Conceptualization, Supervision, Writing – review & editing, Validation, Resources.; **Khalid Amrouch**: Supervision, Writing – review & editing.

Declaration of competing interest

The authors declare that they have no known competing financial

interests or personal relationships that could have appeared to influence the work reported in this paper.

Data availability

Data will be made available on request.

Acknowledgements

References

Ab Rasid, S.A., Mahmood, S.M., Kechut, N.I., Akbari, S., 2022. A review on parameters affecting nanoparticles stabilized foam performance based on recent analyses. J. Petrol. Sci. Eng. 208.

Abeli, B., Miguel, M., Mendes, P., Mendes, R., 2021. Startup flow of gelled waxy crude oils in pipelines: the role of volume shrinkage. Fuel 288.

Abdelaal, A., Aljawad, M.S., Alyousef, Z., Almajid, M.M., 2021. A review of foam-based fracturing fluids applications: from lab studies to field implementations. J. Nat. Gas Sci. Eng. 95.

Ahmed, S., Elraies, K., Hashmet, M., Alnarabiji, M., 2018. Empirical modeling of the viscosity of supercritical carbon dioxide foam fracturing fluid under different downhole conditions. Energies 11 (4).

AlYousef, Z.A., Almobarky, M.A., Schechter, D.S., 2018. The effect of nanoparticle aggregation on surfactant foam stability. J. Colloid Interface Sci. 511, 365–373. Feb 1.

Bayat, A.E., Rajaei, K., Junin, R., 2016. Assessing the effects of nanoparticle type and concentration on the stability of CO 2 foams and the performance in enhanced oil recovery. Colloids Surf. A Physicochem. Eng. Asp. 511, 222–231.

Binks, B., 2002. Particles as surfactants-similarities and differences. Curr. Opin. Colloid Interface Sci. 7 (03/01), 21–41.

Binks, B.P., Campbell, S., Mashinchi, S., Piatko, M.P., 2015. Dispersion behavior and aqueous foams in mixtures of a vesicle-forming surfactant and edible nanoparticles. Langmuir 31 (10), 2967–2978. Mar 17.

Briceño-Ahumada, Z., Soltero-Martínez, J.F.A., Castillo, R., 2021. Aqueous foams and emulsions stabilized by mixtures of silica nanoparticles and surfactants: a state-of-the-art review. Chemical Engineering Journal Advances 7.

Carn, F., Colin, A., Pitois, O., Vignes-Adler, M., Backov, R., 2009. Foam drainage in the presence of nanoparticle-surfactant mixtures. Langmuir 25 (14), 7847–7856. Jul 21.

Emrani, A.S., Nasr-El-Din, Ha, 2017. An experimental study of nanoparticle-polymer-stabilized CO 2 foam. Colloids Surf. A Physicochem. Eng. Asp. 524, 17–27.

Fameau, A.-L., Salonen, A., 2014. Effect of particles and aggregated structures on the foam stability and aging. Compt. Rendus Phys. 15 (8–9), 748–760.

Farhadi, H., Riahi, S., Ayatollahi, S., Ahmadi, H., 2016. Experimental study of nanoparticle-surfactant-stabilized CO2 foam: stability and mobility control. Chem. Eng. Res. Des. 111, 449–460.

Faroughi, S.A., Pruvot, A.J.-C.J., McAndrew, J., 2018. The rheological behavior of energized fluids and foams with application to hydraulic fracturing: review. J. Petrol. Sci. Eng. 163, 243–263.

Fei, Y., Johnson, R.L., Gonzalez, M., Haghighi, M., Pokalai, K., 2018. Experimental and numerical investigation into nano-stabilized foams in low permeability reservoir hydraulic fracturing applications. Fuel 213, 133–143.

Fei, Y., Zhu, J., Xu, B., Li, X., Gonzalez, M., Haghighi, M., 2017. Experimental investigation of nanotechnology on worm-like micelles for high-temperature foam stimulation. J. Ind. Eng. Chem. 50, 190–198.

Fu, C., Liu, N., 2020. Study of the synergistic effect of the nanoparticle-surfactant-polymer system on CO2 foam apparent viscosity and stability at high pressure and temperature. Energy Fuels 34 (11), 13707–13716.

Fu, C., Liu, N., 2021. Rheology and stability of nanoparticle-stabilized CO2 foam under reservoir conditions. J. Petrol. Sci. Eng. 196.

Georgieva, D., Cagna, A., Langevin, D., 2009. Link between surface elasticity and foam stability. Soft Matter 5 (10).

Gidley, J., Holditch, S., Nierode, D., Veatch, R., 1995. Recent Advances in Hydraulic Fracturing (Beijing).

Goel, N., Shad, S., Grady, B., 2002. Correlating viscoelastic measurements of fracturing fluid to particles suspension and solids transport. J. Petrol. Sci. Eng. 35, 59–81.

Gu, M., Mohanty, K.K., 2015. Rheology of polymer-free foam fracturing fluids. J. Petrol. Sci. Eng. 134, 87–96.

Hanamertani, A.S., Pilus, R.M., Manan, N.A., Mutalib, M.I.A., 2018. The use of ionic liquids as additive to stabilize surfactant foam for mobility control application. J. Petrol. Sci. Eng. 167, 192–201, 2018/08/01/.

Harati, S., Esfandyari Bayat, A., Sarvestani, M.T., 2020. Assessing the effects of different gas types on stability of SiO2 nanoparticle foam for enhanced oil recovery purpose. J. Mol. Liq. 313.

Hu, N., Li, Y., Wu, Z., Lu, K., Huang, D., Liu, W., 2018. Foams stabilization by silica nanoparticle with cationic and anionic surfactants in column flotation: effects of particle size. J. Taiwan Inst. Chem. Eng. 88, 62–69.

Hunter, T.N., Pugh, R.J., Franks, G.V., Jameson, G.J., 2008. The role of particles in stabilising foams and emulsions. Adv. Colloid Interface Sci. 137 (2), 57–81. Mar 18.

Isah, A., Hiba, M., Al-Azani, K., Aljawad, M.S., Mahmoud, M., 2021. A comprehensive review of proppant transport in fractured reservoirs: experimental, numerical, and field aspects. J. Nat. Gas Sci. Eng. 88.

Kapetas, L., Vincent Bonnieu, S., Danelis, S., Rossen, W.R., Farajzadeh, R., Eftekhari, A. A., Mohd Shafian, S.R., Kamarul Bahrim, R.Z., 2016. Effect of temperature on foam flow in porous media. J. Ind. Eng. Chem. 36, 229–237.

Kong, X., McAndrew, J., Cisternas, P., 2016. CFD study of using foam fracturing fluid for proppant transport in hydraulic fractures. In: Abu Dhabi International Petroleum Exhibition & Conference. Day 2 Tue, November 08, 2016.

Kumar, S., Mandal, A., 2017. Investigation on stabilization of CO 2 foam by ionic and nonionic surfactants in presence of different additives for application in enhanced oil recovery. Appl. Surf. Sci. 420, 9–20.

Langevin, D., 2000. Influence of interfacial rheology on foam and emulsion properties. Adv. Colloid Interface Sci. 88, 209–222.

Li, C., Huang, Y., Sun, X., Gao, R., Zeng, F., Tontiwachwuthikul, P., Liang, Z., 2017a. Rheological properties study of foam fracturing fluid using CO 2 and surfactant. Chem. Eng. Sci. 170, 720–730.

Li, S., Qiao, C., Li, Z., Wanambwa, S., 2017b. Properties of carbon dioxide foam stabilized by hydrophilic nanoparticles and hexadecyltrimethylammonium bromide. Energy Fuels 31 (2), 1478–1488.

Li, S., Yang, K., Li, Z., Zhang, K., Jia, N., 2019. Properties of CO2 foam stabilized by hydrophilic nanoparticles and nonionic surfactants. Energy Fuels 33 (6), 5043–5054.

Liu, Q., Zhang, S., Sun, D., Xu, J., 2010. Foams stabilized by Laponite nanoparticles and alkylammonium bromides with different alkyl chain lengths. Colloids Surf. A Physicochem. Eng. Asp. 355 (1–3), 151–157.

Luo, X., Wang, S., Wang, Z., Jing, Z., Lv, M., 2014. Experimental research on rheological properties and proppant transport performance of GRF–CO2 fracturing fluid. J. Petrol. Sci. Eng. 120, 154–162.

Lv, Q., Li, Z., Li, B., Li, S., Sun, Q., 2015. Study of nanoparticle–surfactant-stabilized foam as a fracturing fluid. Ind. Eng. Chem. Res. 54 (38), 9468–9477.

Lv, Q., Li, Z., Li, B., Zhang, C., Shi, D., Zheng, C., Zhou, T., 2017. Experimental study on the dynamic filtration control performance of N 2/liquid CO 2 foam in porous media. Fuel 202, 435–445.

Majeed, T., Kamal, M.S., Zhou, X., Solling, T., 2021. A review on foam stabilizers for enhanced oil recovery. Energy Fuels 35 (7), 5594–5612.

Pozrikidis, C., 2001. Numerical investigation of the effect of surfactants on the stability and rheology of emulsions and foam. J. Eng. Math. 41, 237–258.

Schramm, L.L., 1994. Foams: Fundamentals and Applications in the Petroleum Industry. American Chemical Industry, Washington DC, USA.

Singh, R., Mohanty, K.K., 2015. Synergy between nanoparticles and surfactants in stabilizing foams for oil recovery. Energy Fuels 29 (2), 467–479.

Speight, J.G., 2016. Handbook of Hydraulic Fracturing. John Wiley & Sons.

Sun, Q., Li, Z., Li, S., Jiang, L., Wang, J., Wang, P., 2014a. Utilization of surfactant-stabilized foam for enhanced oil recovery by adding nanoparticles. Energy Fuels 28 (4), 2384–2394.

Sun, X., Liang, X., Wang, S., Lu, Y., 2014b. Experimental study on the rheology of CO2 viscoelastic surfactant foam fracturing fluid. J. Petrol. Sci. Eng. 119, 104–111.

Sun, Q., Li, Z., Wang, J., Li, S., Li, B., Jiang, L., Wang, H., Lu, Q., Zhang, C., Liu, W., 2015. Aqueous foam stabilized by partially hydrophobic nanoparticles in the presence of surfactant. Colloids Surf. A Physicochem. Eng. Asp. 471, 54–64.

Tran, T., Gonzalez Perdomo, M.E., Haghighi, M., Amrouch, K., 2022. Study of the synergistic effects between different surfactant types and silica nanoparticles on the stability of liquid foams at elevated temperature. Fuel 315.

Tran, T., Gonzalez Perdomo, M.E., Wilk, K., Kasza, P., Amrouch, K., 2020. Performance evaluation of synthetic and natural polymers in nitrogen foam-based fracturing fluids in the Cooper Basin, South Australia. The APPEA Journal 60 (1).

Verma, A., Chauhan, G., Baruah, P.P., Ojha, K., 2018. Morphology, rheology, and kinetics of nanosilica stabilized gelled foam fluid for hydraulic fracturing application. Ind. Eng. Chem. Res. 57 (40), 13449–13462.

Verma, A., Chauhan, G., Ojha, K., Padmanabhan, E., 2019. Characterization of nano-Fe2O3-stabilized polymer-free foam fracturing fluids for unconventional gas reservoirs. Energy Fuels 33 (11), 10570–10582.

Veyskarami, M., Ghazanfari, M.H., 2018. Synergistic effect of like and opposite charged nanoparticle and surfactant on foam stability and mobility in the absence and presence of hydrocarbon: a comparative study. J. Petrol. Sci. Eng. 166, 433–444.

Wang, L., Yao, B., Cha, M., Alqahtani, N.B., Patterson, T.W., Kneafsey, T.J., Miskimins, J. L., Yin, X., Wu, Y.-S., 2016. Waterless fracturing technologies for unconventional reservoirs-opportunities for liquid nitrogen. J. Nat. Gas Sci. Eng. 35, 160–174.

Wang, P., You, Q., Han, L., Deng, W., Liu, Y., Fang, J., Gao, M., Dai, C., 2018. Experimental study on the stabilization mechanisms of CO2 foams by hydrophilic silica nanoparticles. Energy Fuels 32 (3), 3709–3715.

Wang, W., Gu, B., Liang, L., 2005. Effect of surfactants on the formation, morphology, and surface property of synthesized SiO2 nanoparticles. J. Dispersion Sci. Technol. 25 (5), 593–601.

Wanniarachchi, W.A.M., Ranjith, P.G., Perera, M.S.A., 2017. Shale gas fracturing using foam-based fracturing fluid: a review. Environ. Earth Sci. 76 (2).

Wanniarachchi, W.A.M., Ranjith, P.G., Perera, M.S.A., Lashin, A., Al Arifi, N., Li, J.C., 2015. Current opinions on foam-based hydro-fracturing in deep geological reservoirs. Geomechanics and Geophysics for Geo-Energy and Geo-Resources 1 (3–4), 121–134.

Worthen, A.J., Bagaria, H.G., Chen, Y., Bryant, S.L., Huh, C., Johnston, K.P., 2013. Nanoparticle-stabilized carbon dioxide-in-water foams with fine texture. J. Colloid Interface Sci. 391, 142–151, 2013/02/01/.

Wu, Y., Fang, S., Zhang, K., Zhao, M., Jiao, B., Dai, C., 2018. Stability mechanism of nitrogen foam in porous media with silica nanoparticles modified by cationic surfactants. Langmuir 34 (27), 8015–8023. Jul 10.

Xiao, C., Balasubramanian, S.N., Clapp, L.W., 2017. Rheology of viscous CO2 foams stabilized by nanoparticles under high pressure. Ind. Eng. Chem. Res. 56 (29), 8340–8348.

Yang, K., Li, S., Zhang, K., Wang, Y., 2021. Synergy of hydrophilic nanoparticle and nonionic surfactant on stabilization of carbon dioxide-in-brine foams at elevated temperatures and extreme salinities. Fuel 288.

Yekeen, N., Padmanabhan, E., Idris, A.K., 2018. A review of recent advances in foam-based fracturing fluid application in unconventional reservoirs. J. Ind. Eng. Chem. 66, 45–71.

Yekeen, N., Padmanabhan, E., Idris, A.K., 2019a. Synergistic effects of nanoparticles and surfactants on n-decane-water interfacial tension and bulk foam stability at high temperature. J. Petrol. Sci. Eng. 179, 814–830, 2019/08/01/.

Yekeen, N., Padmanabhan, E., Idris, A.K., Chauhan, P.S., 2019b. Nanoparticles applications for hydraulic fracturing of unconventional reservoirs: a comprehensive review of recent advances and prospects. J. Petrol. Sci. Eng. 178, 41–73.

Yekeen, N., Padmanabhan, E., Idris, A.K., Ibad, S.M., 2019c. Surfactant adsorption behaviors onto shale from Malaysian formations: influence of silicon dioxide nanoparticles, surfactant type, temperature, salinity and shale lithology. J. Petrol. Sci. Eng. 179, 841–854.

Zhang, X., Sun, H., Zhao, H., Qin, Y., Wang, Q., Li, Y., 2020. Formation and stabilization of CO2 bubbles with different sizes and the interaction with solid particles. Colloids Surf. A Physicochem. Eng. Asp. 598.

Zhang, Y., Liu, Q., Ye, H., Yang, L., Luo, D., Peng, B., 2021. Nanoparticles as foam stabilizer: mechanism, control parameters and application in foam flooding for enhanced oil recovery. J. Petrol. Sci. Eng. 202.

Zhou, J., Ranjith, P.G., Wanniarachchi, W.A.M., 2020. Different strategies of foam stabilization in the use of foam as a fracturing fluid. Adv. Colloid Interface Sci. 276, 102104. Feb.

Zhu, J., Yang, Z., Li, X., Song, Z., Liu, Z., Xie, S., 2019. Settling behavior of the proppants in viscoelastic foams on the bubble scale. J. Petrol. Sci. Eng. 181.

Zhu, Y., Tian, J., Hou, Q., Luo, Y., Fan, J., 2017. Studies on nanoparticle-stabilized foam flooding EOR for a high temperature and high salinity reservoir. In: Abu Dhabi International Petroleum Exhibition & Conference. Day 4 Thu, November 16, 2017.

56

5. Simulation study of foam rheology and the effects on hydraulic fracture proppant placement

In this chapter, the fracture simulation modelling is performed on GOHFER software. The details of the software such as its application, advantages, limitations and step-by-step guide, are included in Appendix 9.1 and 9.2.

This paper represents a significant contribution to the field of hydraulic fracturing by studying the interplay between cationic and anionic surfactants in conjunction with silica nanoparticles (SNP) and their impact on fracturing performance, specifically at the demanding conditions of reservoir temperatures. The research explores critical aspects such as foam stability, rheology, proppant-carrying capacity, and fracture modelling simulation. Remarkably, the results demonstrate that cationic surfactants exhibit superior synergy with SNP, enhancing foam properties and ultimately improving fracture conductivity and gas production. This work underscores the interrelationship between fluid characteristics and fracture effectiveness and emphasizes the significance of proppant placement, providing valuable insights that can advance hydraulic fracturing practices in unconventional reservoirs.

Statement of Authorship

Title of Paper	Simulation study of foam rheology and the effects on hydraulic fracture proppant placement
Publication Status	☐ Published ☐ Accepted for Publication ☑ Submitted for Publication ☐ Unpublished and Unsubmitted work written in manuscript style
Publication Details	Tran, T, Nguyen, G, Gonzalez Perdomo, ME, Haghighi, M & Amrouch, K 2023, 'Laboratory investigation and modelling of foam rheology and the effects on hydraulic fracture proppant placement', submitted to Journal of Petroleum Science.

Principal Author

Name of Principal Author (Candidate)	Tuan Huynh Minh Tran		
Contribution to the Paper	Literature review, Data collection, Simulation model development, Result analysis and interpretation, Writing the manuscript		
Overall percentage (%)	60%		
Certification:	This paper reports on original research I conducted during the period of my Higher Degree by Research candidature and is not subject to any obligations or contractual agreements with a third party that would constrain its inclusion in this thesis. I am the primary author of this paper.		
Signature		Date	14/03/2023

Co-Author Contributions

By signing the Statement of Authorship, each author certifies that:

   i.   the candidate's stated contribution to the publication is accurate (as detailed above);

   ii. permission is granted for the candidate in include the publication in the thesis; and

   iii. the sum of all co-author contributions is equal to 100% less the candidate's stated contribution.

Name of Co-Author	Giang Hoang Nguyen		
Contribution to the Paper	Support in simulation work (10%)		
Signature		Date	16/03/2023

Name of Co-Author	Maria Gonzalez Perdomo		
Contribution to the Paper	Support in result analysis, Reviewing the manuscript (15%)		
Signature		Date	14/03/2023

Name of Co-Author	Manouchehr Haghighi		
Contribution to the Paper	Support in result analysis, Reviewing the manuscript (10%)		
Signature		Date	16/03/2023

Name of Co-Author	Khalid Amrouch		
Contribution to the Paper	Support in result analysis, Reviewing the manuscript (5%)		
Signature		Date	17/03/2023

Simulation Study of Foam Rheology and the Effects on Hydraulic Fracture Proppant Placement

Tuan Tran[1], Giang Hoang Nguyen[1], Maria Elena Gonzalez Perdomo[1], Manouchehr Haghighi[1], Khalid Amrouch[1,2]

[1] *Australian School of Petroleum and Energy Resources, University of Adelaide, South Australia 5000, Australia*

[2] *Geology & Sustainable Mining, University Mohammed VI Polytechnic, Lot-660, Benguerir 43150, Morocco*

Corresponding author: Tuan Tran (tuan.tran@adelaide.edu.au)

Keywords

Foam viscosity, hydraulic fracturing, proppant placement, simulation, nanoparticle, surfactant

ABSTRACT

Hydraulic fracture stimulation is one of the most effective methods to recover oil and gas from unconventional resources. In recent years, foam-based fracturing fluids have been increasingly studied to address the limitations of conventional slickwater such as high water and chemical consumption, environmental concerns, and high incompatibility with water-sensitive formations. Due to the gradual breakdown of liquid foams at reservoir conditions, the combination of silica nanoparticles (SNP) and surfactants has attracted a lot of attention to improve liquid foams' characteristics, including their stability, rheology, and proppant-carrying capacity. This paper investigates and compares the effects of cationic and anionic surfactants on the fracturing performance of SNP-stabilized foams at the reservoir temperature of 90°C. The experimental results of viscosity measurements were imported into a 3-D fracture propagation model to evaluate the effectiveness of fracturing foams in transporting and distributing proppants in the fracture system. At both ambient and elevated temperatures, cationic surfactant was experimentally found to have better synergistic effects with SNP than anionic surfactant in improving the apparent viscosity and proppant-carrying capacity of foams. The simulation results demonstrate that fracturing with cationic surfactant-SNP foam delivers greater performance with larger propped area by 4%, higher fracture conductivity by 9% and higher cumulative gas production by 13%, compared to the anionic surfactant-SNP foam. This research work not only helps validate the interrelationship between fluid viscosity, proppant settlement rate and fracture effectiveness, but also emphasizes the importance of proppant placement in enhancing fracture conductivity and well productivity.

1. INTRODUCTION

Liquid foams have been increasingly studied in multiple petroleum applications such as drilling, enhanced oil recovery, carbon sequestration and fracture stimulation (Li et al., 2014; Sherif et al., 2015; Farhadi et al., 2016; Verma et al., 2019; Wang and Elsworth, 2020; Føyen et al., 2020; Wilk-Zajdel et al., 2021; Lyu et al., 2021; Zhao et al., 2021; Du et al., 2022;). Since first introduced in the late 1970s (Fei et al., 2017; Yekeen et al., 2018), foam-based fracturing fluids have brought in many significant benefits, such as their low water and chemical consumption, fast clean-up, reduced formation damage and high compatibility with water-sensitive formations including shale gas reservoirs (Wanniarachchi et al., 2015; Wang et al., 2016; Verma et al., 2017; Tran et al., 2020; Abdelaal et al., 2021; Fu and Liu, 2021).

In recent years, several research works have been conducted to combine surfactants with nanoparticles (NP) as stabilising agents to enhance the stability and thermal resistance of foams (Singh and Mohanty, 2015; Bayat et al., 2016; Wu et al., 2018; Li et al., 2019; Yekeen et al., 2019; Harati et al., 2020). As NP adsorb on the bubble interface, they minimize the contact area between the fluids and increase the film strength and film elasticity. This significantly helps reduce gas diffusion, decrease liquid drainage, delay film thinning and directly improve the foam stability (Yekeen et al., 2017; Majeed et al., 2020). In addition, the adsorption of surfactant molecules on the SNP surface reduces the surface tension of the gas-liquid interface, which directly helps to generate and maintain stable foam bubbles (Langevin, 2000; Karakashev and Mane, 2003; Bournival et al., 2014). It has been found that ionic surfactants have greater synergy with silica nanoparticles (SNP) than non-ionic surfactants in enhancing foams' properties (Tran et al., 2022). Cationic and anionic surfactants have been commonly used with silica nanoparticles (SNP) to improve the stability of both EOR and fracturing foams (Cui et al., 2010; Maestro et al., 2012; Sun et al., 2014; Lv et al., 2015; Li et al., 2017; Xiao et al., 2017; Vatanparast et al., 2017; Kumar and Mandal, 2017; Verma et al., 2018; Veyskarami and Ghazanfari, 2018; Fu and Liu, 2020). Previous studies by Yekeen et al. (2019) and Tran et al. (2022) compared the effects of cationic and anionic surfactants on the stability of SNP dispersions and SNP-stabilized foams at high temperatures. As cationic surfactant molecules have an opposite electric charge with the SNP, they can form multi-adsorption layers on the SNP surface, leading to increased hydrophobization and aggregation among the SNP. As a result, the liquid foams stabilized by SNP and cationic surfactants were found to have lower drainage rate, and higher half-life but lower foamability than those stabilized by the SNP/anionic surfactant system (Tran et al., 2022).

Proppants, such as sand and ceramics, are mixed in fracturing fluids to maintain the fracture width and fracture conductivity after the treatment (Mader, 1989; Fink, 2013). Besides stability, the

rheological properties and proppant suspension capacity of fracturing fluids play essential roles in the success of the stimulation treatment. Fracturing fluids with low viscosity tend to have limited proppant-carrying capacity, which results in inadequate propped area and insufficient fracture conductivity. It is, therefore, critically important for fracturing fluids to have sufficient viscosity to effectively transport and place proppants in the fractures. The impacts of proppant distribution on the fracture dimension can be demonstrated in Figure 1, in which the evenly distributed proppants result in much greater fracture volume than the unevenly distributed ones.
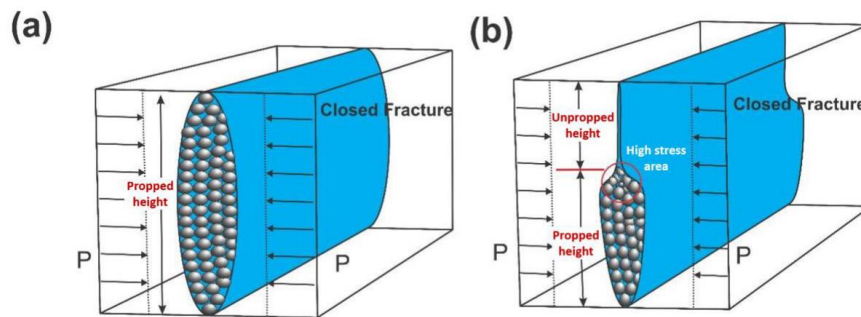

Figure 1: Schematic of fracture dimension with (a) evenly distributed proppants; (b) unevenly distributed proppants (reproduced from Fei et al., 2018)

In the current literature, although the stability and foamability of fracturing foams have received much attention, very few studies have been conducted to investigate the effects of different surfactant types on the rheological properties and proppant suspension capacity of SNP-stabilized fracturing foams, especially at elevated temperatures. Moreover, there has been a significant gap in the simulation of the performance of fracturing foams (Yekeen et al., 2018). The simulation outputs are believed to be an excellent source to validate the experimental results and to evaluate and compare the practical efficacy of the fracturing fluid systems. Due to the presented research gaps, this paper aims to investigate and compare the effects of cationic and anionic surfactants on the fracturing performance of SNP-stabilized foams at the reservoir temperature of 90°C. Two foam-based fracturing fluid cases were considered: cationic CTAB/SNP foam, anionic SDBS/SNP foam; and slickwater case was added as an industry benchmark for comparison. The fluid viscosity and proppant settling rate were first measured. Then, a rheological model was applied to characterise the fracturing fluids, followed by a 3-D fracture propagation simulation modelling. To evaluate and compare the fracturing performance of the fluid systems, the simulation metrics include the proppant distribution, fracture dimension, fracture conductivity and production prediction after the treatment.

3

2. RHEOLOGY & PROPPANT SUSPENSION EXPERIMENTS

2.1 Materials

Two different surfactant types were used as foaming agents in the experiments. The cationic surfactant was Hexadecyltrimethylammonium Bromide (CTAB, >98% purity) and the anionic surfactant was Sodium Dodecylbenzene Sulfonate (SDBS, >99% purity); both were obtained from Sigma Aldrich, Australia. The critical micelle concentrations (CMC) of the surfactants were provided by the supplier, which are 0.61 mM for SDBS and 0.92 mM for CTAB at 25°C. In addition, hydrophilic silica nanoparticles (SNP) in colloidal form were purchased from Sigma Aldrich with a concentration of 34 wt% suspensions in water. The SNP have an average diameter of 22 nm, a molecular weight of 60.08 g/mol and a surface area of 110 - 150 m^2/g. All the chemicals were used without further purification. All experiments used deionised distilled water with a resistivity of 18.2 mΩ as a base fluid.

2.2 Sample preparation

Deionized distilled water was first added with 0.05 wt% surfactant and stirred at a low speed of 50 RPM for 2 hours without interruption. After that, 1.0 wt% SNP were added to the mixture and stirred for another 2 hours. The surfactant-nanoparticle dispersion was then ultra-sonicated at a frequency of 40 Hz for 30 minutes to reach adsorption equilibrium. The dispersion appeared slightly hazy and was sealed for use in experiments. Finally, the prepared dispersion was stirred at 2000 RPM for 2 minutes to produce fine foams.

2.3 Apparent viscosity measurement

The apparent viscosity of SDBS/SNP and CTAB/SNP foams was measured by a SR5 Rheometer (Rheometric Scientific, USA). The measurements were conducted on a cup & bob geometry system with shear rates varying from 10 to 1000 s^{-1}. The testing temperature inside the rheometer is generated, measured and accurately controlled by an integrated heating system. The influence of surfactant type on the foam viscosity was studied at the temperature of 25°C and 90°C and atmospheric pressure.

2.4 Static proppant settling measurement

Sand proppants (20/40 mesh size) with a mass amount of 1 gram were evenly added to the foam column in the glass cylinder. The proppant settling velocity was then calculated by measuring the height of the initial foam column and the time taken for the proppants to settle on the bottom of the cylinder. The diameter of the measuring cylinder was more than 25 times larger than that of the proppants to minimize the effect of confining walls on the proppant-settling velocity (Goel et al., 2002).

4

2.5 Experimental results and discussions

2.5.1 Viscosity measurement

The rheology of the fracturing fluid plays an essential role in determining the success of the fracture stimulation treatment. Figure 2 shows the studied fracturing fluids' apparent viscosity at ambient and elevated temperatures. While the viscosity of the SDBS/SNP and CTAB/SNP foam were obtained from the rheometer measurement, the slickwater viscosity data was extracted from the related literature (Zhang & Chao, 2018). As observed in Figure 2, the fracturing foams had much higher apparent viscosity than the slickwater, and the highest viscosity was recorded in the cationic CTAB/SNP foam. In addition, the viscosity of foams and slickwater became lower at elevated temperatures and decreased gradually as the shear rates increased.
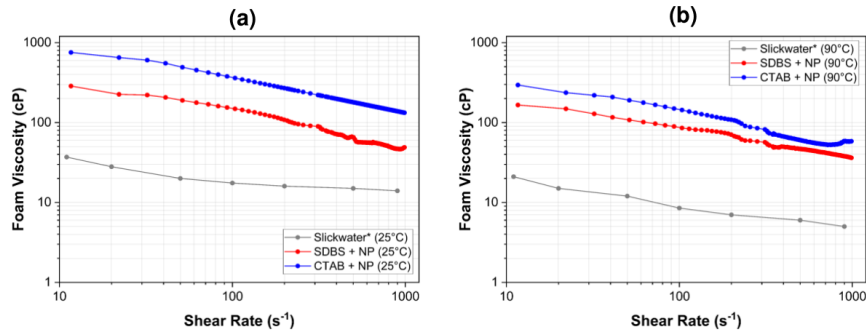
Figure 2: Apparent viscosity of foams and slickwater at (a) 25 °C and (b) 90 °C

Based on the log-log profile of apparent viscosity (μ_{app}) versus shear rate (γ) and the power law equation (Equation 1) (Barree, 1984), the rheological parameters of flow behavior index (n') and fluid consistency index (K') for each fluid were calculated and summarized in Table 1.

$$\mu_{app} = 47879K'\gamma^{(n'-1)} \tag{1}$$

Table 1: Rheological parameters of the fracturing fluids

Parameter	Flow Behavior Index (n') dimensionless	Fluid Consistency Index (K') $\left(\dfrac{lb.\,s}{ft^2}\right)$
Slickwater	0.8820	0.0044
SDBS/SNP foam (90 °C)	0.6305	0.0098
CTAB/SNP foam (90 °C)	0.5565	0.0216

Generally, foam fluids can be classified into 3 main groups based on the flow behaviour index (n'). If 0 < n' < 1, the fluid shows pseudo-plastic or shear thinning behaviour, in which the fluid viscosity decreases with increasing shear rates. On the other hand, if n' > 1, the fluid shows dilatant or shear-thickening behaviour, in which the fluid viscosity increases with increasing shear rates. Lastly, if n' = 1, the fluid has Newtonian behaviour, in which the fluid viscosity is independent of the shear rate change. According to Figure 2 and Table 1, it can be confirmed that all three studied fracturing fluids have shear-thinning behaviour.

The viscosity measurement data and the n' & K' parameters at 90 °C were then imported into the GOHFER database. More details of the rheological characterization process are presented in Section 3.2.

2.5.2   Proppant suspension

The settlement rate of proppants in the fractures is critical to the fracture dimension and conductivity. If the proppants settle too quickly, they tend to accumulate near the wellbore, resulting in limited fracture dimension and even formation damage. Otherwise, at a low settling velocity, proppants are more likely to be further transported and uniformly distributed inside the fractures, helping enhance the fracture area and increase the overall conductivity.

Figure 3 shows the proppant suspension capacity in foams at 25 °C and 90 °C. At the ambient condition, the 20/40-mesh proppants had a settling rate of 0.024 cm/s and 0.0685 mm/s in CTAB/SNP and SDBS/SNP foams, respectively. The velocity difference can be explained by the Stokes' Law theory, in which the settling velocity of proppants is greatly dependent and inversely proportional to the viscosity of the medium fluid (Stokes, 1851). In other words, the fluids with higher viscosity tend to have a better capability of suspending and transporting the proppants.

As the temperature increased to 90 °C, the proppants settled faster at above 0.09 cm/s in both studied foams. The settling velocity of proppants in the anionic SDBS/SNP foam was much less sensitive to the temperature change than the cationic CTAB/SNP foam. Related observation can be seen in the viscosity results (Figure 2), indicating the high thermal resistance of the SDBS/SNP foam.

The proppant suspension capacity of slickwater was collected from previous literature for comparison purposes. Similar experiments have been conducted by Zhang et al. (2016) to measure the settling velocity of proppants in slickwater with several different proppant sizes. At the comparable elevated temperature, the 20/40-mesh proppants in slickwater were found to have a settling velocity of 1.8 - 3.0 mm/s, which is 20 – 30 times higher than the foam-based fracturing fluids in our study. Because of this, slickwater is expected to have lower proppant suspension capacity and

6

65

result in lower fracture performance than liquid foams. Simulation outputs, including the fracture dimension, fracture conductivity and gas production, are compared among the three fluid systems and presented in the next section to validate the prediction.
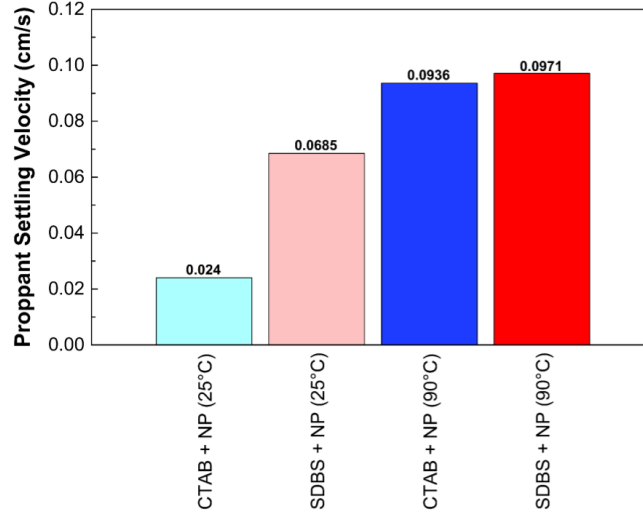
Figure 3: Proppant settling velocity in foams at 25 °C and 90 °C

3. HYDRAULIC FRACTURING SIMULATION

Several simulations were performed on a numerical simulator (GOHFER) developed by Barree (1983) to evaluate the practical performance of the fracturing fluids. The simulator can predict three-dimensional fracture geometry during propagation as a function of time. In addition, the fluid and solid transport models are fully coupled in the simulator.

The GOHFER simulator by Barree (1983) eliminates some simplified assumptions from previous models and incorporates the calculation of the fracture width. Fracture width (w) is assumed to be twice the fracture surface displacement (u), which is calculated from Poisson's ratio (v), Young Modulus (E) (Equation 2).

$$w = 2u = 2 \iint \left(\frac{1 - v^2}{\pi E} \right) P_e \, d\Psi \, dS \qquad (2)$$

Effective pressure (P_e) is the distributed load at the radial deflection distance (S) and angle (Ψ). The fluid pressure determines the effective pressure in fracture (P_f), the least principal earth stress (σ) and the pore pressure in rocks (P_P) (Equation 3). The fluid pressure in fracture (P_f) is related to

7

the apparent fluid viscosity and the volumetric flow rate in fracture, which is determined by the material balance equation (Barree, 1984).

$$P_e = P_f - \sigma - P_P \qquad (3)$$

3.1 Simulation inputs and outputs

The fracture simulations were carried out on a typical tight gas reservoir model. First, the well logs, diagnostic fracture injection test (DFIT) results, reservoir properties and the perforation design were imported into the simulator. The well log data includes the measures of depth, porosity, gamma ray, bulk density, resistivity, sonic waves, and caliper logs. Figure 4 shows the DFIT results, which are used to determine the geomechanical parameters such as the breakdown pressure, shut-in pressure, and closure pressure, as well as the average permeability of the reservoir. After that, a single perforation interval was added to the model. The details of the perforation design and reservoir properties are included in Table 2.

Finally, the fracture treatment design was added to the simulator. Three different fracturing fluids were investigated, which are the SDBS/SNP foam, CTAB/SNP foam and the slickwater. Table 3 demonstrates the treatment stages and parameters used in the study. The injection rate was set fixed at 30 bbl/min. In order to assess the fracturing performance among the fluid systems, the key comparison metrics used are the simulation outputs of the fracture dimension, fracture conductivity, proppant distribution and the post-frac gas production forecast.
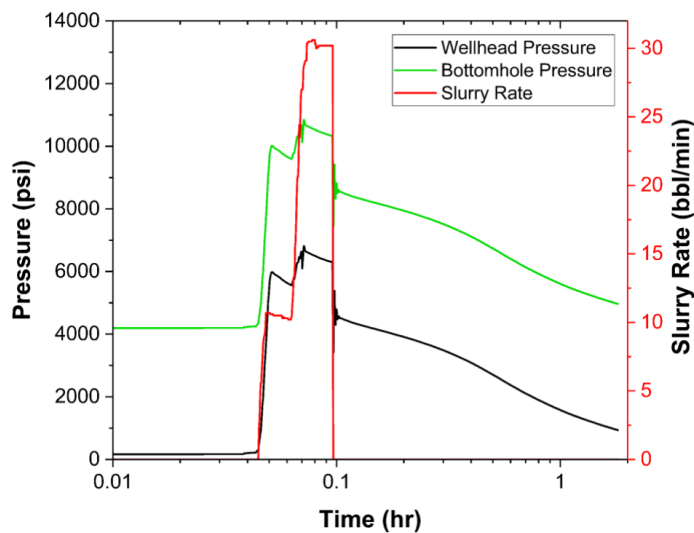
Figure 4: Diagnostic Fracture Injection Test (DFIT) data

8

67

Table 2: Input data for reservoir properties and perforation design

Parameters	Value
Reservoir Properties	
Reservoir depth	9,410 ft
Reservoir pressure	4,339 psi
Reservoir temperature	200 °F (93 °C)
Average reservoir porosity	11%
Gas saturation	65%
Water saturation (%)	35%
Perforation Design	
Perforation interval	9,400 – 9,420 ft
Number of shots	30
Perforation phasing	60°
Perforation diameter	0.4 inch
DFIT Analysis	
Breakdown pressure	10,942 psi
Instantaneous shut-in pressure	8,726 psi
Fracture closure pressure	6,818 psi
Average reservoir permeability	0.06 mD

Table 3: Input data for fracturing treatment

Stage	Fluid Type	Clean stage volume (gal)	Proppant amount (lb)	Proppant type	Injection rate (bbl/m)
1	Pad fluid	15,000	0	None	30
2	SDBS/SNP foam, CTAB/SNP foam, Slickwater	10,000	10,000	Ceramic Sand 20/40	30
3		8,000	24,000	Ceramic Sand 20/40	30
4		6,000	30,000	Ceramic Sand 20/40	30
5		4,000	28,000	Ceramic Sand 20/40	30
6	Flush fluid	3,000	0	None	30
	Total	**46,000**	**92,000**		

3.2 Rheological characterization

Before performing the simulations, the experimental viscosity results of the studied foams and slickwater were imported into the fluid database of GOHFER. A Carreau rheological model was used to characterize the properties of the fluids (Equations 4 & 5). Four fluid parameters are required in the Carreau model, which are the power law exponent (n'), fluid consistency index (K'), zero-shear fluid viscosity (μ_0) and the high-shear viscosity (μ_∞) (Halliburton, 2019). Most of these parameters can be obtained from the laboratory plot of viscosity versus shear rate, which is demonstrated in Figure 2.

$$\mu_{app} = \mu_\infty + \frac{s_f \mu_0 - \mu_\infty}{\left(1 + \left(\frac{s_f \gamma}{\gamma_l}\right)^2\right)^{\frac{1-n'}{2}}} \tag{4}$$

$$\gamma_l = \left(\frac{\mu_0 K'}{47879}\right)^{\left(\frac{1}{n'-1}\right)} \tag{5}$$

where s_f is the sand factor, γ is the shear rate, and γ_l is the low shear transition.

3.3 Simulation results and discussions

3.3.1 Proppant distribution and fracture dimension

Figure 5 shows the simulation results of the proppant distribution from the three fracturing fluid cases: slickwater, SDBS/SNP foam, and CTAB/SNP foam. The simulation results show that the fracture generated by slickwater stimulation has a much smaller propped area than those generated by foam stimulation. Moreover, in the slickwater case, very high concentrations of proppants accumulate at the bottom of the fracture, indicating limited transportation and ineffective placement of proppants in the fracture. This behaviour is mainly due to the low viscosity and high leak-off rate of slickwater, both of which promote early and rapid proppant settlement at the near-wellbore region.

On the other hand, foam-based fracturing fluids result in larger propped areas with the fracture length extension and the fracture height growth. In contrast to the slickwater, liquid foams generate very uniform and homogenous proppant distributions, which can be attributed to the superior rheological properties of the nanoparticle-surfactant-stabilized foams. As the SDBS/SNP and CTAB/SNP foams have high viscosity characteristics and rigid bubble structures strengthened by nanoparticle layers, they tend to effectively suspend proppants in their bubble networks, thereby delaying the proppant settlement. According to Zhu et al. (2019), when settling through foams, proppants are exerted by two uplift forces: the drag force from the bulk foam movement and the elastic force from the foam compressibility and lamella movement. These forces are essential to

counter the gravitational force and resist the downward trend of the proppants (Jing et al., 2016). As a result, in the foam fracturing cases, proppants are effectively transported and uniformly placed towards the fracture tips, helping to enhance the fracture dimension and conductivity.
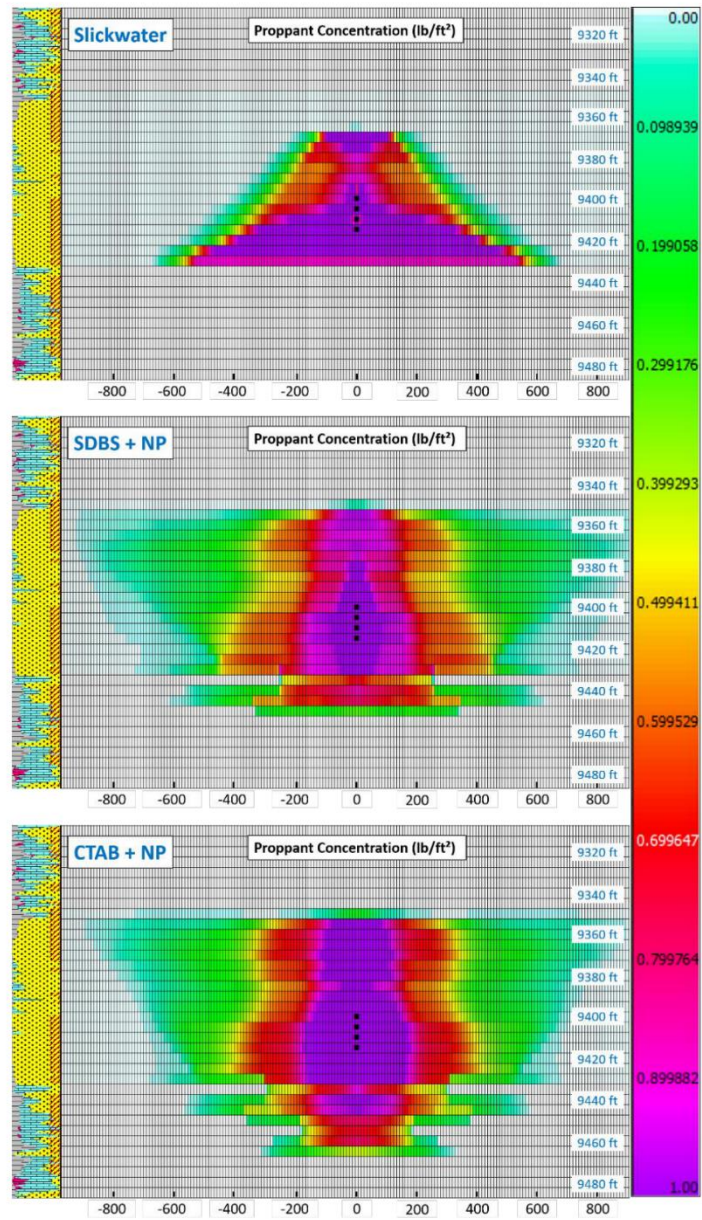

Figure 5: Concentration and distribution of proppants in fractures using slickwater and liquid foams

The predicted fracture geometries of the SDBS/SNP and CTAB/SNP foams appear nearly identical in Figure 5. A quantitative measure, therefore, is required to evaluate the fracturing performance of the three fluid systems. Table 4 summarizes the fracture dimensions, average fracture conductivity and cumulative fluid lost for each simulation scenario.

As expected from the proppant distribution results, the fracture created by slickwater has the smallest dimensions out of the three simulation cases. While the anionic SDBS/SNP foam results in the longest fracture half-length, the cationic CTAB/SNP foam achieves the largest propped area due to its outstanding fracture height and average width. The estimated propped area of the CTAB/SNP case is 350,400 ft^2, which is 87% higher than the slickwater case and 4% higher than the SDBS/SNP case. Furthermore, the cumulative fluid loss is recorded as lowest in the CTAB/SNP stimulation and highest in the slickwater fracturing. There seems to be a strong correlation between the fluid viscosity, its leak-off rate, and the resulting fracture dimension. It is demonstrated that fracturing fluids with higher viscosity tend to have a lower leak-off rate and produce greater height and openness for the fractures, and vice versa.

Besides the fracture dimensions, fracture conductivity is another critical parameter to evaluate fracturing performance. Based on the summary results in Table 4, the fracture conductivity of the cationic CTAB/SNP case is 62.7 mD.ft, which is 9% higher than that of the anionic SDBS/SNP case. On the other hand, slickwater has the highest average fracture conductivity of 109.3 mD.ft. However, this high value is caused by the poor proppant transportation of the slickwater, leading to the excessive accumulation of proppants at the bottom of the fracture. Consequently, an undesirable fracture pathway with great length and very high conductivity is created, which acts as an outlier to increase the conductivity average of the whole propped area. An analogous observation can be found in Fei et al. (2017), in which the least stable foam generated the highest fracture conductivity due to the high accumulation of proppants in the near wellbore area. Therefore, it is essential to note that the interpretation of the fracture conductivity results alone might be misleading and not reflect the situation accurately. Instead, a comprehensive evaluation of the fracture dimensions, fracture conductivity and the leak-off behaviour is strongly required when evaluating the stimulation performance of a fracturing fluid.

Parameter	Unit	Slickwater	SDBS/SNP foam	CTAB/SNP foam
Fracture height	ft	70	105	120
Fracture length	ft	670	800	730
Average fracture width	inch	0.310	0.319	0.324
Propped area	ft^2	187,600	336,000	336,000
Cumulative fluid loss	gal	1198	997	961
Fracture conductivity	mD.ft	109.3	336,000	336,000

3.3.2 Gas production after treatment

To demonstrate the impacts of the resulting fracture dimension and conductivity on productivity, simulations were conducted to predict production at the stimulated well. In GOHFER software, the average proppant concentration over the net pay, the closure stress, pore pressure, and reservoir properties are used to calculate the formation's effective conductivity and deliverability. A transient production model is then applied to estimate the gas flow rate at a given time.

Figure 6 shows the cumulative gas production of the three studied cases over the first five years after the treatments. The slickwater case has the lowest productivity, with a total gas production of 136 MMscf. On the other hand, the CTAB/SNP foam achieves the highest cumulative gas production of 238 MMscf, which is 13% higher than the SDBS/SNP foam case. Furthermore, Figure 7 shows the total recoverable gas production before the economic limit is reached. Over the life span of the well, the anionic SDBS/SNP and cationic CTAB/SNP foam stimulations can recover up to 2.05 and 2.24 Bscf of gas volume, compared to only 0.84 Bscf from the slickwater fracturing.

It is evident that foam-based fracturing fluids can provide greater access and extract more gas volume from the reservoir than slickwater. The excellent productivity results of the foam stimulation are attributed to the large propped area and the uniform distribution of proppants in the fractures, both of which are caused by the high viscosity and the effective proppant-carrying characteristics of the liquid foams. Nevertheless, it is important to emphasise that the performance of the fracturing fluid heavily depends on the reservoir properties. By generating significant fracture height growth and having slow settlement of proppants, foam-based fracturing fluids have huge advantages to expand the propped area and enhance the field productivity, especially on the studied reservoir with thick net pay and low permeability. However, in some other cases, foam fracturing might not be a good stimulation option as the excessive fracture height growth can cause negative consequences to the structure confinement, seal rocks and the water aquifer. In addition, Fei et al. (2018) reported that

13

foam stimulation does not prevent proppant settlement in a high permeability reservoir due to the rapid closure of the fractures.
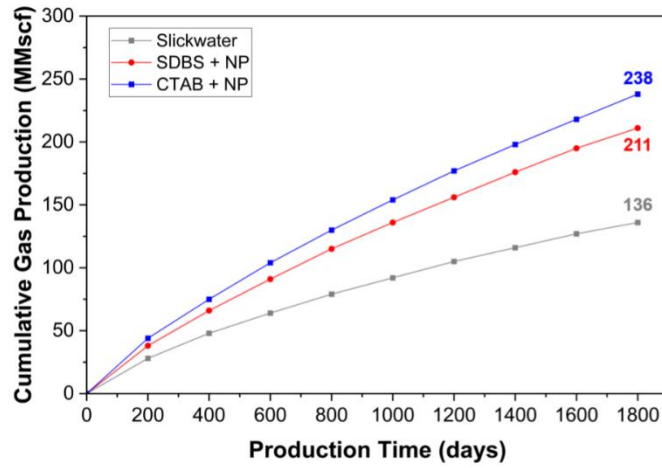

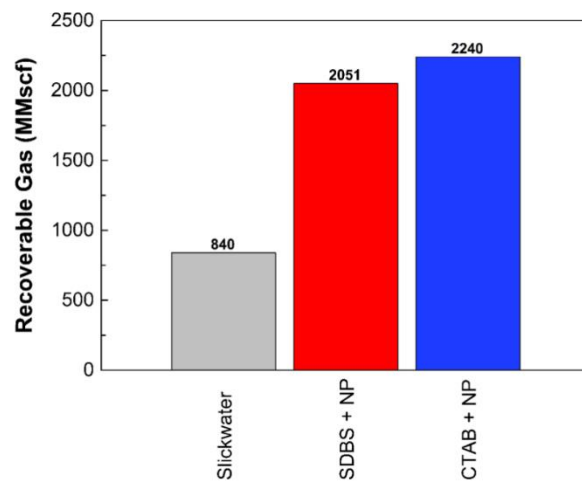*Figure 6: Cumulative gas production in the first 5-year period*

Figure 7: Total recoverable gas over the life span of the well

4 CONCLUSIONS

This paper aims to investigate the relationship between the foams' rheological and proppant suspension properties and their fracturing performance at elevated reservoir temperatures. Through the experimental and simulation results, the effectiveness and practicality of the nanoparticle-surfactant-stabilized fracturing foams have been highlighted. The key conclusions can be summarized as follows:

1. At both ambient and elevated temperatures, SNP have stronger synergy with cationic CTAB surfactant than anionic SDBS surfactant in enhancing liquid foams' rheological and proppant suspension properties. Because of this, CTAB/SNP foam was observed to provide larger propped area, lower leak-off rate, and higher fracture conductivity than the SDBS/SNP foam.

2. SNP-surfactant-stabilized foams have significantly higher apparent viscosity and proppant-carrying capacity than the benchmark slickwater. Simulation results suggest the tremendous impact of foam-based fracturing fluids on delaying proppant settlement and generating uniform distributions of proppants in the fractures.

3. The productivity of the stimulated well is controlled by the combination of the fracture dimension and the fracture conductivity. High fracture conductivity itself does not necessarily guarantee high productivity.

4. In the given tight gas reservoir model, the highest gas production is achieved by fracturing with CTAB/SNP foam, followed by SDBS/SNP foam, and then the slickwater.

5 DECLARATION OF COMPETING INTEREST

The authors declared that they have no known competing interest in this work.

6 CREDIT AUTHORSHIP CONTRIBUTION STATEMENT

Tuan Tran: Investigation, Methodology, Data curation, Formal analysis, Writing – original draft. **Giang Hoang Nguyen:** Simulation, Formal Analysis. **M.E Gonzalez Perdomo**: Conceptualization, Supervision, Writing – review & editing, Validation, Resources. **Manouchehr Haghighi**: Conceptualization, Supervision, Writing – review & editing, Validation, Resources. **Khalid Amrouch**: Supervision, Conceptualization.

7 ACKNOWLEDGEMENTS

8 REFERENCES

Abdelaal, A, Aljawad, MS, Alyousef, Z & Almajid, MM 2021, 'A review of foam-based fracturing fluids applications: From lab studies to field implementations', *Journal of Natural Gas Science and Engineering*, vol. 95.

Barree, RD 1983, 'A Practical Numerical Simulator for Three-Dimensional Fracture Propagation in Heterogeneous Media', *SPE Reservoir Simulation Symposium*, San Francisco, California, November 1983.

Barree, RD 1984, *Development of a numerical simulator for three-dimensional hydraulic fracture propagation in heterogeneous media*, Colorado School of Mines, Colorado, USA.

Bayat, AE, Rajaei, K & Junin, R 2016, 'Assessing the effects of nanoparticle type and concentration on the stability of CO 2 foams and the performance in enhanced oil recovery', *Colloids and Surfaces A: Physicochemical and Engineering Aspects*, vol. 511, pp. 222-231.

Bournival, G, Du, Z, Ata, S & Jameson, GJ 2014, 'Foaming and gas dispersion properties of non-ionic surfactants in the presence of an inorganic electrolyte', *Chemical Engineering Science*, vol. 116, pp. 536-546.

Cui, ZG, Cui, YZ, Cui, CF, Chen, Z & Binks, BP 2010, 'Aqueous foams stabilized by in situ surface activation of CaCO3 nanoparticles via adsorption of anionic surfactant', *Langmuir*, vol. 26, no. 15, pp. 12567-12574.

Du, L, Lu, T & Li, B 2022, 'CO2 capture and sequestration in porous media with SiO2 aerogel nanoparticle-stabilized foams', *Fuel*, vol. 324.

Farhadi, H, Riahi, S, Ayatollahi, S & Ahmadi, H 2016, 'Experimental study of nanoparticle-surfactant-stabilized CO2 foam: Stability and mobility control', *Chemical Engineering Research and Design*, vol. 111, pp. 449-460.

Fei, Y, Johnson, RL, Gonzalez, M, Haghighi, M & Pokalai, K 2018, 'Experimental and numerical investigation into nano-stabilized foams in low permeability reservoir hydraulic fracturing applications', *Fuel*, vol. 213, pp. 133-143.

16

75

Fei, Y, Pokalai, K, Johnson, R, Gonzalez, R & Haghighi, M 2017, 'Experimental and simulation study of foam stability and the effects on hydraulic fracture proppant placement', *Journal of Natural Gas Science and Engineering*, vol. 46, pp. 544-554.

Fink, JK 2013, Hydraulic Fracturing Chemicals and Fluids Technology, *Gulf Professional Publishing*.

Føyen, T, Brattekås, B, Fernø, MA, Barrabino, A & Holt, T 2020, 'Increased CO2 storage capacity using CO2-foam', *International Journal of Greenhouse Gas Control*, vol. 96.

Fu, C & Liu, N 2020, 'Study of the Synergistic Effect of the Nanoparticle-Surfactant-Polymer System on CO2 Foam Apparent Viscosity and Stability at High Pressure and Temperature', *Energy & Fuels*, vol. 34, no. 11, pp. 13707-13716.

Fu, C & Liu, N 2021, 'Rheology and stability of nanoparticle-stabilized CO2 foam under reservoir conditions', *Journal of Petroleum Science and Engineering*, vol. 196.

Goel, N, Shad, S & Grady, B 2002, 'Correlating viscoelastic measurements of fracturing fluid to particles suspension and solids transport', *Journal of Petroleum Science and Engineering*, vol. 35, pp. 59-81.

Halliburton 2019, 'GOHFER 3D User Manual', Halliburton, Texas, USA.

Harati, S, Esfandyari Bayat, A & Sarvestani, MT 2020, 'Assessing the effects of different gas types on stability of SiO2 nanoparticle foam for enhanced oil recovery purpose', *Journal of Molecular Liquids*, vol. 313.

Jing, Z, Wang, S & Wang, Z 2016, 'Detailed Structural and Mechanical Response of Wet Foam to the Settling Particle', *Langmuir*, vol. 32, no. 10, pp. 2419-2427.

Karakashev, SI & Manev, ED 2003, 'Correlation in the properties of aqueous single films and foam containing a nonionic surfactant and organic/inorganic electrolytes', *Journal of Colloid and Interface Science*, vol. 259, no. 1, pp. 171-179.

Kumar, S & Mandal, A 2017, 'Investigation on stabilization of CO 2 foam by ionic and nonionic surfactants in presence of different additives for application in enhanced oil recovery', *Applied Surface Science*, vol. 420, pp. 9-20.

Langevin, D 2000, 'Influence of interfacial rheology on foam and emulsion properties', *Advances in Colloid and Interface Science*, vol. 88, pp. 209-222.

Li, J, Pan, R, Guo, B & Shan, J 2014, 'Thermal stability of brine foams for shale gas drilling', *Journal of Natural Gas Science and Engineering*, vol. 17, pp. 131-135.

17

Li, S, Qiao, C, Li, Z & Wanambwa, S 2017, 'Properties of Carbon Dioxide Foam Stabilized by Hydrophilic Nanoparticles and Hexadecyltrimethylammonium Bromide', *Energy & Fuels*, vol. 31, no. 2, pp. 1478-1488.

Li, S, Yang, K, Li, Z, Zhang, K & Jia, N 2019, 'Properties of CO2 Foam Stabilized by Hydrophilic Nanoparticles and Nonionic Surfactants', *Energy & Fuels*, vol. 33, no. 6, pp. 5043-5054.

Lv, Q, Li, Z, Li, B, Li, S & Sun, Q 2015, 'Study of Nanoparticle–Surfactant-Stabilized Foam as a Fracturing Fluid', *Industrial & Engineering Chemistry Research*, vol. 54, no. 38, pp. 9468-9477.

Lyu, X, Voskov, D & Rossen, W 2021, 'Numerical investigations of foam-assisted CO2 storage in saline aquifers', *International Journal of Greenhouse Gas Control*, vol. 108.

Mader, D 1989, Hydraulic Proppant Fracturing and Gravel Packing, 1st edn, *Elsevier Science*.

Maestro, A, Guzmán, E, Santini, E, Ravera, F, Liggieri, L, Ortega, F & Rubio, RG 2012, 'Wettability of silicananoparticle–surfactant nanocomposite interfacial layers', *Soft Matter*, vol. 8, no. 3, pp. 837-843.

Majeed, T, Sølling, TI & Kamal, MS 2020, 'Foamstability: The interplay between salt-, surfactant- and critical micelle concentration', *Journal of Petroleum Science and Engineering*, vol. 187.

Sherif, T, Ahmed, R, Shah, S & Amani, M 2015, 'Rheological behavior of oil-based drilling foams', *Journal of Natural Gas Science and Engineering*, vol. 26, pp. 873-882.

Singh, R & Mohanty, KK 2015, 'Synergy between Nanoparticles and Surfactants in Stabilizing Foams for Oil Recovery', *Energy & Fuels*, vol. 29, no. 2, pp. 467-479.

Stokes, GG 1851, 'On the Effect of the Internal Friction of Fluids on the Motion of Pendulums', *Transactions of the Cambridge Philosophical Society*, vol. 9, pp. 8-106.

Sun, Q, Li, Z, Li, S, Jiang, L, Wang, J & Wang, P 2014, 'Utilization of Surfactant-Stabilized Foam for Enhanced Oil Recovery by Adding Nanoparticles', *Energy & Fuels*, vol. 28, no. 4, pp. 2384-2394.

Tran, T, Gonzalez Perdomo, ME, Haghighi, M & Amrouch, K 2022, 'Study of the synergistic effects between different surfactant types and silica nanoparticles on the stability of liquid foams at elevated temperature', *Fuel*, vol. 315.

Tran, T, Gonzalez Perdomo, ME, Wilk, K, Kasza, P & Amrouch, K 2020, 'Performance evaluation of synthetic and natural polymers in nitrogen foam-based fracturing fluids in the Cooper Basin, South Australia', *The APPEA Journal*, vol. 60, no. 1.

Vatanparast, H, Samiee, A, Bahramian, A & Javadi, A 2017, 'Surface behavior of hydrophilic silica nanoparticle-SDS surfactant solutions: I. Effect of nanoparticle concentration on foamability and foam stability', *Colloids and Surfaces A: Physicochemical and Engineering Aspects*, vol. 513, pp. 430-441.

Verma, A, Chauhan, G & Ojha, K 2017, 'Synergistic effects of polymer and bentonite clay on rheology and thermal stability of foam fluid developed for hydraulic fracturing', *Asia-Pacific Journal of Chemical Engineering*, vol. 12, pp. 872-883.

Verma, A, Chauhan, G, Baruah, PP & Ojha, K 2018, 'Morphology, Rheology, and Kinetics of Nanosilica Stabilized Gelled Foam Fluid for Hydraulic Fracturing Application', *Industrial & Engineering Chemistry Research*, vol. 57, no. 40, pp. 13449-13462.

Verma, A, Chauhan, G, Ojha, K & Padmanabhan, E 2019, 'Characterization of Nano-Fe2O3-Stabilized Polymer-Free Foam Fracturing Fluids for Unconventional Gas Reservoirs', *Energy & Fuels*, vol. 33, no. 11, pp. 10570-10582.

Veyskarami, M & Ghazanfari, MH 2018, 'Synergistic effect of like and opposite charged nanoparticle and surfactant on foam stability and mobility in the absence and presence of hydrocarbon: A comparative study', *Journal of Petroleum Science and Engineering*, vol. 166, pp. 433-444.

Wang, J & Elsworth, D 2020, 'Fracture penetration and proppant transport in gas- and foam-fracturing', *Journal of Natural Gas Science and Engineering*, vol. 77.

Wang, L, Yao, B, Cha, M, Alqahtani, NB, Patterson, TW, Kneafsey, TJ, Miskimins, JL, Yin, X & Wu, Y-S 2016, 'Waterless fracturing technologies for unconventional reservoirs-opportunities for liquid nitrogen', *Journal of Natural Gas Science and Engineering*, vol. 35, pp. 160-174.

Wanniarachchi, WAM, Ranjith, PG, Perera, MSA, Lashin, A, Al Arifi, N & Li, JC 2015, 'Current opinions on foam-based hydro-fracturing in deep geological reservoirs', *Geomechanics and Geophysics for Geo-Energy and Geo-Resources,* vol. 1, no. 3-4, pp. 121-134.

Wilk-Zajdel, K, Kasza, P & Maslowski, M 2021, 'Laboratory testing of fracture conductivity damage by foam-based fracturing fluids in low permeability tight gas formations', *Energies*, vol. 14.

Wu, Y, Fang, S, Zhang, K, Zhao, M, Jiao, B & Dai, C 2018, 'Stability Mechanism of Nitrogen Foam in Porous Media with Silica Nanoparticles Modified by Cationic Surfactants', *Langmuir*, vol. 34, no. 27, pp. 8015-8023.

Xiao, C, Balasubramanian, SN & Clapp, LW 2017, 'Rheology of Viscous CO2 Foams Stabilized by Nanoparticles under High Pressure', *Industrial & Engineering Chemistry Research*, vol. 56, no. 29, pp. 8340-8348.

Yekeen, N, Manan, MA, Idris, AK & Samin, AM 2017, 'Influence of surfactant and electrolyte concentrations on surfactant adsorption and foaming characteristics', *Journal of Petroleum Science and Engineering*, vol. 149, pp. 612-622.

Yekeen, N, Padmanabhan, E & Idris, AK 2018, 'A review of recent advances in foam-based fracturing fluid application in unconventional reservoirs', *Journal of Industrial and Engineering Chemistry*, vol. 66, pp. 45-71.

Yekeen, N, Padmanabhan, E & Idris, AK 2019, 'Synergistic effects of nanoparticles and surfactants on n-decane-water interfacial tension and bulk foam stability at high temperature', *Journal of Petroleum Science and Engineering*, vol. 179, pp. 814-830.

Zhang, G & Chao, K 2018, 'Downward flow of proppant slurry through curving pipes during horizontal well fracturing', *Oil & Gas Science and Technology*, vol. 73.

Zhang, G, Li, M, Geng, K, Han, R, Xie, M & Liao, K 2016, 'New integrated model of the settling velocity of proppants falling in viscoelastic slick-water fracturing fluids', *Journal of Natural Gas Science and Engineering*, vol. 33, pp. 518-526.

Zhao, J, Torabi, F & Yang, J 2021, 'The synergistic role of silica nanoparticle and anionic surfactant on the static and dynamic CO2 foam stability for enhanced heavy oil recovery: An experimental study', *Fuel*, vol. 287.

Zhu, J, Yang, Z, Li, X, Song, Z, Liu, Z & Xie, S 2019, 'Settling behavior of the proppants in viscoelastic foams on the bubble scale', *Journal of Petroleum Science and Engineering*, vol. 181.

6. Experimental study of the effects of salinity on nanoparticle-surfactant foams for fracture stimulation application

The application of foam-based fracturing fluids is considerably sensitive to salinity, a factor that can greatly affect foam stability and efficiency. This paper investigates the relationship between salinity and the properties of silica nanoparticle (SNP)-surfactant-stabilized foams, crucial for hydraulic fracturing operations. The research provides critical insights into how increased salt concentrations impact foam stability, rheology and proppant suspension. Notably, the findings highlight the limitations of foams at high salinity levels, a critical consideration when dealing with reservoir brines and recycled water as base fluids for foam generation. This study enhances our understanding of foam behavior and compatibility and lays the foundation for developing practical guidelines to fight off the challenges of high-salinity reservoir conditions. As hydraulic fracturing continues to be a pivotal technology in the energy industry, the knowledge gained from this research can significantly advance its practices under even the harshest reservoir conditions.

Statement of Authorship

Title of Paper	Experimental study of the effects of salinity on nanoparticle-surfactant foams for fracture stimulation application
Publication Status	☑ Published ☐ Accepted for Publication ☐ Submitted for Publication ☐ Unpublished and Unsubmitted work written in manuscript style
Publication Details	Tran, T, Gonzalez Perdomo, ME, Haghighi, M & Amrouch, K 2023, 'Experimental study of the effects of salinity on nanoparticle-surfactant foams for fracture stimulation application', Journal of Gas Science and Engineering, vol. 115.

Principal Author

Name of Principal Author (Candidate)	Tuan Huynh Minh Tran		
Contribution to the Paper	Literature review, Data collection, Result analysis and interpretation, Writing the manuscript		
Overall percentage (%)	70%		
Certification:	This paper reports on original research I conducted during the period of my Higher Degree by Research candidature and is not subject to any obligations or contractual agreements with a third party that would constrain its inclusion in this thesis. I am the primary author of this paper.		
Signature		Date	14/03/2023

Co-Author Contributions

By signing the Statement of Authorship, each author certifies that:

    i.   the candidate's stated contribution to the publication is accurate (as detailed above);

    ii.   permission is granted for the candidate in include the publication in the thesis; and

    iii.   the sum of all co-author contributions is equal to 100% less the candidate's stated contribution.

Name of Co-Author	Maria Gonzalez Perdomo		
Contribution to the Paper	Support in result analysis, Reviewing the manuscript (15%)		
Signature		Date	14/03/2023

Name of Co-Author	Manouchehr Haghighi		
Contribution to the Paper	Support in result analysis, Reviewing the manuscript (10%)		
Signature		Date	16/03/2023

81

Name of Co-Author	Khalid Amrouch		
Contribution to the Paper	Support in result analysis, Reviewing the manuscript (5%)		
Signature		Date	17/03/2023

Experimental study of the effects of salinity on nanoparticle-surfactant foams for fracture stimulation application

Tuan Tran [a,*], Maria Elena Gonzalez Perdomo [a], Manouchehr Haghighi [a], Khalid Amrouch [a,b]

[a] *Australian School of Petroleum and Energy Resources, University of Adelaide, South Australia, 5000, Australia*
[b] *Geology & Sustainable Mining, University Mohammed VI Polytechnic, Lot-660, Benguerir, 43150, Morocco*

ABSTRACT

Liquid foams have been increasingly studied and used in hydraulic fracturing application to develop unconventional resources. In recent years, silica nanoparticles (SNP) have been commonly applied to improve foams' thermal stability and performance under reservoir conditions. While liquid foams are highly affected by salt concentration, the influences of salinity on the foams' characteristics have yet to be clearly understood. This paper investigates the effects of salinity on the properties of SNP-surfactant-stabilized foams. The key experiments included the zeta potential and particle size measurements of SNP in surfactant solutions and the foamability, stability, rheology and proppant suspension tests on the studied foams. The results showed that the increase in the NaCl salt concentration reduced the electrostatic repulsion and promoted the aggregation behaviour among the SNP. At higher salinity, the SNP-surfactant-stabilized foams were found to have lower initial volumes, shorter half-lives, reduced apparent viscosity and faster proppant settlement. Furthermore, it was observed that all the studied foams became extremely unstable with very low foamability and had limited proppant suspension capacity when the salinity was increased to 5%. This observation is critical to evaluate the compatibility of fracturing foams when interacting with the formation brine and to improve the process of recycling produced water as a base fluid to generate foams. The outcomes of this study enhance our understanding of the influences of salinity on the properties of liquid foams and contribute to developing a practical guideline for the foam-fracturing application under harsh reservoir conditions.

1. Introduction

In the last 30 years, global energy consumption has increased gradually by nearly 70%, from 8507 Mtoe to 14,221 Mtoe in 2021 (Enerdata, 2022). Due to the rising energy demand and the depletion of conventional resources, there has been an increasing need to produce hydrocarbon from unconventional resources. Throughout history, fracture stimulation has been widely applied to recover oil and gas from unconventional resources. However, conventional water-based fracturing fluids, including slickwater possess several significant field limitations, such as inefficient flowback, and high water and chemical additives consumption. More importantly, they can cause clay swelling when interacting with water-sensitive formations (Wanniarachchi et al., 2017; Abdelaal et al., 2021; Fu and Liu, 2021). Some alternative fracturing systems have been introduced to address these limitations, and one of the most effective ones is foam-based fluid.

Liquid foams are typically generated by using surface-active agents

known as surfactants. The surfactants are important in reducing interfacial tension so gas bubbles can form (Langevin, 2000). The key properties of foams in the hydraulic fracturing application are their stability, rheology, and proppant-carrying capability. In comparison, foam-based fracturing fluids have several advantages over conventional water-based fluids, such as low water consumption, high proppant-carrying capacity, effective flowback, efficient clean-up, minimal formation damage and improved fracture dimension (Yekeen et al., 2018b; Speight, 2016; Isah et al., 2021; Tran et al., 2020; Fei et al., 2018).

Despite having many substantial benefits, the biggest challenge of fracturing foams in practice is their instability and reduced properties under high-temperature reservoir conditions (Lv et al., 2015; Luo et al., 2014; Yang et al., 2021). At elevated temperatures, the surfactants tend to become degraded and, therefore, cannot provide durable foams (Kapetas et al., 2016; Abdelaal et al., 2021). To address this challenge, silica nanoparticles (SNP) have been studied and found to be very

effective in improving the thermal stability of surfactant foams (Faroughi et al., 2018; Fei et al., 2017, 2018; Lv et al., 2015, 2017; Fu and Liu, 2020; Verma et al., 2018). As NP absorb on the gas-liquid interface, they act as a steric barrier to enhance the film strength, delay liquid drainage, prevent gas diffusion, and improve foam viscosity (Lv et al., 2015; Zhang et al., 2021; Ab Rasid et al., 2022). This, as a result, helps increase the overall stability and improve the thermal resistance of the liquid foams.

In addition to temperature, salinity also significantly affects the foams' performance. In the current literature, there are divided opinions on the effects of salinity on the properties of liquid foams. On the one hand, the addition of salts was observed to improve the foamability, stability and viscosity of the surfactant foams (Wang et al., 2017; Yekeen et al., 2017; Vatanparast et al., 2018; Majeed et al., 2020; Da et al., 2018; Obisesan et al., 2021; Rudyk et al., 2021). In addition, NP was found to have higher hydrophobicity with increasing salt concentration (Worthen et al., 2013; San et al., 2017; Rahmani, 2018). This allows NP to be easier adsorbed on the gas-liquid interface and to enhance the foams' properties. On the other hand, some researchers concluded that liquid foams had reduced properties with lower foamability, half-life and viscosity in the presence of salts (Wang et al., 2017; Tang et al., 2020; Yang et al., 2021; Majeed et al., 2021; Ab Rasid et al., 2022). Due to the existing literature contrast, more research is needed to validate the findings and clarify the controversy.

Many previous studies have been conducted to evaluate the effects of salt concentration on liquid foams. However, most of them focus on EOR/water-flooding foams, which are stabilized by either surfactants or nanoparticles (NP) but rarely by a combination of both. Thus, there has been a very limited understanding of how salinity affects the properties of NP-surfactant-stabilized foams, particularly for hydraulic fracturing applications. Moreover, while the key properties of NP-stabilized foams have a strong relationship with the colloidal stability, the influences of salinity on the stability of the NP-surfactant dispersion have yet to be clearly demonstrated.

Due to the presented research gaps, this paper aimed to investigate the effects of salinity on the critical properties of NP-surfactant-stabilized fracturing foams, including colloidal dispersion stability, foamability, foam stability, and foam stability rheology, and proppant suspension capacity. An anionic surfactant and SNP were used to generate foams and were studied at varied NaCl salt concentrations. The paper is expected to provide a comprehensive study of the influences of salinity on the characteristics of the NP-surfactant-stabilized fracturing foams and to enhance our understanding of the foam fracturing practice under high salinity conditions.

2. Experimental section

2.1. Materials

An anionic surfactant, sodium dodecyl benzene sulfonate (SDBS, >99% purity), has a molecular weight of 348.48 g/mol and a critical micelle concentration (CMC) of 0.61 mM, which is equivalent to 0.021 wt% in water. The hydrophilic SNP in colloidal form were used in the experiment with a concentration of 34 wt% suspensions in water. The SNP has a molecular weight of 60.08 g/mol and a surface area of 110–150 m^2/g. Both SDBS and SNP were obtained from Sigma Aldrich. Sodium chloride NaCl (99.6% purity) was supplied by Rowe Scientific. All chemical substances were of analytical grades and were used as received without further modification. All experiments used deionised distilled water with a resistivity of 18.2 mΩ as a base fluid.

2.2. Experimental procedures

2.2.1. Sample preparation

Firstly, anionic SDBS surfactant was added to distilled water and continuously stirred for 2 h without interruption. Different concentrations of SDBS at 0.01 wt%, 0.02 wt%, 0.05 wt% and 0.08 wt% were prepared. NaCl salt was then mixed and dissolved in the solution. After that, 1.0 wt% SNP were added to the mixture and stirred for another 2 h. The SNP/SDBS dispersion was ultra-sonicated at a frequency of 40 Hz for 30 min to reach adsorption equilibrium. The dispersion appeared slightly hazy and was sealed for use in experiments.

2.2.2. Zeta-potential and aggregate size measurement

The zeta potential and particle size of SNP in the SDBS solutions were measured at room temperature using a Zetasizer Nano Series (Malvern Instrument, UK). The instrument is operated based on the dynamic light scattering principle and can measure particles ranging from 1 nm up to 6 μm. Each experiment was repeated at least three times and averaged to ensure the reliability and accuracy of the results. The electrostatic interaction between SNP and surfactants and the aggregation behaviour can be investigated and discussed by determining the zeta potential values and particle sizes.

2.2.3. Foam static stability measurement

The prepared SNP/SDBS dispersion was stirred at 2000 RPM for 2 min to produce fine foams. Immediately after foam generation, the initial foam volume was recorded as a measure of foamability. The foam was then transferred into a glass cylinder. The top of the cylinder was sealed to prevent environmental contamination and disturbance. Foam half-life, which is the duration taken to drain 50% liquid from the foam (Verma et al., 2018; Li et al., 2017; Li et al., 2019), was recorded and used as a standard measure for foam stability. All stability measurements were conducted under ambient conditions.

2.2.4. Apparent viscosity measurement

The apparent viscosities of SNP/SDBS foams at room temperature were measured using a SR5 Rheometer (Rheometric Scientific, USA) equipped with a cup & bob geometry. Power Law model was applied to characterise the foam rheology (Equation (1)):

$$\mu_{app} = \frac{\sigma}{\gamma} = K\gamma^{n-1} \#$$ (1)

where μ_{app} is the apparent viscosity, σ is the measured shear stress, γ is the shear rate, K is the consistency index, and n is the flow behaviour index of the fluid. The foam viscosity measurements were carried out at varied NaCl salt and SDBS surfactant concentrations. Atmospheric pressure and temperature were applied in this experiment to match the testing conditions of the foam stability and proppant settling experiments.

2.2.5. Static proppant settling measurement

In the static proppant suspension test, 2g of sand proppants (20/40 mesh size) was evenly added to the foam column in the glass cylinder. The proppant settling velocity was determined by measuring the height of the initial foam column and the time taken for the proppants to settle at the bottom of the cylinder. The diameter of the measuring cylinder was more than 25 times larger than that of the proppants to minimize the effect of confining walls on the proppant-settling velocity (Goel et al., 2002). The settling velocity of a spherical particle (V_s) in a fluid can be demonstrated by the classical Stokes' Law as in Equation (2) (Stokes, 1851):

$$V_s = \frac{g(\rho_p - \rho_f)d_p^2}{18\mu_f} \#$$ (2)

where g is the gravitational acceleration, ρ_p is the particle density, ρ_f is the fluid density, d_p is the particle diameter, and μ_f is the fluid viscosity. It is evident that the proppant settling velocity is inversely proportional to the fluid viscosity.

3. Results & discussions

3.1. Stability of silica nanoparticles

It is well-accepted in the literature that the properties of NP-surfactant-stabilized foams greatly depend on the stability of the NP dispersions. According to DLVO theory (Derjaguin and Landau, 1941; Verwey and Overbeek, 1948), the stability of a colloidal system is determined by the sum of the van der Waals (VdW) attractive and the electric double layer (EDL) repulsive forces exerted on the particles.

Fig. 1 demonstrates the relationship between separation distance and the interaction energy from VdW and EDL forces (Cardellini et al., 2016). At a considerable separation distance, the EDL repulsion is the predominant force to prevent particles from approaching each other due to the Brownian motion. However, under extreme conditions such as high temperatures, the attractive force on the particles may overcome the repulsion and result in irreversible particle aggregation. At a considerable level of aggregation, particle flocculates are formed within the dispersions, which decreases the stability of the colloidal system (Freitas and Müller, 1998).

3.1.1. Zeta potential

Zeta potential and aggregate size are the two key measures to assess the stability of the SNP dispersion (Vatanparast et al., 2018). Fig. 2 shows the adsorption mechanism of ions on a SNP in distilled water. As SNP are negatively charged, the hydronium cations (H_3O^+) with positive charge tend to adsorb and form two layers on the SNP surface. The inner layer (Stern layer) contains strongly bounded cations, while the outer layer (diffuse layer) carries the loosely attached cations and anions. Zeta potential (ζ), by definition, is the electrical potential at the boundary of the diffuse layer (Barhoum et al., 2018). According to the DLVO theory, the repulsive potential energy (V_{EDL}) acting on particles is a function of squared zeta potential ($V_{EDL} = f(\zeta^2)$). Therefore, high absolute values of zeta potential indicate high repulsion between the particles, resulting in increased stability of SNP dispersion and a low likelihood of particle aggregation, and vice versa.

Fig. 3 shows the effects of salinity on the zeta potential of SNP in SDBS solutions. Without NaCl salt, SNP had relatively high absolute zeta potential between -34 mV and -43 mV. As the NaCl concentration increased from 0% to 5%, the absolute zeta potential of SNP decreased gradually towards the isoelectric point of 0 mV. This observation can be
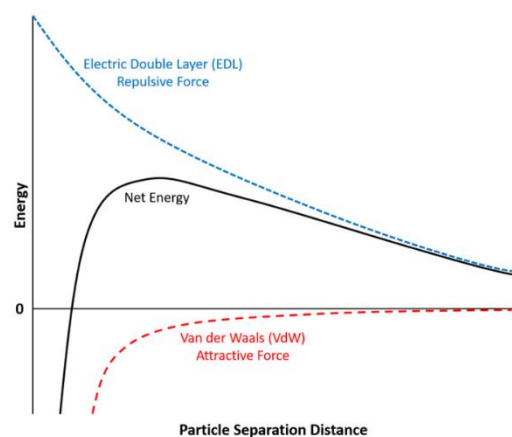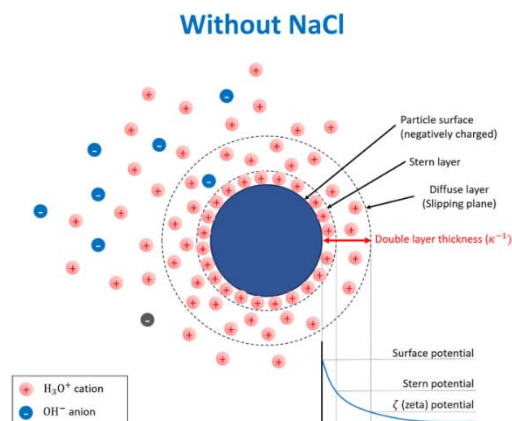

Fig. 2. Electrical layers and ion adsorption on a negatively charged SNP in distilled water.
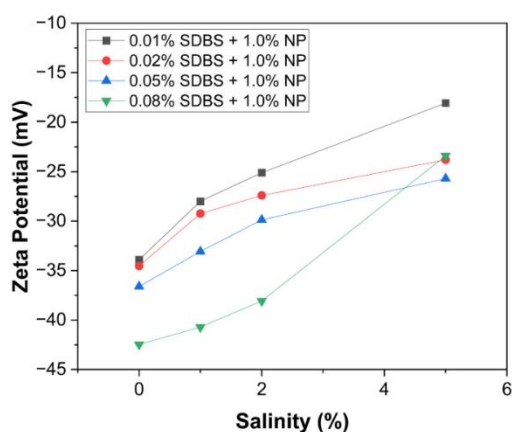

Fig. 3. Influence of salinity on the zeta potential of the SNP/SDBS dispersions.

explained by the ion adsorption mechanism of SNP in the saline environment shown in Fig. 4. In the presence of NaCl salt, the sodium ions (Na^+) and chloride ions (Cl^-) are released into the SNP/SDBS dispersions. As SNP is negatively charged, the Na^+ cations tend to adsorb on the SNP surface due to the electrical attraction. With increasing salinity, a higher amount of Na^+ cations will adsorb and enter the Stern and diffuse layers of the SNP. Consequently, the SNP surface charge becomes less negative due to the increased concentration of cations within the layers (Behera et al., 2014; Vatanparast et al., 2018), resulting in lower absolute zeta potential as measured.

According to Fig. 3, as the SDBS concentration increased from 0.01% to 0.08%, the absolute zeta potential of SNP increased considerably from -33.9 mV to -42.5 mV at 0% NaCl, and from -18.1 mV to -25.7 mV at 5% NaCl. Two possible reasons can explain this observation. Firstly, with increasing surfactant concentration, more SDBS molecules can be adsorbed on the SNP surface via the ion association mechanism (Liu et al., 2020). In specific, the H_3O^+ cations available on the SNP surface would serve as bridges to attract the negative head groups of SDBS and
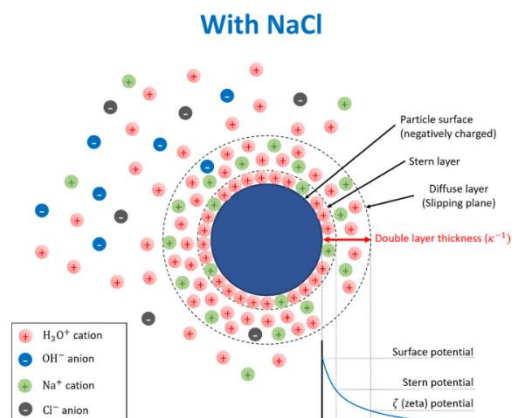

Fig. 1. Schematic of repulsive and attractive energy on particles in dispersion (reproduced from Cardellini et al., 2016)).

3

Fig. 4. Electrical layers and ion adsorption on a negatively charged SNP with NaCl salts.

Fig. 5. Influence of salinity on the particle average size in the SNP/SDBS dispersions.

establish connections between SDBS molecules and the SNP surface. As a result, due to the increased adsorption of SDBS molecules, SNP tends to have higher charge density at the surface and more negative zeta potential values (Onaizi, 2022; Behera et al., 2014; Awan et al., 2022).

The second reason can be linked to the pH of the SNP/SDBS dispersion. In our experiments, the unmodified silica nanofluid has a neutral pH of 7, while the SDBS solution has a pH of 9. When adding them together, the pH value of the SNP/SDBS mixture is undoubtedly higher than 7 and increases with increasing SDBS concentration. As the pH increases, more free hydroxyl anions (OH^-) are released and become available in the medium. Because of this, the silanol groups on the SNP surface generate a greater number of negative sites based on Reaction 1 (Dehghan Monfared et al., 2015):

$$SiOH + OH^- \rightleftharpoons SiO^- + H_2O \ \# \qquad\qquad \text{Reaction (1)}$$

As a result, the negative charge on the SNP surface is promoted, leading to a higher absolute zeta potential of the SNP at higher pH. Some previous studies have observed similar behaviours (Cacua et al., 2019; Zhao et al., 2018; Veyskarami and Ghazanfari, 2018; Eftekhari et al., 2015).

3.1.2. Aggregate size

In addition to zeta potential, the measurement results of SNP size in different salinities and surfactant concentrations are demonstrated in Fig. 5. As the NaCl concentration increased from 0% to 5%, the average size of SNP in SDBS solutions increased considerably. This observation is mainly attributed to the aggregation of SNP under saline conditions.

As discussed previously, the DLVO theory suggests that the EDL repulsive force plays an essential role in preventing particles from approaching and aggregating with others. However, the addition of NaCl salts was found to reduce the absolute zeta potential of SNP considerably (Fig. 3). As a result, the magnitude of EDL repulsive force on SNP is reduced, and SNP aggregates are formed due to the dominance of the existing electrostatic attractive force. Moreover, the SNP aggregates can interact with each other via silanol-silanol hydrogen bonding to generate even larger structures such as flocculates and coagulates (Russel et al., 1989). These structures might be visible by the naked eye and are strong indicators of the instability of the SNP/SDBS dispersion.

Fig. 6 shows the photos of SNP/SDBS dispersion samples at varied NaCl concentrations. The dispersions remained clear and transparent at 0% and 1% NaCl, indicating none or a minor aggregation of SNP. At 2% NaCl, the dispersion became translucent, and several snowy tiny solids
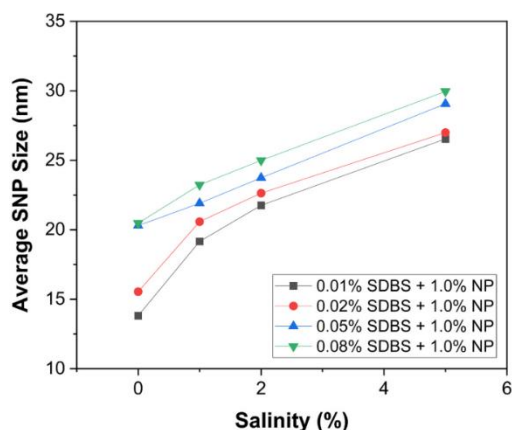
can be seen in the medium. These solids are most likely SNP flocculates formed by a substantial level of SNP aggregation. At 5% NaCl, the SNP/SDBS dispersion appeared to be opaque and cloudy, possibly due to the presence of SNP flocculates and undissolved salt particles at extreme salinity. Fig. 6 provides excellent evidence to conclude the effects of salinity on promoting aggregation and flocculation of SNP, leading to the increased average SNP size and reduced stability of the SNP/SDBS dispersions.

According to Fig. 5, the average SNP size in SDBS solutions increased by 3–5 nm when increasing the SDBS concentration from 0.01% to 0.08%. In this case, particle aggregation is not a rational reason because as SDBS concentration increases, SNP have higher absolute zeta potential, thus stronger electrostatic repulsion to secure the separation (Fig. 3). Instead, the growth of SNP size is most likely due to the incremental surfactant adsorption on the SNP surface. As the surfactant concentration increases, a greater number of free SDBS molecules are generated and SDBS micelles are formed when the concentration exceeds the CMC of 0.021 wt%. As a result, when silica nanofluid is added to the mixture, these SDBS molecules and micelles tend to adsorb and form a monolayer or even a double layer on the SNP surface (Wang et al., 2007; Zhao et al., 2018). This consequently leads to an increment of the hydraulic radius of the SNP, as shown in Fig. 5.

3.2. Foamability

Fig. 7 shows the foaming ability of SNP/SDBS dispersions in different salinities and surfactant concentrations. It is evident that the initial volume of foams increased with increasing SDBS concentration. As more SDBS molecules are added to the dispersions, they migrate towards the gas-liquid interface and further reduce the surface tension at the interface, increasing the foamability (Bournival et al., 2014; Karakashev and Manev, 2003). The same trends have been reported previously for other surfactants (Simjoo et al., 2013; Xu et al., 2009).

On the other hand, adding NaCl salt had detrimental effects on the foamability of SNP/SDBS foams. At all studied SDBS concentrations, the initial volumes of foams had the highest values at 0% NaCl. As the salinity increased, the foamability decreased gradually and reduced to around 120–130 mL at 5% NaCl. The negative impacts of salinity on the foamability are mainly due to the reduced solubility of surfactants under brine conditions. In previous studies, the presence of electrolytes was found to decrease the solubility of surfactants in dispersions (Zhou et al., 2020; Xue et al., 2015). This directly hinders the surfactants' ability to

4
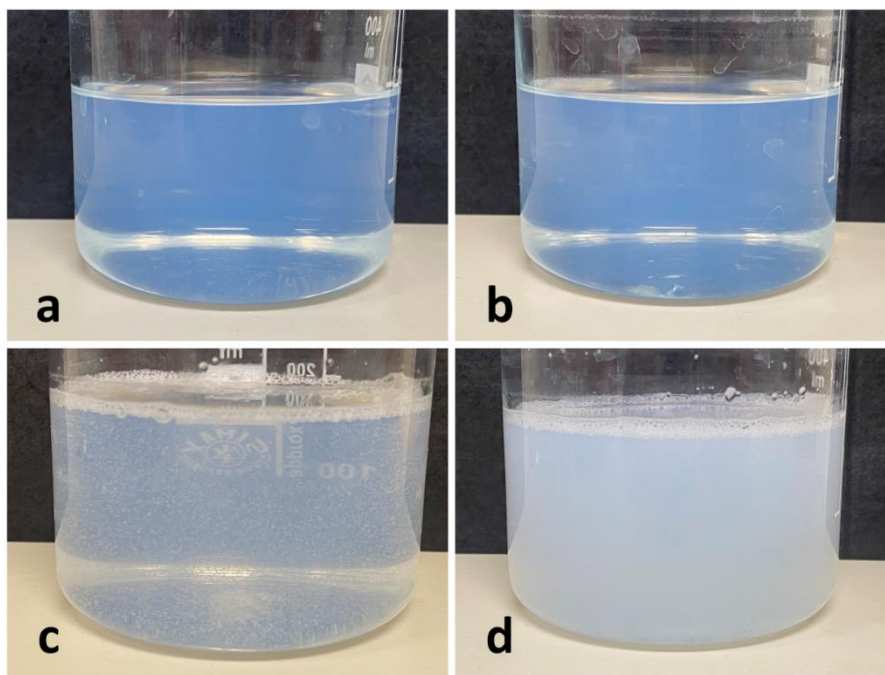
Fig. 6. Dispersions of 0.08% SDBS +1% SNP with (a) 0% NaCl, (b) 1% NaCl, (c) 2% NaCl, and (d) 5% NaCl.
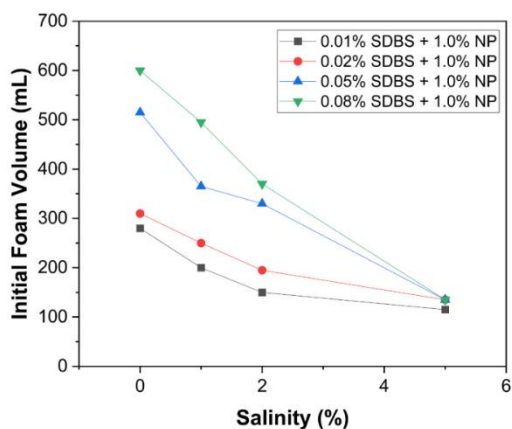
Fig. 7. Influence of salinity on the foamability of SNP/SDBS foams.

reduce the interfacial tension and eventually lowers their ability to generate foams (Yang et al., 2021, Eftekhari et al., 2015).

Fig. 8 shows the photo of 0.08% SDBS +1.0% SNP foams in different salinities. At low salinities, the gas volumes dominate the liquid volumes, indicating the high quality of foams. However, at 5% NaCl, the liquid is the main component, with very few foam bubbles on top, demonstrating very low foam quality.

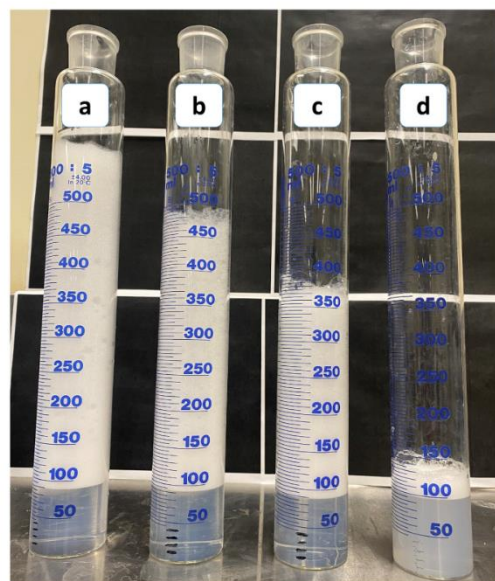**Fig. 8.** Columns of 0.08% SDBS +1.0% SNP foams with (a) 0% NaCl, (b) 1% NaCl, (c) 2% NaCl, and (d) 5% NaCl.

5

87

3.3. Foam stability

Besides foamability, the stability and rheology of foams are critical factors to the success of the foam fracturing application. The foam destabilization is driven by three main mechanisms: liquid drainage, gas diffusion, and bubble coalescence (Majeed et al., 2020). Among these mechanisms, gravitational liquid drainage has the most impacts on the stability of foams (Langevin, 2000; Li et al., 2017, 2019).

Fig. 9 shows the drainage half-lives of SNP-SDBS foams in varied NaCl and surfactant concentrations. The foam half-life was found to increase with increasing surfactant concentration. This is because as the SDBS concentration increases, a higher number of active SDBS molecules are attached on the SNP surface and adsorbed on the gas-liquid interface. The incremental surfactant adsorption not only increases the film strength and integrity but also improves the interfacial elasticity of the lamellae (Firouzi and Nguyen, 2014). As a result, the liquid drainage and bubble coalescence rates in foams are delayed, leading to an increased foam half-life, as observed in Fig. 9.

However, the stability of foams decreased dramatically when adding salts to the SNP/SDBS dispersions. The destabilization effects are more severe with increasing salinity and more evident on foams with lower SDBS concentrations. For example, as the salinity increased to 5%, all studied foams became extremely unstable with drainage half-lives of less than 5 s. The destructive impacts of salts on foam stability can be attributed to two main reasons. Firstly, surfactants are very likely to precipitate under brine conditions due to their interaction with mono-valent or multi-valent cations (Wang et al., 2018). This leads to the degradation of surfactants, thereby reducing their stabilization effects on foams (Emrani et al., 2017).

The second reason is linked to the aggregation behaviour of NP. According to Yekeen et al. (2018a), the aggregation of NP could enhance or reduce foam stability depending on the location and extent of the aggregation. If accumulating on the gas-liquid interface or Plateau borders at a moderate extent, the NP aggregate network acts as a thick solid barrier on foam bubbles to reduce direct contact between the fluids and keep the bubbles separated (Tran et al., 2022). This network helps delay liquid drainage, reduce gas diffusion rate and prevent bubble coalescence, leading to more stable foams with longer half-lives (Yekeen et al., 2018a; Carn et al., 2009; AlYousef et al., 2018). On the other hand, if excessive NP aggregates accumulate in the continuous liquid phase or bulk solution, these large-sized structures require very high energy to migrate to the gas-liquid interface (Yang et al., 2017; Aktas et al., 2008). Consequently, the amount of NP is insufficient enhance the stability of foams, leading to lower foam half-life and viscosity.
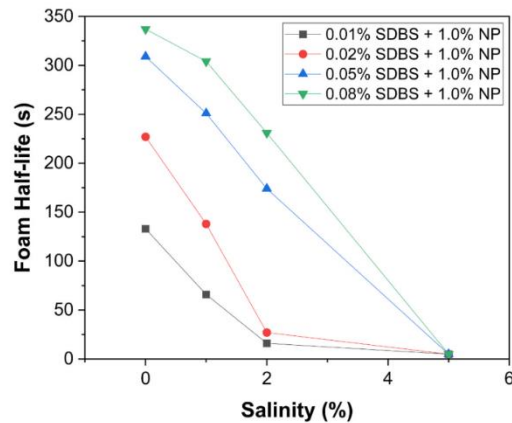
In this study, it was previously found that adding NaCl salts promotes particle aggregation due to the reduced electrostatic repulsion between SNP and the reduced absolute zeta potential (Figs. 3 and 5). According to Fig. 6, the majority of SNP aggregation is believed to occur in the continuous liquid phase and appear as the visible snowy solids in the medium. As these flocculates and aggregates are much larger than the individual SNP, they are very difficult to be placed onto the gas-liquid interface and, thereby, do not effectively stabilize foams.

3.4. Foam rheology

The viscosity behaviour is crucial for any fracturing fluid as it determines the proppant-carrying capacity and filtration property. Fig. 10 shows the apparent viscosity of SNP/SDBS foams in different NaCl and SDBS concentrations at a fixed shear rate of $100\ \text{s}^{-1}$. The viscosity of the studied foams was found to increase with increasing surfactant concentration but decrease with increasing salinity.

According to the Young-Laplace equation (Equation (3)), the pressure inside the bubble (P_{in}) is a function of the pressure outside the bubble (P_{out}), surface tension (γ), and the bubble radius (R_b) (Stevenson, 2010).

$$P_{in} = P_{out} + \frac{2\gamma}{R_b} \ \# \tag{3}$$

Due to the pressure difference, gas is diffused from small bubbles to larger ones, which eventually causes film rupture (Farajzadeh et al., 2008). Furthermore, as the SDBS concentration increases, the incremental adsorption of active surfactant molecules on the gas-liquid interface results in higher foam quality, finer foam texture, thicker lamellae and higher viscoelasticity to resist deformation of bubbles (Fu and Liu, 2021; Worthen et al., 2013). Besides that, with increasing surfactant concentration, foam bubbles tend to have a smaller size and, thereby, have higher inner pressure to prevent gas diffusion (Yang et al., 2021). This makes the deformation process much more difficult, and eventually enhances the foam viscosity.

On the other hand, the addition of salts has devastating effects on the foam viscosity. For example, as the NaCl concentration increased to 5%, the 0.01% SDBS foam became liquid-like with a very low viscosity of 2 cP, while other foams had their viscosity reduced by 36–38%, compared to the cases without salts. Similar to the previous discussion on foam stability, the negative impacts of salts on the foam viscosity are mainly
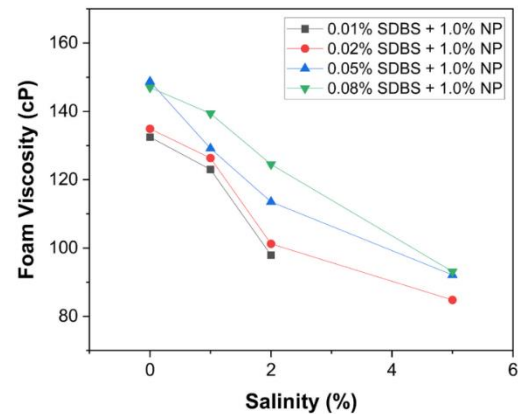
Fig. 9. Influence of salinity on the stability of SNP/SDBS foams.

Fig. 10. Influence of salinity on the viscosity of SNP/SDBS foams at a shear rate of $100\ \text{s}^{-1}$..

attributed to surfactant degradation and the increased aggregation of SNP.

At medium and high NaCl concentrations, the aggregation behaviour of SNP was highly promoted due to the reduced electrostatic repulsion, which produces SNP aggregates and flocculates in the foam system. However, these aggregation structures were believed to assemble in the bulk dispersion, reducing adsorption of active SNP on the gas-liquid interface. Because of low adsorption, SNP has very limited capabilities of improving the interfacial strength, enhancing the structural integrity of foams, or resisting disturbances in foams. In addition, foam bubbles tend to have larger sizes; therefore, they have lower inner pressure and are more vulnerable to gas diffusion. As a result, these lower the flow resistance and decrease the viscosity of foams with increasing salinity.

The aggregation of NP at high electrolyte concentration was also reported in Kostakis et al. (2006), which caused the disproportionation and insufficient adsorption of NP onto the interface to cover the foam bubbles. The negative effects of salts on foam viscosity have been observed in some previous studies (Xiao et al., 2017; Yang et al., 2021; Tang et al., 2020).

3.5. Proppant suspension of foams

The placement of proppants at the fracture surfaces plays a critical role in the success of the fracture stimulation process (Goel et al., 2002; Harris and Reidenbach., 1987). If the proppants settle too quickly, they will accumulate near the wellbore region and only affect a very limited portion of the fracture. On the other hand, if the proppants settle slower, they can be transported deeper towards the fracture tips to increase the propped area and enhance the fracture conductivity (Tong et al., 2019).

The proppant suspension capacity of foam is best evaluated by the proppant settling velocity (Yekeen et al., 2018b). In general, foams have lower proppant settling velocity than water-based fracturing fluids due to their high viscosity and the uplift force acting on the proppants against gravity. This uplift force includes two components: a drag force from the bulk movement of the foams and an elastic force due to foam compressibility and lamella movement (Jing et al., 2016; Zhu et al., 2019).

Fig. 11 shows the impacts of salinity and surfactant concentration on the proppant suspension capacity of SNP/SDBS foams under ambient conditions. As the SDBS concentration increased from 0.01% to 0.08%, the settling velocity of proppants decreased noticeably. This observation is mainly due to the dependent relationship between proppant settling
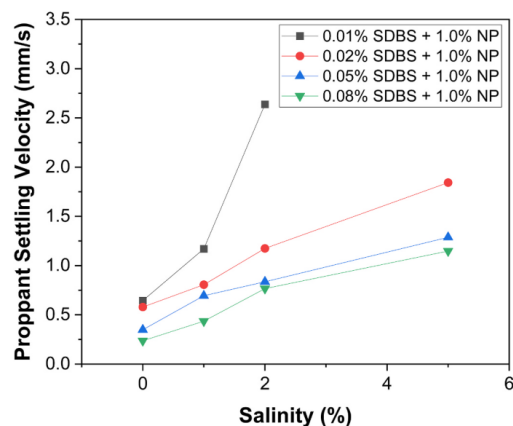

Fig. 11. Influence of salinity on the proppant suspension behaviour of SNP/SDBS foams.

velocity and the rheology and stability of foams. As discussed previously, at higher surfactant concentrations, foams were found to have higher half-life, lower drainage rate, finer texture, improved bubble strength and higher flow resistance. These effects are very beneficial in delaying the downward movement of proppants and, thereby, significantly enhancing their suspension in the medium.

In addition, the settling velocities of proppants in SNP/SDBS foams were found to increase gradually with increasing salinity. Among all foam systems, the 0.01% SDBS + SNP foam was most sensitive to the salinity change. At 5% NaCl, the proppant settling velocity in this foam system became extremely high at around 40 mm/s due to the significant drop in the foam viscosity. For other foams with higher SDBS concentrations, the proppant settling velocity also increased but for a maximum of 3–5 times at 5% salinity.

The progressive settlement behaviour of proppants with increasing salinity is mainly attributed to the effects of salts on reducing the foam stability and viscosity. As foam becomes less viscous and less stable with fragile bubbles, it tends to have lower capabilities of generating uplift forces to counter the gravitational movement of proppants. Besides that, the excessive aggregation of SNP at high salt concentrations is also believed to contribute to the increased proppant settling velocity. The adsorption of the large-sized aggregates on the gas-liquid interface might have positive effects on blocking the liquid channels and reducing gravitation drainage; however, these aggregates tend to interact with proppants via attachment and possibly collision. This interaction, as a result, exerts undesirable forces on proppants and makes them settle faster in the liquid foams.

3.6. Practical recommendations

From the experimental results, the increase in salinity had negative impacts on the stability of the SNP dispersions and the key properties of the SNP-surfactant-stabilized fracturing foams. For example, as the salinity increased to 5%, all the studied foams were found to become extremely unstable with very low foamability and limited proppant suspension capacity. Therefore, in the foam fracturing practice, SNP-surfactant-stabilized foams should not be used to stimulate formations with an excessive salt concentration in their brines – for instance, at 5% salinity or higher. These formations are considered highly incompatible with foam-based fluids.

In addition, it is a common practice that the produced water from the underground is recycled, and then used as a base solution to generate liquid foams. Therefore, it is suggested that this recycled water should have as low salinity as possible to avoid any undesirable synergy with the foam, NP or surfactants. Otherwise, if the produced water contains a high salt concentration, it should be diluted to meet the salinity requirement.

4. Conclusions

In this paper, the effects of salinity on the properties of SNP-surfactant-stabilized fracturing foams have been thoroughly investigated. The results and findings of the study help enhance understanding of the characteristics of fracturing foams and their operating practice under high salinity conditions. The increase of NaCl concentration was found to lower the surface charge and promote the aggregation behaviour of SNP, which leads to the increased SNP average size and reduced stability of the SNP/SDBS dispersion. At high salinity, surfactant molecules become degraded while the SNP aggregates tend to accumulate in the bulk solution, causing the insufficient adsorption of SNP and surfactants on the gas-liquid interface to stabilize foams. As a result, SNP/SDBS foams had lower foamability, lower half-life, reduced apparent viscosity and faster proppant settlement with increasing salinity. In addition, the SNP/SDBS foams were observed to be extremely unstable with very low foamability and limited proppant suspension at 5% salinity. It is imperative to carefully evaluate the formation brine and

monitor the recycled water to avoid reaching this salinity limit and ensure the compatibility of the fracturing foams.

Future works are strongly required to further investigate the effects of salinity on the properties and behaviours of liquid foams in the fracturing application. In addition, other common salt types such as KCl, $MgCl_2$, $CaCl_2$ or a combination of them with/without NaCl, should be studied intensively to compare and validate the results and findings from this project. Finally, it is recommended to include laboratory experiments to evaluate the hydrophobicity, wettability of NP, and the interfacial tension of surfactants under the influence of salinity. This would certainly add a lot of insightful discussions and explanations to our observations.

Credit authors statement

Tuan Tran: Investigation, Methodology, Data curation, Formal analysis, Writing – original draft.**M.E Gonzalez Perdomo**: Conceptualization, Supervision, Writing – review & editing, Validation, Resources.**Manouchehr Haghighi**: Conceptualization, Supervision, Writing – review & editing, Validation, Resources.**Khalid Amrouch**: Supervision, Writing – review & editing.

Declaration of competing interest

The authors declare that they have no known competing financial interests or personal relationships that could have appeared to influence the work reported in this paper.

Data availability

Data will be made available on request.

Acknowledgements

References

Ab Rasid, S.A., Mahmood, S.M., Kechut, N.I., Akbari, S., 2022. A review on parameters affecting nanoparticles stabilized foam performance based on recent analyses. J. Petrol. Sci. Eng. 208.

Abdelaal, A., Aljawad, M.S., Alyousef, Z., Almajid, M.M., 2021. A review on foam-based fracturing fluids applications: from lab studies to field implementations. J. Nat. Gas Sci. Eng. 95.

Aktas, Z., Cilliers, J.J., Banford, A.W., 2008. Dynamic froth stability: particle size, airflow rate and conditioning time effects. Int. J. Miner. Process. 87 (1–2), 65–71.

AlYousef, Z.A., Almobarky, M.A., Schechter, D.S., 2018. The effect of nanoparticle aggregation on surfactant foam stability. J. Colloid Interface Sci. 511, 365–373.

Awan, F.U.R., Al-Yaseri, A., Akhondzadeh, H., Iglauer, S., Keshavarz, A., 2022. Influence of mineralogy and surfactant concentration on zeta potential in intact sandstone at high pressure. J. Colloid Interface Sci. 607 (1), 401–411.

Barhoum, A., García-Betancourt, M.L., Rahier, H., Van Assche, G., 2018. Chapter 9 - physicochemical characterization of nanomaterials: polymorph, composition, wettability, and thermal stability. In: Barhoum, A., ASH Makhlouf (Eds.), Emerging Applications of Nanoparticles and Architecture Nanostructures. Elsevier, pp. 255–278.

Behera, M.R., Varade, S.R., Ghosh, P., Paul, P., Negi, A.S., 2014. Foaming in micellar solutions: effects of surfactant, salt, and oil concentrations. Ind. Eng. Chem. Res. 53 (48), 18497–18507.

Bournival, G., Du, Z., Ata, S., Jameson, G.J., 2014. Foaming and gas dispersion properties of non-ionic surfactants in the presence of an inorganic electrolyte. Chem. Eng. Sci. 116, 536–546.

Cacua, K., Ordoñez, F., Zapata, C., Herrera, B., Pabón, E., Buitrago-Sierra, R., 2019. Surfactant concentration and pH effects on the zeta potential values of alumina nanofluids to inspect stability. Colloids Surf. A Physicochem. Eng. Asp. 583.

Cardellini, A., Fasano, M., Bozorg Bigdeli, M., Chiavazzo, E., Asinari, P., 2016. Thermal transport phenomena in nanoparticle suspensions. J. Phys. Condens. Matter 28 (48), 483003.

Carn, F., Colin, A., Pitois, O., Vignes-Adler, M., Backov, R., 2009. Foam drainage in the presence of nanoparticle-surfactant mixtures. Langmuir 25 (14), 7847–7856.

Da, C., Alzobaidi, S., Jian, G., Zhang, L., Biswal, S.L., Hirasaki, G.J., Johnston, K.P., 2018. Carbon dioxide/water foams stabilized with a zwitterionic surfactant at temperatures up to 150 °C in high salinity brine. J. Petrol. Sci. Eng. 166, 880–890.

Dehghan Monfared, A., Ghazanfari, M.H., Jamialahmadi, M., Helalizadeh, A., 2015. Adsorption of silica nanoparticles onto calcite: equilibrium, kinetic, thermodynamic and DLVO analysis. Chem. Eng. J. 281, 334–344.

Derjaguin, B., Landau, L., 1941. Theory of the stability of strongly charged lyophobic sols and of the adhesion of strongly charged particles in solutions of electrolytes. Prog. Surf. Sci. 43, 30–59.

Eftekhari, A.A., Krastev, R., Farajzadeh, R., 2015. Foam stabilized by fly ash nanoparticles for enhancing oil recovery. Ind. Eng. Chem. Res. 54 (50), 12482–12491.

Emrani, A.S., Nasr-El-Din, Ha, 2017. An experimental study of nanoparticle-polymer-stabilized CO 2 foam. Colloids Surf. A Physicochem. Eng. Asp. 524, 17–27.

Enerdata, 2022. Total Energy Consumption. Enerdata. (Accessed 9 March 2023).

Farajzadeh, R., Krastev, R., Zitha, P.L., 2008. Foam film permeability: theory and experiment. Adv. Colloid Interface Sci. 137 (1), 27–44.

Faroughi, S.A., Pruvot, A.J.-C.J., McAndrew, J., 2018. The rheological behavior of energized fluids and foams with application to hydraulic fracturing: review. J. Petrol. Sci. Eng. 163, 243–263.

Fei, Y., Zhu, J., Xu, B., Li, X., Gonzalez, M., Haghighi, M., 2017. Experimental investigation of nanotechnology on worm-like micelles for high-temperature foam stimulation. J. Ind. Eng. Chem. 50, 190–198.

Fei, Y., Johnson, R.L., Gonzalez, M., Haghighi, M., Pokalai, K., 2018. Experimental and numerical investigation into nano-stabilized foams in low permeability reservoir hydraulic fracturing applications. Fuel 213, 133–143.

Firouzi, M., Nguyen, A.V., 2014. Effects of monovalent anions and cations on drainage and lifetime of foam films at different interface approach speeds. Adv. Powder Technol. 25 (4), 1212–1219.

Freitas, C., Müller, R.H., 1998. Effect of light and temperature on zeta potential and physical stability in solid lipid nanoparticle (SLN™) dispersions. Int. J. Pharm. 168 (2), 221–229.

Fu, C., Liu, N., 2020. Study of the synergistic effect of the nanoparticle-surfactant-polymer system on CO2 foam apparent viscosity and stability at high pressure and temperature. Energy Fuels 34 (11), 13707–13716.

Fu, C., Liu, N., 2021. Rheology and stability of nanoparticle-stabilized CO2 foam under reservoir conditions. J. Petrol. Sci. Eng. 196.

Goel, N., Shad, S., Grady, B., 2002. Correlating viscoelastic measurements of fracturing fluid to particles suspension and solids transport. J. Petrol. Sci. Eng. 35, 59–81.

Harris, P.C., Reidenbach, V.G., 1987. High-temperature rheological study of foam fracturing fluids. J. Petrol. Technol. 39 (5), 613–619.

Isah, A., Hiba, M., Al-Azani, K., Aljawad, M.S., Mahmoud, M., 2021. A comprehensive review of proppant transport in fractured reservoirs: experimental, numerical, and field aspects. J. Nat. Gas Sci. Eng. 88.

Jing, Z., Wang, S., Wang, Z., 2016. Detailed structural and mechanical response of wet foam to the settling particle. Langmuir 32 (10), 2419–2427.

Kapetas, L., Vincent Bonnieu, S., Danelis, S., Rossen, W.R., Farajzadeh, R., Eftekhari, A. A., Shafian, Mohd, SR, Bahrim, Kamarul, Rz, 2016. Effect of temperature on foam flow in porous media. J. Ind. Eng. Chem. 36, 229–237.

Correlation in the properties of aqueous single films and foam containing a nonionic surfactant and organic/inorganic electrolytes. In: Karakashev, S.I., Manev (Eds.), J. Colloid Interface Sci. 259 (1), 171–179.

Kostakis, T., Ettelaie, R., Murray, B.S., 2006. Effect of high salt concentrations on the stabilization of bubbles by silica particles. Langmuir 22 (3), 1273–1280.

Langevin, D., 2000. Influence of interfacial rheology on foam and emulsion properties. Adv. Colloid Interface Sci. 88, 209–222.

Li, S., Qiao, C., Li, Z., Wanambwa, S., 2017. Properties of carbon dioxide foam stabilized by hydrophilic nanoparticles and hexadecyltrimethylammonium bromide. Energy Fuels 31 (2), 1478–1488.

Li, S., Yang, K., Li, Z., Zhang, K., Jia, N., 2019. Properties of CO2 foam stabilized by hydrophilic nanoparticles and nonionic surfactants. Energy Fuels 33 (6), 5043–5054.

Liu, Z., Hedayati, P., Sudholter, E.J.R., Haaring, R., Shaik, A.R., Kumar, L., 2020. Adsorption behavior of anionic surfactants to silica surfaces in the presence of calcium ion and polystyrene sulfonate. Colloids Surf., A 602.

Luo, X., Wang, S., Wang, Z., Jing, Z., Lv, M., 2014. Experimental research on rheological properties and proppant transport performance of GRF–CO2 fracturing fluid. J. Petrol. Sci. Eng. 120, 154–162.

Lv, Q., Li, Z., Li, B., Li, S., Sun, Q., 2015. Study of nanoparticle–surfactant-stabilized foam as a fracturing fluid. Ind. Eng. Chem. Res. 54 (38), 9468–9477.

Lv, Q., Li, Z., Li, B., Zhang, C., Shi, D., Zheng, C., Zhou, T., 2017. Experimental study on the dynamic filtration control performance of N 2/liquid CO2 foam in porous media. Fuel 202, 435–445.

Majeed, T., Sølling, T.I., Kamal, M.S., 2020. Foamstability: the interplay between salt-, surfactant- and critical micelle concentration. J. Petrol. Sci. Eng. 187.

Majeed, T., Kamal, M.S., Zhou, X., Solling, T., 2021. A review on foam stabilizers for enhanced oil recovery. Energy Fuels 35 (7), 5594–5612.

Obisesan, O., Ahmed, R., Amani, M., 2021. The effect of salt on stability of aqueous foams. Energies 14 (2).

Onaizi, S.A., 2022. 'Characteristics and pH-responsiveness of SDBS-stabilized crude oil/ water nanoemulsions'. Nanomaterials 12 (10).

Rahmani, O., 2018. Mobility control in carbon dioxide-enhanced oil recovery process using nanoparticle-stabilized foam for carbonate reservoirs. Colloids Surf. A Physicochem. Eng. Asp. 550, 245–255.

Rudyk, S., Al-Khamisi, S., Al-Wahaibi, Y., 2021. Effects of water salinity on the foam dynamics for EOR application. J. Pet. Explor. Prod. Technol. 11 (8), 3321–3332.

Russel, W., Saville, D., Schowalter, W., 1989. Colloidal Dispersions. Cambridge University Press, Cambridge.

San, J., Wang, S., Yu, J., Liu, N., Lee, R., 2017. Nanoparticle-stabilized carbon dioxide foam used in enhanced oil recovery: effect of different ions and temperatures. SPE J. 22 (5), 1416–1423.

Simjoo, M., Rezaei, T., Andrianov, A., Zitha, P.L.J., 2013. Foam stability in the presence of oil: effect of surfactant concentration and oil type. Colloids Surf. A Physicochem. Eng. Asp. 438, 148–158.

Speight, J.G., 2016. Handbook of Hydraulic Fracturing. John Wiley & Sons.

Stevenson, P., 2010. Inter-bubble gas diffusion in liquid foam. Curr. Opin. Colloid Interface Sci. 15 (5), 374–381.

Stokes, G.G., 1851. On the effect of the internal friction of fluids on the motion of pendulums. Transactions of the Cambridge Philosophical Society 9, 8–106.

Tang, Q., Huang, Z., Wang, B., Lu, H., 2020. Surfactant-free aqueous foams stabilized with synergy of xanthan-based amphiphilic biopolymer and nanoparticle as potential hydraulic fracturing fluids. Colloids Surf. A Physicochem. Eng. Asp. 603.

Tong, S., Gu, M., Singh, R., Mohanty, K.K., 2019. Proppant transport in foam fracturing fluid during hydraulic fracturing. J. Petrol. Sci. Eng. 182.

Tran, T., Gonzalez Perdomo, M.E., Wilk, K., Kasza, P., Amrouch, K., 2020. Performance evaluation of synthetic and natural polymers in nitrogen foam-based fracturing fluids in the Cooper Basin, South Australia. The APPEA Journal 60 (1).

Tran, T., Gonzalez Perdomo, M.E., Haghighi, M., Amrouch, K., 2022. Study of the synergistic effects between different surfactant types and silica nanoparticles on the stability of liquid foams at elevated temperature. Fuel 315.

Vatanparast, H., Shahabi, F., Bahramian, A., Javadi, A., Miller, R., 2018. The role of electrostatic repulsion on increasing surface activity of anionic surfactants in the presence of hydrophilic silica nanoparticles. Sci. Rep. 8 (1), 7251.

Verma, A., Chauhan, G., Baruah, P.P., Ojha, K., 2018. Morphology, rheology, and kinetics of nanosilica stabilized gelled foam fluid for hydraulic fracturing application. Ind. Eng. Chem. Res. 57 (40), 13449–13462.

Verwey, E.J.W., Overbeek, J.T.G., 1948. Theory of the Stability of Lyophobic Colloids: the Interaction of Sol Particles Having an Electric Double Layer. Elsevier.

Veyskarami, M., Ghazanfari, M.H., 2018. Synergistic effect of like and opposite charged nanoparticle and surfactant on foam stability and mobility in the absence and presence of hydrocarbon: a comparative study. J. Petrol. Sci. Eng. 166, 433–444.

Wang, W., Gu, B., Liang, L., 2007. Effect of anionic surfactants on synthesis and self-assembly of silica colloidal nanoparticles. J. Colloid Interface Sci. 313 (1), 169–173.

Wang, Y., Zhang, Y., Liu, Y., Zhang, L., Ren, S., Lu, J., Wang, X., Fan, N., 2017. The stability study of CO2 foams at high pressure and high temperature. J. Petrol. Sci. Eng. 154, 234–243.

Wang, S., Chen, C., Kadum, M.J., Shiau, B.-J., Harwell, J.H., 2018. Enhancing foam stability in porous media by applying nanoparticles. J. Dispersion Sci. Technol. 39 (5), 734–743.

Wanniarachchi, W.A.M., Ranjith, P.G., Perera, M.S.A., 2017. Shale gas fracturing using foam-based fracturing fluid: a review. Environ. Earth Sci. 76 (2).

Worthen, A.J., Bagaria, H.G., Chen, Y., Bryant, S.L., Huh, C., Johnston, K.P., 2013. Nanoparticle-stabilized carbon dioxide-in-water foams with fine texture. J. Colloid Interface Sci. 391, 142–151.

Xiao, C., Balasubramanian, S.N., Clapp, L.W., 2017. Rheology of viscous CO2 foams stabilized by nanoparticles under high pressure. Ind. Eng. Chem. Res. 56 (29), 8340–8348.

Xu, Q., Nakajima, M., Ichikawa, S., Nakamura, N., Roy, P., Okadome, H., Shiina, T., 2009. Effects of surfactant and electrolyte concentrations on bubble formation and stabilization. J. Colloid Interface Sci. 332 (1), 208–214.

Xue, Z., Panthi, K., Fei, Y., Johnston, K.P., Mohanty, K.K., 2015. CO2-Soluble ionic surfactants and CO2 foams for high-temperature and high-salinity sandstone reservoirs. Energy Fuels 29 (9), 5750–5760.

Yang, W., Wang, T., Fan, Z., Miao, Q., Deng, Z., Zhu, Y., 2017. Foams stabilized by in situ-modified nanoparticles and anionic surfactants for enhanced oil recovery. Energy Fuels 31 (5), 4721–4730.

Yang, K., Li, S., Zhang, K., Wang, Y., 2021. Synergy of hydrophilic nanoparticle and nonionic surfactant on stabilization of carbon dioxide-in-brine foams at elevated temperatures and extreme salinities. Fuel 288.

Yekeen, N., Manan, M.A., Idris, A.K., Samin, A.M., 2017. Influence of surfactant and electrolyte concentrations on surfactant Adsorption and foaming characteristics. J. Petrol. Sci. Eng. 149, 612–622.

Yekeen, N., Manan, M.A., Idris, A.K., Padmanabhan, E., Junin, R., Samin, A.M., Gbadamosi, A.O., Oguamah, I., 2018a. A comprehensive review of experimental studies of nanoparticles-stabilized foam for enhanced oil recovery. J. Petrol. Sci. Eng. 164, 43–74.

Yekeen, N., Padmanabhan, E., Idris, A.K., 2018b. A review of recent advances in foam-based fracturing fluid application in unconventional reservoirs. J. Ind. Eng. Chem. 66, 45–71.

Zhang, Y., Liu, Q., Ye, H., Yang, L., Luo, D., Peng, B., 2021. Nanoparticles as foam stabilizer: mechanism, control parameters and application in foam flooding for enhanced oil recovery. J. Petrol. Sci. Eng. 202.

Zhao, M., Lv, W., Li, Y., Dai, C., Zhou, H., Song, X., Wu, Y., 2018. A study on preparation and stabilizing mechanism of hydrophobic silica nanofluids. Materials 11 (8).

Zhou, J., Ranjith, P.G., Wanniarachchi, WAM, 2020. 'Different strategies of foam stabilization in the use of foam as a fracturing fluid'. Adv. Colloid Interface Sci. 276, 102104.

Zhu, J., Yang, Z., Li, X., Song, Z., Liu, Z., Xie, S., 2019. Settling behavior of the proppants in viscoelastic foams on the bubble scale. J. Petrol. Sci. Eng. 181.

9

91

7. Performance evaluation of synthetic and natural polymers in nitrogen foam-based fracturing fluids in the Cooper Basin, South Australia

In this chapter, the fracture simulation modelling is performed on GOHFER software. The details of the software, such as its application, advantages, limitations and step-by-step guide, are included in Appendix 9.1 and 9.2.

Traditional fracturing fluids like slickwater have their own limitations, including high water consumption, clay swelling issues, and low flowback recovery. As the industry seeks more efficient and environmentally friendly alternatives, foam-based fracturing fluids have emerged as promising candidates. However, foam's inherent instability, especially in high-temperature reservoirs, poses a significant challenge. This paper explores the impacts of natural and synthetic polymers on the rheological properties of nitrogen foam-based fluids at high-temperature conditions. The laboratory experiments are integrated with a 3D hydraulic fracture propagation model, using real field data from the Toolachee Formation in the Cooper Basin. The study presents the superiority of synthetic PAM polymers in stabilizing foam viscosity under high temperatures, and the simulation results demonstrate the clear advantage of foam-based fluids over slickwater in field application. The paper highlights the significance of thermal stability and opens the door to further investigation into the role of crosslinkers in high-temperature foam-based fracturing, offering a pathway for optimizing hydraulic fracturing practices at reservoir conditions.

Statement of Authorship

Title of Paper	Performance evaluation of synthetic and natural polymers in nitrogen foam-based fracturing fluids in the Cooper Basin, South Australia
Publication Status	☑ Published ☐ Accepted for Publication ☐ Submitted for Publication ☐ Unpublished and Unsubmitted work written in manuscript style
Publication Details	Tran, T, Gonzalez Perdomo, ME, Wilk, K, Kasza, P & Amrouch, K 2020, 'Performance evaluation of synthetic and natural polymers in nitrogen foam-based fracturing fluids in the Cooper Basin, South Australia', Journal of the Australian Petroleum Production & Exploration Association, vol. 60, no. 1.

Principal Author

Name of Principal Author (Candidate)	Tuan Huynh Minh Tran		
Contribution to the Paper	Literature review, Data collection, Simulation model development, Result analysis and interpretation, Writing the manuscript		
Overall percentage (%)	50%		
Certification:	This paper reports on original research I conducted during the period of my Higher Degree by Research candidature and is not subject to any obligations or contractual agreements with a third party that would constrain its inclusion in this thesis. I am the primary author of this paper.		
Signature		Date	14/03/2023

Co-Author Contributions

By signing the Statement of Authorship, each author certifies that:

    i.   the candidate's stated contribution to the publication is accurate (as detailed above);

   ii.   permission is granted for the candidate in include the publication in the thesis; and

  iii.   the sum of all co-author contributions is equal to 100% less the candidate's stated contribution.

Name of Co-Author	Maria Gonzalez Perdomo		
Contribution to the Paper	Support in result analysis, Reviewing the manuscript (15%)		
Signature		Date	14/03/2023

Name of Co-Author	Klaudia Wilk		
Contribution to the Paper	Support in all laboratory work and result analysis, Reviewing the manuscript (15%)		
Signature		Date	17.03. 2023

Name of Co-Author	Piotr Kasza
Contribution to the Paper	Support in all laboratory work and result analysis, Reviewing the manuscript (15%)

		Date	17.03.2023
Signature			

Name of Co-Author	Khalid Amrouch
Contribution to the Paper	Support in result analysis, Reviewing the manuscript (5%)

		Date	17/03/2023
Signature			

Performance evaluation of synthetic and natural polymers in nitrogen foam-based fracturing fluids in the Cooper Basin, South Australia

Tuan Tran [A,C], *M. E. Gonzalez Perdomo* [A], *Klaudia Wilk* [B], *Piotr Kasza* [B] *and Khalid Amrouch* [A]

[A]Australian School of Petroleum and Energy Resources, University of Adelaide, Adelaide, SA 5000, Australia.
[B]Oil and Gas Institute – National Research Institute, Lubicz 25A, 31-503 Kraków, Poland.
[C]Corresponding author. Email: tuan.tran@adelaide.edu.au

Abstract. Hydraulic fracturing is a well-known stimulation technique for creating fractures in a subsurface formation to achieve profitable production rates in low-permeability reservoirs. Slickwater has been widely used as a traditional fracturing fluid. However, it has multiple disadvantages, such as high consumption of water, clay swelling and low flowback recovery. Foam, as an alternative fracturing fluid, consumes less liquid and provides additional energy. However, foam bubbles are typically unstable due to the degradation of surfactants, particularly in high temperature reservoirs, which reduces their capabilities of carrying and placing proppants into fractures. The purpose of this study is to provide general guidelines for an optimised application of polymers to improve the foam stability in high temperature reservoirs while increasing the proppant placement and water usage efficiencies. In this paper, the effects of natural hydroxypropyl guar (HPG) and synthetic polyacrylamide (PAM) polymers on the rheological properties of nitrogen foam-based fluids were examined by laboratory experiments conducted using temperatures up to 110°C. Then, a 3D hydraulic fracture propagation model was developed to study the fracturing performance of HPG-foamed and PAM-foamed fluids in the Toolachee Formation, Cooper Basin. It was found that synthetic PAM polymers were more effective than natural HPG polymers in stabilising foam viscosity under high temperature conditions. The simulation results indicate that foam-based fluids totally outperform slickwater in the field case application. This paper emphasises the significance of crosslinkers, foam quality and thermal stability on the performance of foams in high temperature environments.

Keywords: experiment, hydraulic fracturing, simulation, synthetic polymer.

Received 20 December 2019, accepted 3 February 2020, published online 15 May 2020

Introduction

Unconventional hydrocarbon reservoirs, such as tight sands, shales and coals, are becoming important resources for existing and future oil and gas supply; however, because of their low-permeable nature, they require hydraulic fracturing treatment to be economically viable. Since first introduced in the late 1940s, fracturing treatment has been performed in more than 2.5 million wells and has become a fundamental engineering tool to enhance hydrocarbon production from low-permeable formations (Smith and Montgomery 2015). In hydraulic fracturing operations, fracturing fluid is pressurised and pumped downhole through perforations or an open-hole interval to create fractures. Proppants, which are normally small natural sands, are mixed and injected with

the fluids to keep fractures open, thereby maintaining a conductive path from the formation to wellbore. Besides proppants, some other chemical additives are mixed in to fracturing fluids: viscosifiers, friction reducers, pH control agents, fluid loss control agents, breaker and clay stabilisers (Gottardo *et al.* 2016). These additives adjust the fracturing fluid's properties to assist with fracture propagation and minimise formation damage near to the fracturing area (Harris 1988). According to Speight (2016), some of the key features of an ideal fracturing fluid are:

- High apparent viscosity to carry and transport proppant into the fractures;
- Rapid break down to low-viscosity fluid for effective flowback and quick recovery;

- Compatibility with formation rock, reservoir fluid, the chemical additives and proppants;
- Low-formation damage;
- Environmentally friendly; and
- Economical.

Water-based fluid is the most common type of fracturing fluid and has been widely used for several decades. Generally, water-based fluid is easy to handle and cost-effective if there is high availability of water (Barati and Liang 2014). However, in field applications, water-based fluid has numerous limitations, such as formation damage, water blocking, clay swelling, low flowback recovery, water disposal issues and inefficient proppant transportation (Yekeen *et al*. 2018). Due to these disadvantages, foams have become an alternative fracturing fluid.

Foam as a fracturing fluid

Foams are stable mixtures of liquid and gas, where liquid acts as the external phase and gas as the internal phase. Foams can be defined by their stability and texture, but they are best characterised by their quality (Schramm 1994). The mathematical equation for calculating foam quality is simply described in Eqn 1:

$$Q = \frac{V_{gas}}{V_{foam}} \times 100. \tag{1}$$

where, Q is the foam quality in percentage, V_{gas} is the gas volume and V_{foam} is the foam volume, which is the total volume of gas and liquid existing in the foam. Foam quality usually ranges between 52% and 95%. A foam with less than 52% quality is considered unstable, as no bubble–bubble, interactions exist (Economides and Nolte 2000). In this case, the foam-based fluid can be considered as 'energised fluid'. On the other hand, in a foam with 95% quality, gas is the dominant and continuous phase, which makes foam become mist and unsuitable for fracturing operation.

Foam-based fracturing fluid has been extensively studied and implemented since late 1970s, as it has multiple benefits over conventional fluids. First, by using foams, a significant amount of water and chemical additives are reduced, thereby lowering operating costs and preventing formation damage and contamination issues. According to Economides and Nolte (2000), foam-based fluid performs effectively in water-sensitive formations where there is bentonite or smectite, which causes clay swelling. Second, due to the high apparent viscosity of foam-based fluid in porous media, the capability of proppant transportation and sedimentation are considerably improved (Speight 2016). Wanniarachchi *et al*.'s (2017) test concludes that foams help increase the proppant-carrying capability and decrease the proppant settling velocity by 85% when compared to water-based fluid.

In foam-based fluids, liquid is commonly mixed with compressed nitrogen gas, which is safe to use and compatible with most of the formation fluids. As nitrogen is injected underground, the interfacial tension in porous media is

lowered, thereby helping the hydrocarbon trapped in small pores to flow more easily (Economides and Nolte 2000). Moreover, as the compressed gas expands under downhole conditions, pressure is released and more energy is added to the reservoirs. Due to the increase in reservoir pressure and the low density of foam, the well can achieve excellent flowback with rapid clean-up of the fracturing fluid (Schramm 1994). Finally, by using foam-based fluid, less water is required to be recovered and disposed, which largely reduces the amount of possible hazardous and radioactive materials at the surface.

Besides the significant benefits over conventional fracturing fluids, there are some considerable limitations of foam-based fluids in field applications. First, the hydrostatic pressure of foams is relatively low due to its low density. Therefore, higher surface treating pressure is required, leading to an increase in the pumping costs. Additionally, nitrogen is normally contained as liquid phase in pressurised tanks, with a temperature of –196°C and a pressure of 30 kPa (Schramm 1994). Thus, the process of compressing, storing and transporting nitrogen can sometimes be challenging. The most critical challenge of foam-based fluid is the foam stability at reservoir conditions, where high temperature and pressures are encountered (Yekeen *et al*. 2018). Foam stability is the key factor contributing to the fracturing performance of foam-based fluid. With increasing temperature, gas bubbles start to move together and coalescence, leading to the decrease in foam's apparent viscosity. As foam becomes less viscous, the proppant settling velocity increases, resulting in the poor and non-uniform distribution of proppant. Consequently, the fracture dimensions decrease, and the foam's performance is negatively affected (Fei 2017). Several studies have been conducted to improve foam stability (Wilk *et al*. 2019), and one of the most effective solutions is to incorporate polymers in the foam mixture (Economides and Nolte 2000).

Generally, polymers help to viscosify the liquid content of the foam-based fluid. As liquid phase gets thicker, gas bubbles are harder to break or coalesce, leading to an increase in foam stability (Wendorff and Ainley 1981). Polymers have been used in hydraulic fracturing operations for decades, but mainly to viscosify the water-based fracturing fluids. Very limited research has been done to study the application of polymers in foam-based fracturing fluids. There are two main types of polymers used in fracturing: natural polymer and synthetic polymer. Natural polymers are a product of guar, which is a naturally occurring material produced from beans. Guar-based polymers are traditionally used in fracture stimulation due to their desirable rheological properties and cost-effectiveness (Al-Muntasheri 2014). Some of the popular examples of natural polymers are hydroxypropyl guar (HPG) and carboxymethyl hydroxypropyl guar (CMHPG) (Fink 2012). On the other hand, synthetic polymer application is quite new in hydraulic fracturing and is used as a friction reducer. Synthetic polyacrylamide (PAM) has been reported to have better thermal stability than natural polymers in water-based fracturing fluids (Al-Muntasheri 2014).

In this paper, laboratory experiments were conducted to examine the effects of HPG and PAM polymers on the rheology of the nitrogen foam-based fluids with 50% and 70% foam quality. The testing conditions were up to 110°C with three

different shear rates of 40, 100 and 170 1/s. The experimental results were then imported into the 3D fracture propagation model, which was developed based on the log data, reservoir properties from the well completion report, geomechanical properties from diagnosed fracture injection test (DFIT) results and the well production history. Finally, multiple simulations were run to predict the generated fracture geometry, conductivity and the proppant distribution of the HPG- and PAM-foamed fluids in the Toolachee Formation, Cooper Basin. The performances of these foam-based fluids were compared with slickwater and the industry-based fluid used in an actual fracture stimulation operation.

Geological background and hydraulic fracturing at the Cooper Basin

The Cooper Basin is a Late Carboniferous–Middle Triassic, non-marine sedimentary basin in eastern–central Australia that produces oil and gas from fluvial, deltaic and shoreface sandstones from eight formations (Alqahtani 2015). The basin is the largest hydrocarbon-producing province and the primary onshore source for natural gas in Australia. It is estimated that 8.2 TCF of recoverable gas and 43.9 MMSTB of recoverable oil have been found in the Cooper Basin (Alqahtani 2015). The basin covers an area of ~130 000 km² with a total thickness of 2500 m (Hill and Gravestock 1995). Located on the border between South Australian and Queensland, the Cooper Basin underlies the Eromanga Basin and overlyies the Warburton Basin (Fig. 1). The geological column of the Cooper Basin is illustrated in Fig. 2. Since the 1960s, oil and gas have been produced from the Cooper Basin and supplied for the domestic and international markets, also as liquefied natural gas.

Fracture treatment has been implemented in the Cooper Basin since the late 1960s to stimulate oil and gas production.

According to (Fei *et al.* 2016), as of 2013, more than 1500 fracture treatment stages were carried out on 700 wells in the basin. The common fracture targets are the Tirrawarra, Patchawarra and Toolachee formations. In this paper, we mainly focus on the Toolachee Formation, as it is the primary production zone of the study field. The Toolachee Formation (Late Permian), which is widespread across the entire Cooper Basin, consists of interbedded sandstone, siltstone, clay and occasional coal seams. The Toolachee Sand is one of the most productive reservoir rock types in the basin with the permeability ranging from 0.5–50 mD (Alqahtani 2015; Fei 2017).

The well used in this study was a vertical gas producing well in a mature oil and gas field in the Cooper Basin. The field has a large north-east–south-west anticline bounded on its north-western edge by a dominant normal fault. In 2012, the well was drilled and initially completed as a 4–1/2″ monobore completion, primarily targeting gas production from the Toolachee Formation with a reservoir depth of around 7300 ft. According the wireline log interpretation, the Toolachee Formation was estimated to have a total net pay of 34.8 ft, an average effective porosity of 10.1% and a water saturation of 44% (Santos 2012*a*, 2012*c*). One month after drilling, the well was fracture stimulated at the Toolachee intervals as part of the completion program. More details of fracturing scope and operations will be discussed in the next section.

Methodology

The methodology for this paper can be divided into two main sections: experimental and simulation. The general workflow of the integration is illustrated in Fig. 3.
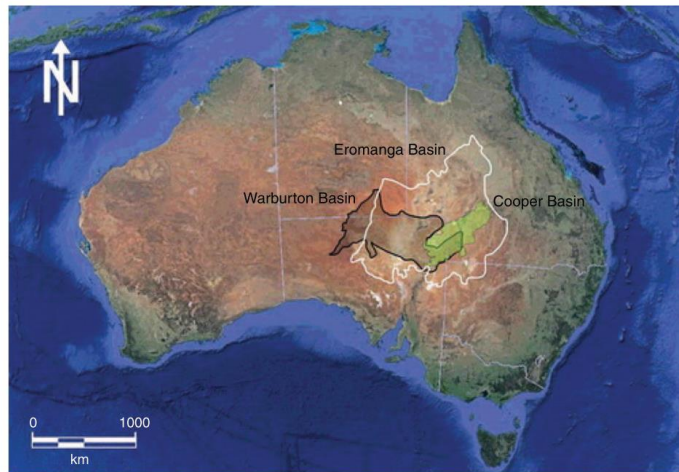

Fig. 1.   Locations of Cooper Basin, overlying Eromanga Basin and underlying Warburton Basin (Kulikowski *et al.* 2016).
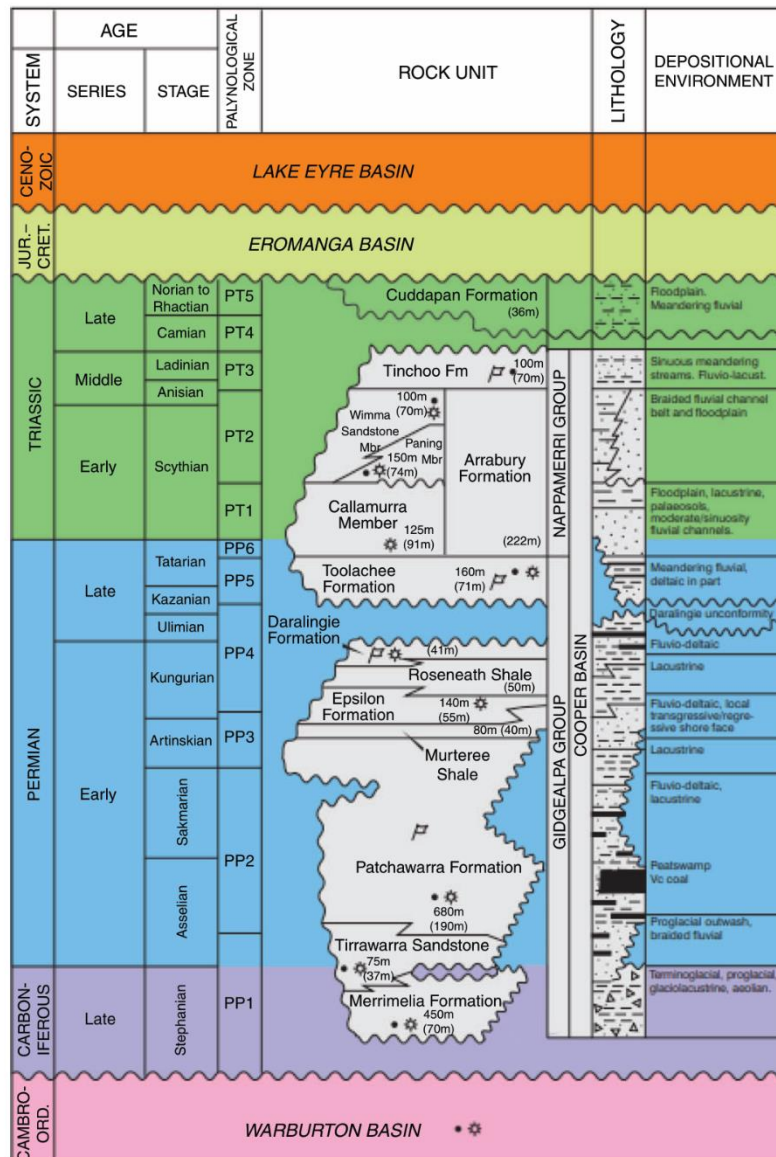
Fig. 2. Geological column of the Cooper Basin (Energy Mining South Australia 2019).
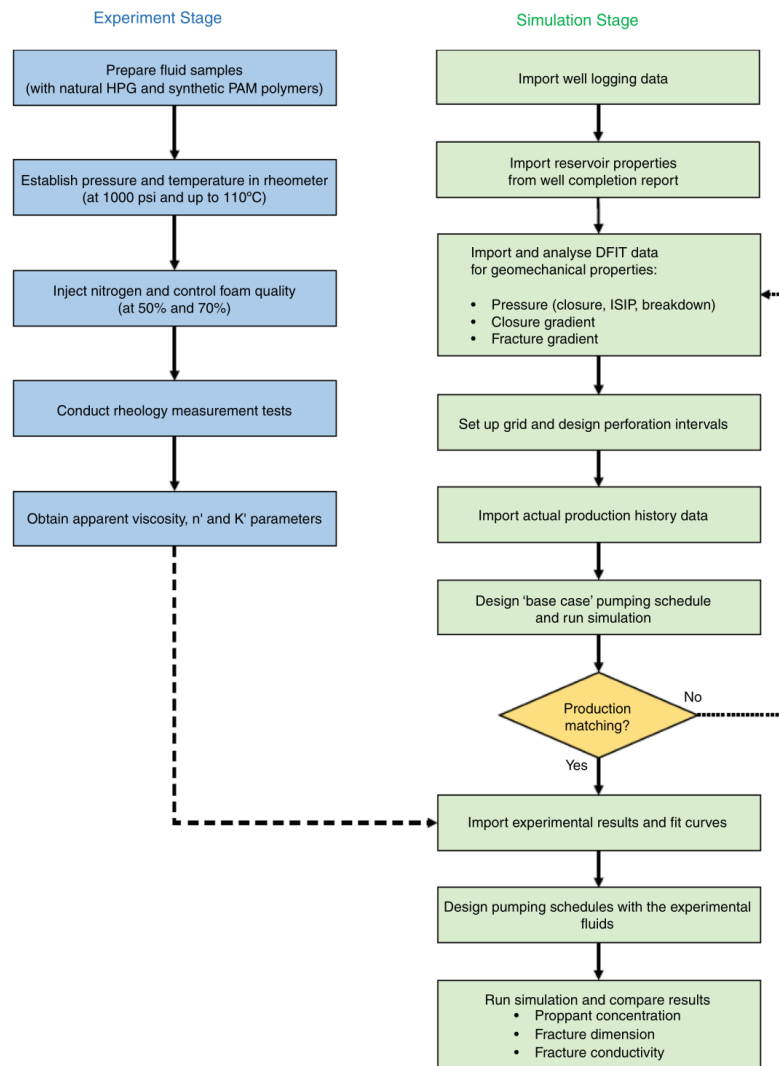
Experiment Stage | Simulation Stage

Prepare fluid samples
(with natural HPG and synthetic PAM polymers)

Establish pressure and temperature in rheometer
(at 1000 psi and up to 110°C)

Inject nitrogen and control foam quality
(at 50% and 70%)

Conduct rheology measurement tests

Obtain apparent viscosity, n' and K' parameters

Import well logging data

Import reservoir properties
from well completion report

Import and analyse DFIT data
for geomechanical properties:

- Pressure (closure, ISIP, breakdown)
- Closure gradient
- Fracture gradient

Set up grid and design perforation intervals

Import actual production history data

Design 'base case' pumping schedule
and run simulation

Production matching?

No

Yes

Import experimental results and fit curves

Design pumping schedules with the experimental fluids

Run simulation and compare results
- Proppant concentration
- Fracture dimension
- Fracture conductivity

Fig. 3. Integrated workflow of methodology. ISIP = instantaneous shut-in pressure.

Experimental stage

Sample preparation

The foam-based fracturing fluids were prepared at atmospheric pressure and at a temperature of 23°C. The experiments did not involve any core testing on formation rocks; therefore, clay control agent and biocide were not added into the samples. Hence, the samples were simply mixtures of tap water, foaming agents and polymer additives.

At first, an anionic foaming agent P-1 was mixed with tap water with an additive concentration of 4 mL/L. After that, two types of samples were generated from different types of polymers.

- **Sample A – Natural**: The foamed fluid was mixed with polymer W at a concentration of 1.2 g/L. Polymer W is an HPG, which is a natural and fast hydrating guar gum. HPG has been commonly used in hydraulic fracturing application for decades as it helps thicken the fracturing fluid, thereby increasing its viscosity. In this study, the used concentration of HPG is low, and it is referred as a linear gel 10# (10 lb/1000 gal)
- **Sample B – Synthetic:** Instead of adding polymer W, the foamed fluid was mixed with polymer N at a concentration of 0.5 mL/L. Polymer N is a synthetic PAM polymer. The concentration of PAM polymer used is typical for slickwater fracturing fluids. This low concentration in one-phase fluids helps to reduce the friction pressure.

Rheological measurements

When the sample preparation stage was finished, a pipe rheometer was used to measure the rheological properties of the foamed fluids. First, after entering the pipe rheometer, the fluid samples were circulated in a closed 1/8″ tubing system with a standard shear rate of 350 1/s. In the meantime, pressure was introduced and maintained in the measurement system at 1000 psi. After that, nitrogen gas was injected into the system while the samples were being stirred at 350 1/s. At the same time, the base fluid was slowly removed from the system, increasing the gas volume in the sample. The process of liquid withdrawal continued until the desired foam quality was reached. The foam quality was controlled and monitored by a densimeter, which measures the density of fluid sample in the system. For example, water has a density of 1.0 g/cm^3. With a 70% foam quality, the water volume is 30% of the total volume, resulting in a sample density of around 0.33–0.35 g/cm^3. Each type of fluid sample was studied with two foam qualities: 50% and 70%.

After the foam quality was obtained and stabilised, rheological measurements were conducted using the pipe rheometer. For each foam quality, the total test duration was 430 min, in which the testing temperature started from room temperature of 23°C, then increased to 90°C and finally to 110°C. During the experiment duration, the rheological properties were measured at three shear rates of 40, 100 and 170 1/s. At each measurement point, key rheological parameters, such as n′, K′ and the dynamic apparent viscosity, were recorded. In the rheology study, n′ is the dimensionless flow index and K′ is the consistency index

Simulation stage

The fracture propagation model was built and calibrated using the grid-orientated hydraulic fracture extension replicator (GOHFER) software. First, the wireline log data was imported to generate the formation and rock data of the well. After that, using the completion report of Well X, reservoir properties were updated into the model, as described in Table 1.

The actual responses of DFIT was then imported into the model (Fig. 4). The DFIT results were analysed to determine the geomechanical parameters of the reservoir, which are shown in Table 2.

Table 1.   Reservoir properties of Well X (Santos 2012*c*)

Parameter	Value	Unit
Reservoir depth	7315	ft
Reservoir thickness	88.9	ft
Gas net pay	34.8	ft
Permeability	0.016	mD
Porosity	10.1–12.0	%
Reservoir temperature	122	°C
Reservoir pressure	1913	psi
Gas saturation	56	%
Water saturation	44	%

Subsequently, two perforation intervals of the Toolachee Formation were included, and perforation depths were correlated using the log analysis report of Well X. The details of the perforation intervals are shown in Table 3. According to the post frac report, the well was fracture stimulated with an energised fracturing fluid in 2012. The base fluid was a Hybor fluid system, which uses an HPG gelling agent and delayed borate-crosslinker as viscosifiers. The base fluid was mixed with nitrogen gas at 50% foam quality for the main treatment. The actual pumping schedule for Well X is summarised in Table 4.

In GOHFER, a 'base case' simulation was set up with the same fracturing fluid system to reproduce the actual pumping schedule. The foam injection rate, surface proppant concentration and the treating pressures of the base case schedule are illustrated in Fig. 5. The actual production data from Well X was then imported to assess the calibration and the prediction ability of the model.

After the production history was matched, the results from the experimental stage were imported into GOHFER. The n′ and K′ parameters were then adjusted to match the reference rheological curves, thereby establishing the experimental fracturing fluids with HPG and PAM polymers into the software database. Finally, the fracture propagation simulator was run to evaluate the performance of different types of fracturing fluids in the Cooper Basin. In total, four fracturing fluid systems were simulated and compared: slickwater, 'base case' fluid, HPG-foamed fluids and PAM-foamed fluids. Key parameters obtained from the simulator were the fracture dimension (half-length, height, width), proppant concentration and fracture conductivity. Finally, the gas production of each case was simulated and compared. The total production period was selected as 800 days. Some assumptions were made in the production simulation, such as a drainage ratio of 200 acres and a flowing surface pressure of 200 psi.

Results and discussion

Experimental results

Rheological properties of the fracturing fluid are critically important to the success of any fracture stimulation treatment.
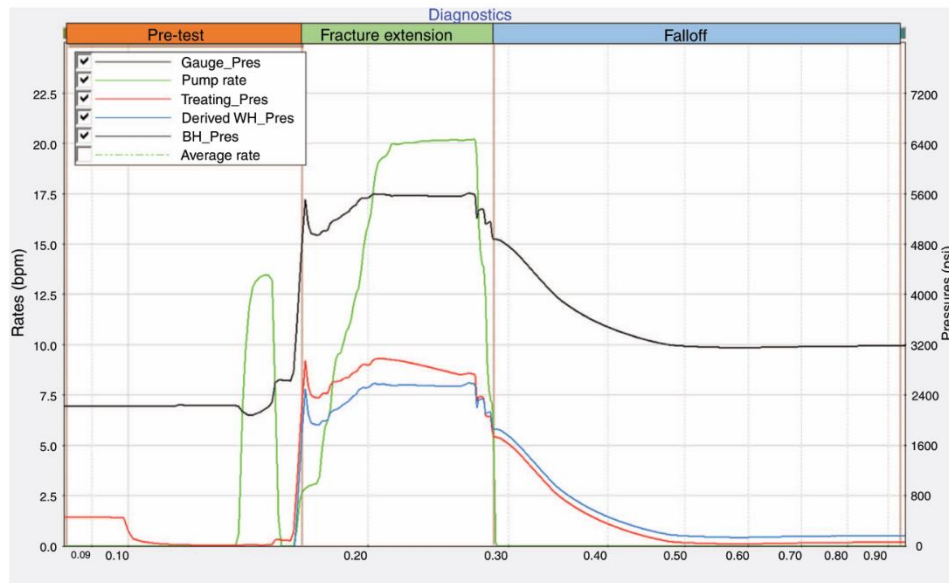
100

Fig. 4. DFIT response data (Santos 2012*b*).

Table 2. Geomechanical properties from analysed DFIT data (Santos 2012*b*)

Parameter	Value	Unit
Closure pressure	4058	psi
Bottomhole ISIP (instantaneous shut-in pressure)	4903	psi
Bottomhole breakdown pressure	5534	psi
Closure gradient	0.55	psi/ft
Fracture gradient	0.67	psi/ft

Table 3. Perforation intervals at the Toolachee Formation (Santos 2012*b*)

Interval	Measured depth (ft)	Perf length (ft)	Number of shots	Perf density (shots/ft)	Perf phasing (°)	Perf diameter (inch)
1	7307–7319	14	85	6.0	60	0.3
2	7333–7343	10	61	6.0	60	0.3

The rheological properties determine the fluid's capabilities of transporting and placing proppants into fractures, and therefore, strongly affect the proppant distribution as well as the fracture dimensions and conductivity. In this study, the viscosity of the foamed fluids was dependent on two variables: the foam quality and the type of polymer. The effects of each variable are shown and discussed below.

Table 4. Actual pumping schedule for the main treatment of Well X (Santos 2012*b*)

Stage	Pad	Slurry	Flush
Duration (minutes)	15	24	9
Fluid type	#40 HyborH	#40 HyborH	Linear gel
N2 foam quality (%)	50	50	50
N2 injected volume (scf)	163000	187000	46000
N2 injection rate (scf/m)	11000	11000	11000
Slurry clean volume (gal)	13184	11559	3429
Average slurry rate (bpm)	20	20	20
Average foam rate (bpm)	29	27	26
Proppant type	None	20/40 sand	None
Proppant concentration (ppa)	0	0–7.11	0

First is the effect of foam quality on foam-based fluids. Figs. 6 and 7 present the test results for foamed fracturing fluids with the inclusion of natural HPG and synthetic PAM polymers, respectively. For each fluid type, the viscosity at 50% and 70% foam quality were measured at the shear rates of 40, 100 and 170 1/s with increasing temperature.

It can be easily observed from both figures that higher foam quality results in higher fluid viscosity for all the testing shear rates. That is because as the gas content increases, more bubbles are generated with a higher degree of bubble interaction and collision, leading to a rise in viscosity. In both cases, the viscosity
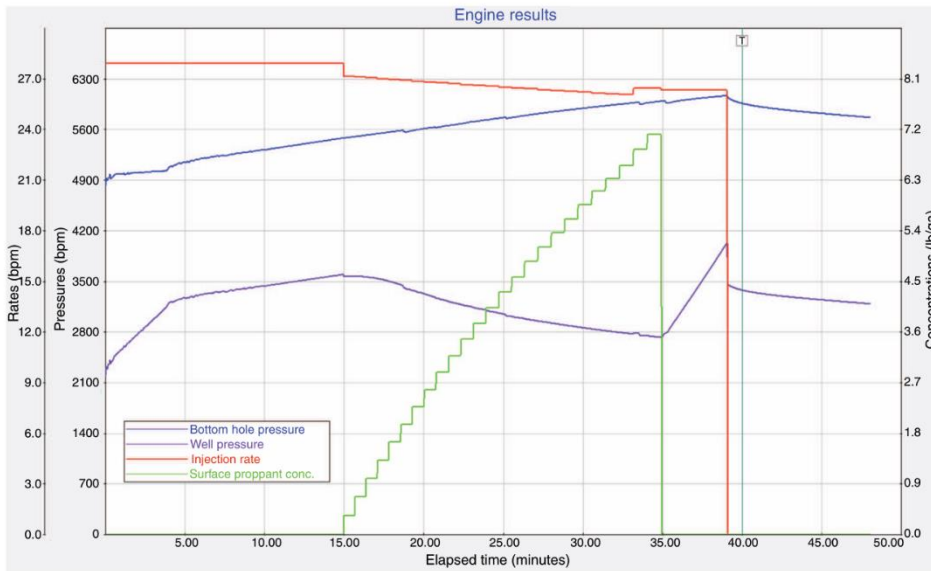
Fig. 5.   Foam injection rate, proppant concentration and pressure responses from the base case pumping schedule.
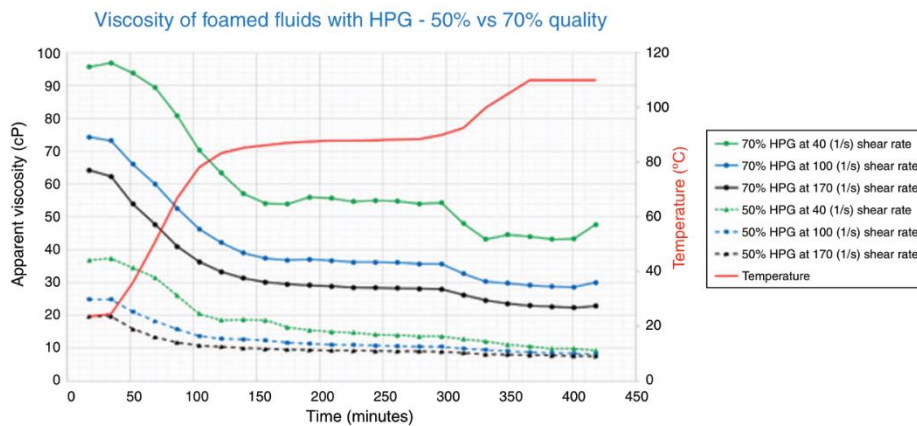

Fig. 6.   Viscosity of HPG-foamed fluids at 50% and 70% quality at different shear rates.

increased significantly by 3.1–3.3 times as the foam quality increased from 50% to 70%. Moreover, the effects of temperature and shear rates can also be seen from the figures. With the increasing temperature or shear rate, the fluid viscosity considerably decreased due to foam degradation. For a foam quality of 70%, the viscosity of HPG-foamed and PAM-foamed fluids were more sensitive to the changes in temperature and shear rates, compared to those from the 50% quality cases.

Next, the effects of different polymer types on the rheological property of foam-based fluids were taken into consideration. Fig. 8 compares the test results between HPG- and PAM-foamed fluid for a foam quality of 50%, while Fig. 9 shows the difference for a 70% foam quality.
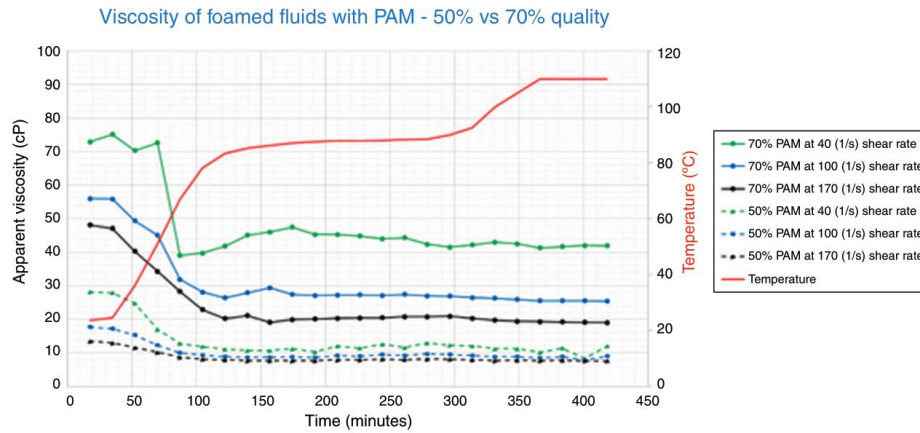
102

Fig. 7. Viscosity of PAM-foamed fluids at 50% and 70% quality at different shear rates.
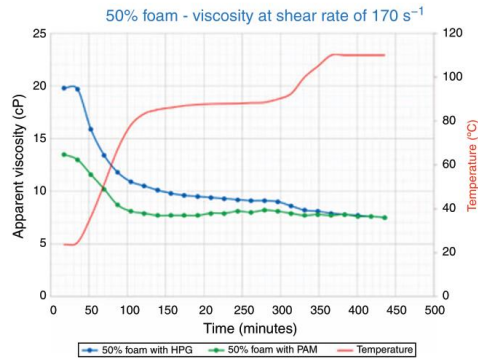

Fig. 8. Viscosity of HPG- and PAM-foamed fluid at 50% foam quality.
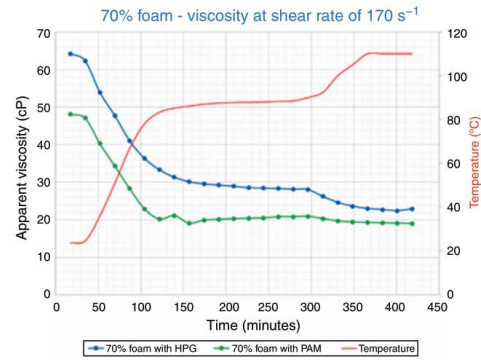

Fig. 9. Viscosity of HPG- and PAM-foamed at 70% foam quality.

For both cases, the viscosity measurement at a standard shear rate of 170 1/s were selected to be displayed as the results from other shear rates share very similar trend.

At both 50% and 70% foam quality, it is evident that HPG polymer generated more viscous fluid than the PAM polymer, which contradicts some previous research. A reasonable explanation for this behaviour is the difference in the polymer concentrations. When preparing the testing samples, the HPG polymer was used at a concentration of 1.2 g/L in powder form, while the PAM polymer was consumed at 0.5 mL/L concentration in liquid solution. As the active substance content of PAM solution is unknown, it is extremely challenging to compare the concentrations between the two polymers. However, in this test, it is believed that the concentration of PAM is less than that of HPG, which results in lower viscosity, as observed. The

importance of polymer concentration is highlighted and requires further investigation in future studies.

In Fig. 8, PAM-foamed fluid has the initial viscosity of 12.5 cP, which is 37% lower than that of the HPG-foamed fluid. In the first 100 min, as temperature increases from 23°C to 90°C, the viscosity of HPG-foamed fluid declines dramatically, while a lower decline rate is observed in PAM-foamed fluid. In the next 200 min, the temperature increases to and stabilises at 90°C. During this period, the foam-based fluid with HPG polymer experiences a slight viscosity decline, whereas the viscosity of PAM-foamed fluid remains stable at 8 cP. In the last 130 min, as the testing temperature jumps to 110°C, the viscosity of HPG-foamed fluid considerably decreases with a steeper slope. In comparison, a very small change is observed in the PAM-foamed fluid's viscosity. Not much difference can be seen compared to its viscosity at 90°C.

In addition, similar behaviour can also be observed in the 70% foam quality case. According to Fig. 9, the viscosity of HPG-foamed fluid is largely dependent on and very sensitive to the testing temperature. As the temperature increases from 90°C to 110°C, the viscosity of HPG-foams decreases by ~18%. On the other hand, at above 90°C, the effects of temperature become insignificant on the viscosity of PAM-foamed fluid. The viscosity of PAM-foams remains unchanged throughout the middle and late stages of the experiment.

Overall, it can be concluded that even though synthetic PAM polymers result in lower initial viscosity due to low polymer concentration, they are more effective than natural HPG polymers in improving thermal stability and preventing degradation of foams under higher temperature conditions. PAM polymers have been tested to stabilise foamed fluid's viscosity at up to 110°C.

Simulation results

After running the 'base case' scenario in GOHFER and calibrating the model based in the geomechanical properties, the production simulation was successfully matched with the production history of well X. Fig. 10 shows the curve matching in gas production rate, while Fig. 11 illustrates matching of the cumulative gas production. In both figures, the red line represents simulation results and the green crosses represent the actual production data points. Therefore, the model is considered well-calibrated and ready for prediction mode.

The experimental foam-based fracturing fluids were successfully added into the software database with their rheological curves fitted. Overall, there were a total of six types of fracturing fluids to be studied and compared:

(1) Slickwater
(2) Base case fluid (nitrogen foam-based fluid at 50% quality, added with HPG gelling agent, borate-crosslinker and buffer);

(3) HPG-foamed fluid at 50% quality;
(4) HPG-foamed fluid at 70% quality;
(5) PAM-foamed fluid at 50% quality; and
(6) PAM-foamed fluid at 50% quality.

In the fracture designs of these six fluid systems, the 20/40 proppants were equally consumed at the same total mass of 76 273 lbs with the same injecting concentration. However, in terms of the total clean volume, the slickwater design used ~30 000 gallons, which is much higher than the 50% foam quality case (20 800 gallons) and the 70% foam quality case (15 700 gallons).

Fig. 12 displays the simulation of proppant distribution for the six cases, with the proppant concentration ranging from 0 to 2.0 lb/ft^2. Generally, the foam-based fracturing fluids outperform slickwater in this field case simulation. Due to the low viscosity of slickwater, proppants are not effectively suspended and transported, leading to the short, narrow and poorly propped fractures at the target intervals. By using foams, better fracture dimensions are created with a reduction of 30%–47% of total water consumption.

It can also be observed that the fractures generated by 70% quality foams are shorter but greater in height and have higher proppant concentration at the target intervals, compared to the experimental 50% quality foams. This proves that foams with higher quality are better at carrying and placing proppants into the fractures due to their high viscosity.

When observing Fig. 12, the fracturing performance of HPG-foams and PAM-foams at the same foam quality appear relatively similar. Therefore, the numerical results of the simulation stage were summarised to study and compare the effects of the polymers. Table 5 provides a summary of the fracture dimensions and average proppant concentrations, while Fig. 13 demonstrates the simulation outputs of the fracture conductivity.
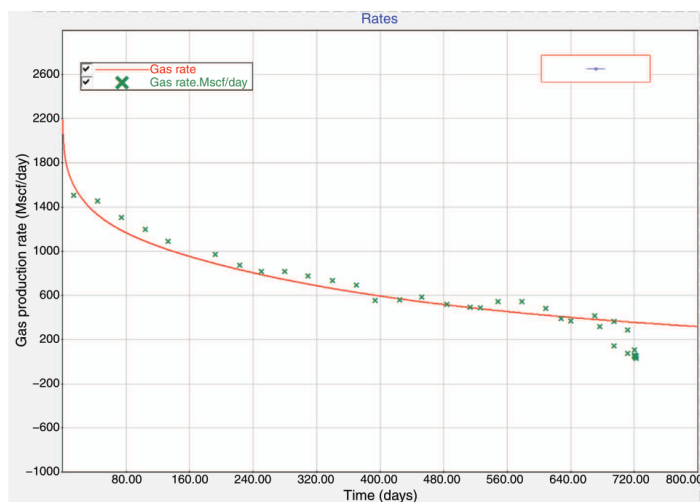

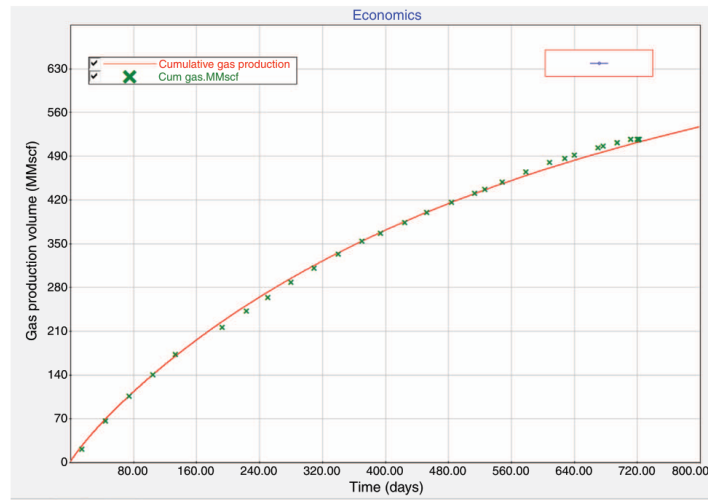**Fig. 10.**   Gas production rate matching.

Fig. 11.   Cumulative gas production matching.

In slickwater fracturing, the highest proppant concentration was observed at a value of 1.049 lb/ft^2. However, this high value was due to the rapid settlement of proppants, which causes over-accumulation at the near-wellbore area. Moreover, by using slickwater, a large amount of proppants travelled upwards and accumulated in the upper non-target fracture, forming a very highly conductive, but unbeneficial, pathway. Thus, the fracture conductivity in the slickwater case appears as noise and is not taken into consideration in Fig. 13.

It is clear that the base case fluid outperformed the experimental fluids in terms of the simulation outputs. Specifically, the fracture generated by the base case fluid has the largest width of 0.298 inch and the highest average proppant concentration of 1.022 lb/ft^2. Even though the fracture is short with a moderate height, it has the highest conductivity of up to 4200 mD/ft at near wellbore and 2500 mD/ft within the 100 ft half-length. The reason for this observation is mainly due to the effects of the borate-crosslinker, which was not included in any of our experimental fluids during the sample preparation. With the inclusion of borate-crosslinker, the base case fluid's viscosity as improved and maintained at 100–200 cP with a standard shear rate of 170 1/s at the temperature of 120°C (Fig. 14). Therefore, the importance of crosslinkers is demonstrated and highlighted in this study. Further investigation into the incorporation of crosslinkers in experimental foams is required.

From the experimental stage, PAM-foamed fluids have lower viscosity than HPG-foamed fluids at both 50% and 70% quality due to the lower polymer concentration. However, the simulation outputs show very surprising results for the PAM-foamed fluids. At 50% foam quality,

despite having lower viscosity, PAM-foamed fluid achieved very similar fracture geometry and average proppant concentration as HPG-foamed fluid. The fracture conductivity obtained from 50% quality PAM foam was also very close to that of the HPG foam. In addition, the performance of PAM foams was even better with higher foam quality. At 70% foam quality, despite larger difference in viscosity, PAM foam outperformed HPG foam in both fracture conductivity and fracture geometry, including an increase of 240 ft in the fracture half-length. Therefore, it can be concluded that apart from the foam viscosity, the thermal stability of foams also plays a very important role in the success of the fracture stimulation operation. In this field case, under reservoir temperature condition, a stable foam with lower viscosity and lower polymer concentration can achieve the similar or even better performance than a foamed fluid with higher viscosity. Therefore, the polymer consumption and polymer loading are considerably reduced, lessening their impacts on the environment.

Finally, the production capabilities of the designed fracture models were evaluated and compared. The simulated cumulative gas production of the foam-based fluids and slickwater over a period of 800 days is shown in Fig. 15. After 800 days, the base case fluid had the highest cumulative gas production (537 MMscf), while the lowest production belongs to the slickwater system (345 MMscf). At 70% foam quality, the PAM-foamed fluid had higher total gas production than HPG-foamed fluid (509 MMscf and 468 MMscf, respectively). On the other hand, at 50% foam quality, the HPG-foam resulted in a total of 423 MMscf gas, which was 7% higher than that of the PAM-foam.
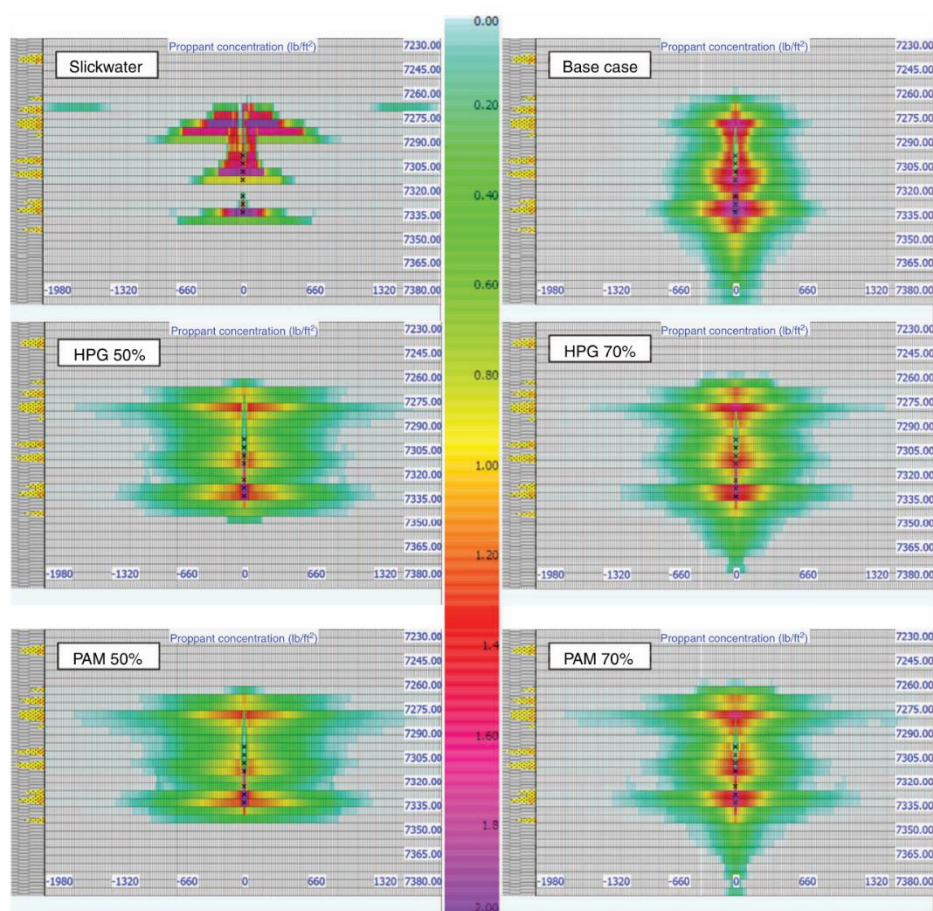
Fig. 12.   Results of proppant distribution versus depth and fracture half-length; black crosses represent the perforation locations.

According to the simulation results, it is evident that the recoverable gas production after fracture stimulation is directly proportional to the fracture conductivity. As the fracturing fluid is more viscous, proppants are transported more effectively and settle with higher concentrations. This helps to increase the fracture dimensions (in length, height and width), which significantly induce the fracture conductivity, and therefore, increase the hydrocarbon production.

Conclusions

This paper studies the rheological properties and performance of nitrogen foam-based fracturing fluids with the application of natural HPG and synthetic PAM polymers under high temperature conditions. Actual field data from the Toolachee

Table 5.   Summary of the simulated fracture dimensions and average proppant concentrations

Fluid type	Propped half-length (ft)	Fracture height (ft)	Average fracture width (inch)	Average proppant concentration (lb/ft^2)
Slickwater	700	60	0.130	1.049
Base case	820	95	0.298	1.022
HPG 50%	1700	80	0.196	0.850
PAM 50%	1720	75	0.190	0.850
HPG 70%	1480	110	0.227	0.941
PAM 70%	1720	115	0.237	0.944

106
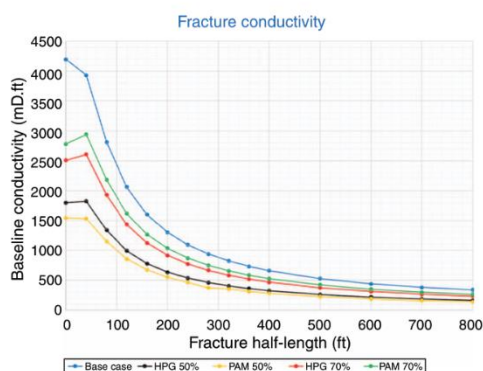
Fig. 13. Simulated fracture conductivity of the foam-based fracturing fluids.
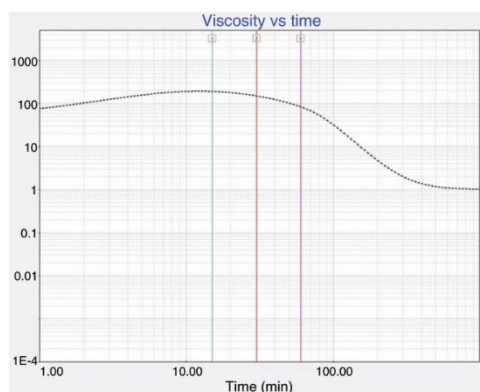

Fig. 14. Viscosity of the base case fluid with a shear rate of 170 s^{-1} at 120°C. (obtained from the GOHFER's fluid database).

Formation in the Cooper Basin was used to develop the simulation model.

In the experimental stage, foam viscosity increased by 3.1–3.3 times as the foam quality increased from 50% to 70%. Despite generating less viscous fluids, PAM polymers were much more effective than HPG polymers in improving the thermal stability of foams under high temperature conditions. PAM polymers successfully maintained foam viscosity at up to 110°C.

In the simulation, foam-based fluids totally outperformed slickwater by having larger fracture geometry, better proppant distribution, higher fracture conductivity and a water reduction of 30%–47%. The simulation outputs show that there is a strong correlation between the fracture conductivity and the gas production after fracture treatment. At high temperature, synthetic PAM polymers generated very stable foams, which achieved similar or even better fracturing results than the

Fig. 15. Simulation results of the cumulative gas production.

HPG-foamed fluids with higher viscosity. The importance of thermal stability on the performance of foams is therefore highlighted and emphasised. Finally, the industry foam used in the actual operation performed much better than the experimental foams due to the inclusion of crosslinker in the mixture. More investigation on the effects of crosslinkers on foam-based fluids in high temperature environment is recommended for future studies.

Conflicts of interest

The authors declare no conflicts of interest.

References

Al-Muntasheri, G. A. (2014). A Critical Review of Hydraulic-Fracturing Fluids for Moderate- to Ultralow-Permeability Formations Over the Last Decade. *SPE Production & Operations* **29**, 243–260. doi:10.2118/169552-PA

Alqahtani, F. A. (2015). Subsurface analysis of fluvial systems of Epsilon and Toolachee formations, Cooper Basin, Australia. *Arabian Journal of Geosciences* **8**(5), 3285–3297. doi:10.1007/s12517-014-1344-8

Barati, R., and Liang, J.-T. (2014). A review of fracturing fluid systems used for hydraulic fracturing of oil and gas wells. *Journal of Applied Polymer Science* **131**(16), 40735. doi:10.1002/app.40735

Economides, M. J., and Nolte, K. G. (2000). 'Reservoir Stimulation'. (John Wiley & Sons Ltd: West Sussex, UK.

Energy Mining South Australia (2019). *Cooper Basin*, Available at http://www.energymining.sa.gov.au/petroleum/prospectivity/cooper_basin [verified 12 October 2019].

Fei, Y. (2017). Experimental and Numerical Investigation of Nanotechnology on Foam Stability for Hydraulic Fracturing Application. PhD Thesis, Australian School of Petroleum, University of Adelaide, Australia.

Fei, Y., Gonzalez Perdomo, M., Nguyen, V., Lei, Z., Pokalai, K., Sarkar, S., and Haghighi, M. (2016). Simulation of hydraulic fracturing with propane-based fluid using a fracture propagation model coupled with multiphase flow simulation in the Cooper Basin, South Australia. *The APPEA Journal* **56**, 415–426. doi:10.1071/AJ15030

Fink, J. K. (Ed.) (2012). Chapter 17 - Fracturing Fluids. In 'Petroleum Engineer's Guide to Oil Field Chemicals and Fluids.' pp. 519–583. (Gulf Professional Publishing: Boston, USA)

Gottardo, S., Mech, A., Gavriel, M., Gaillard, C., and Sokull-Kluettgen, B. (2016). Use of nanomaterials in fluids, proppants, and downhole tools for hydraulic fracturing of unconventional hydrocarbon reservoirs. JRC Technical Report. Publications Office of the European Union. Luxembourg. Available at https://publications.jrc.ec.europa.eu/repository/bitstream/JRC103851/jrc103851_report_nanomaterials-fracturing-final-20161129.pdf [verified 12 February 2020]

Harris, P.C. (1988). Fracturing-Fluid Additives. *Journal of Petroleum Technology* **40**, 1277–1279. doi:10.2118/17112-PA

Hill, A. J., and Gravestock, D. I. (1995). The Cooper Basin. In 'The geology of South Australia, vol. 2: The Phanerozoic.' (Eds J.F. Drexel and W. V. Preiss.) pp. 78–87. (Geological Survey of South Australia: Adelaide, SA.)

Kulikowski, D., Amrouch, K., and Cooke, D. (2016). Geomechanical modelling of fault reactivation in the Cooper Basin, Australia. *Australian Journal of Earth Sciences* **63**(3), 295–314. doi:10.1080/08120099.2016.1212925

Santos (2012*a*). Well X - Log Analysis Report.

Santos (2012*b*). Well X - Post Job Report - Stage 1, Halliburton, Moomba, South Australia.

Santos (2012*c*). Well X - Well Completion Report, Adelaide, South Australia.

Schramm, L. L. (1994). 'Foams: Fundamels and Applications in the Petroleum Industry'. (American Chemical Industry: Washington DC, USA).

Smith, M. B., and Montgomery, C. (2015). 'Hydraulic Fracturing'. 1st edn. (CRC Press: Boca Raton, FL)

Speight, J. G. (2016). 'Handbook Of Hydraulic Fracturing'. (John Wiley & Sons, Inc: Hoboken, NJ).

Wanniarachchi, W. A. M., Ranjith, P. G., and Perera, M. S. A. (2017). Shale gas fracturing using foam-based fracturing fluid: a review. *Environmental Earth Sciences* **76**(2), 91. doi:10.1007/s12665-017-6399-x

Wendorff, C. L., and Ainley, B. R. (1981). Massive Hydraulic Fracturing Of High-Temperature Wells With Stable Frac Foams. In 'SPE Annual Technical Conference and Exhibition, 4-7 October, San Antonio, Texas.' (Society of Petroleum Engineers.) doi:10.2118/10257-MS

Wilk, K., Kasza, P., and Labus, K. (2019). Impact of Nitrogen Foamed Stimulation Fluids Stabilized by Nanoadditives on Reservoir Rocks of Hydrocarbon Deposits *Nanomaterials (Basel, Switzerland)* **9**(5), 766. doi:10.3390/nano9050766

Yekeen, N., Padmanabhan, E., and Idris, A. K. (2018). A review of recent advances in foam-based fracturing fluid application in unconventional reservoirs *Journal of Industrial and Engineering Chemistry* **66**, 45–71. doi:10.1016/j.jiec.2018.05.039

The authors

Tuan Huynh Minh Tran is a first year PhD student in Petroleum Engineering at the Australian School of Petroleum and Energy Resource (ASPER). After completing his Honours degree in December 2018, he has been working as a Production Engineer in the Gas Production Optimisation Team at Santos Ltd. He is responsible for identifying opportunities and preparing programs for gas well activities in the Cooper Basin, including capacity add, capacity maintenance and surveillance projects. Tuan's areas of expertise are in production engineering, reservoir simulation and hydraulic fracturing. His Honours research project was on simulating and comparing two assisted-history matching approaches on a Cooper–Eromanga Basin oil field model: one is a popular commercial software and the other is an interface recently developed in the ASPER. His doctoral research focuses on developing general guidelines for an optimal design of foam-based fracturing fluid that works well under high pressure, high temperature environments and evaluating its performance using both experimental and numerical simulation methods. Tuan is an active member of SPE, and is currently a postgraduate representative at ASPER and at SPE (South Australian chapter). Contact email: tuan.tran@adelaide.edu.au

Mary Gonzalez is a senior lecturer of Petroleum Engineering for the ASPER. Her research and teaching focus are on reservoir and production engineering, particularly production enhancement and optimisation. She joined the ASPER in 2009 after several years of experience in the oil and gas industry, where she provided practical petroleum engineering, consultancy services and solutions in the areas of subsurface and production engineering. Mary has published several articles in peer-reviewed journals and presented t international conferences. She has served as a reviewer for different journals, a mentor of young professionals and is the Community Education Chair and the ASPER Faculty Advisor for the Society of Petroleum Engineers. Contact email: maria.gonzalezperdomo@adelaide.edu.au

Klaudia Wilk graduated from the Faculty of Chemical Technology of the Rzeszow University of Technology. From 2011 she has held the position of Research Assistant in the Oil and Gas Institute – National Research Institute (INIG-PIB), and since 2017, she has been a Polish representative of the World Petroleum Council Youth Committee. In 2020, she obtained a PhD degree in Chemical Engineering at the Silesian University of Technology, which focused on the impact of energised fracturing fluids on rock reservoirs. Her scientific interests include intensification of hydrocarbons production and hydraulic fracturing, especially the use of alternative techniques to explore for non-conventional hydrocarbons deposits. She is a member of SPE and the Polish Association of Engineers and Technicians of the Oil and Gas Industry. Contact email: wilkk@inig.pl

Piotr Kasza is Head of the Reservoir Stimulation Department at the INIG-PIB. Kasza graduated from the Faculty of Drilling Department at the AGH University of Science and Technology, Cracow, Poland. At the same faculty in 2002, he obtained a PhD degree in technical sciences. From the beginning of his 30-year professional career he dealt with issues related to the reservoir stimulation. He participated in many foreign courses and internships, improving his work technique. He authored and co-authored numerous technological solutions in his field, many of which have been patented and published in Poland and abroad. Together with his team, he has received many awards at national and international fairs and exhibitions, promoting inventive and innovative activities. In recent years, he has been particularly active in developing technologies for unconventional hydrocarbons reservoir completion. He is a member of the Scientific Council of the INIG-PIB. Since 2017, he has represented INIG-PIB in the Board of the International Centre of Excellence on Coal Mine Methane operating at the United Nations Economic Commission for Europe. He is a member of the Social and Program Council on Faculty of Mining, Safety Engineering and Industrial Automation at Silesian University of Technology and the SPE. Contact email: kasza@inig.pl

Khalid Amrouch is a Structural Geologist with expertise in geomechanics. He graduated from Sorbonne University (Paris) with a BSc-Hons in Earth Sciences, MSc in Geosciences and a PhD in structural geology. His main interest relates to brittle tectonics, fracture characterisation and 4D stress analyses. Khalid started his career in 2005 at the Institut Français du Pétrole (IFP), which sponsored his studies, followed, in 2010, by a Research Engineer position at the Mines PariTech. In 2012, Khalid spent one year working for BHP as an Exploration Geologist in Chile, before joining the ASPER in February 2013. Since then, Khalid has been an active member of the S3 Research Group, one of the largest geoscience research groups at the University of Adelaide. Contact email: khalid.amrouch@adelaide.edu.au

8. Conclusions and Recommendations

8.1. Conclusions

This thesis presents a comprehensive investigation of the properties and performance of foam-based fracturing fluids stabilized by surfactants, silica nanoparticles (SNP) and polymers. Laboratory experiments and simulation modelling of fracturing foams at reservoir conditions allow drawing the following conclusions:

1. The addition of SNP positively influences the stability, rheology and proppant suspension capacity of surfactant foams at both ambient and elevated temperatures. The improved properties are attributed to the formation of SNP adsorption layers and SNP network on the gas-liquid interface. These SNP structures help increase liquid films' strength, improve foam texture and enhance the interface viscoelasticity, which eventually leads to the reduced drainage rate, higher half-life, higher apparent viscosity and lower proppant settling velocity in foams.

2. The stability of SNP-surfactant colloidal dispersions significantly impacts the properties and performance of fracturing foams. It has been concluded that the increase in temperature and salinity lowers the surface charge and promotes extreme aggregation behaviour of SNP. This, as a result, reduces the stability of the SNP-surfactant dispersions and negatively affects the stability, viscosity and proppant suspension capacity of liquid foams. The effects of temperature and salinity on the surface characteristics of SNP are explained by the DLVO electrostatic interaction theory.

3. The presence of surfactants increases the hydrophobicity of SNP. The contact angle of SNP depends heavily on the adsorption favourability of surfactants on the SNP surface. The cationic surfactant was found to result in the highest increase in the SNP's contact angle, followed by non-ionic surfactants and then anionic surfactants.

4. The synergy between surfactants and SNP plays a vital role in determining foams' properties. At both ambient and elevated temperatures, the combination of SNP and ionic surfactants produces higher foam stability and foamability than that of SNP and non-ionic surfactants.

5. Cationic surfactant has greater synergistic effects with SNP than anionic surfactant in enhancing liquid foams' stability, viscosity and proppant-carrying properties at sufficient surfactant concentrations. This suggests that the electrostatic attraction between cationic surfactant molecules and SNP is preferable in the fracturing foam application, compared to the electrostatic repulsion in the anionic surfactant-SNP system. However, when mixing very high concentrations of cationic surfactant with SNP, careful consideration must be taken to monitor the formation of SNP flocculates and corks in the dispersion, as these large-sized aggregation structures have a very high tendency to destabilize and reduce the properties of foams.

6. Foams stabilized by synthetic polymers have lower viscosity but higher thermal resistance than those stabilized by natural polymers. As the foam quality increases from 50% to 70%, the viscosity of polymer-stabilized foams was found to increase by 3.1 – 3.3 times.

7. Shear thinning and non-Newtonian behaviours are observed in the rheological properties of both SNP-surfactant-stabilized and polymer-surfactant-stabilized foams. The simulation modelling on two different tight gas reservoirs suggests that due to the high apparent viscosity and high proppant suspension capacity, the studied foams can achieve very uniform and effective distributions of proppants in the fracture system. Consequently, the foam cases generated larger fracture dimensions, lower leak-off rate, greater fracture conductivity and higher well productivity than the benchmark slickwater case at reservoir conditions.

8.2. Recommendations

Based on the findings and understandings gained from this research study, the following recommendations are suggested for future work:

1. Conduct bulk-scale experiments with high-grade observation columns to investigate the foamability, foam stability and proppant suspension capacity of fracturing foams at high-pressure high-temperature conditions of up to 3000 psi and 200 °C. Furthermore, it is suggested to study the effects of other gas types, such as N_2 and CO_2, on the properties of foams in the experiments.

2. Include a wide range of nanoparticle types in the study, which could be either negatively charged or positively charged, hydrophilic or hydrophobic, and with particle surface modified or unmodified.

3. Include bubble and micro-scale visualization experiments to observe the changes in size, shape and distribution of gas bubbles and particle aggregates in foams. These could be achieved by a stereo microscope, a scanning electron microscope (SEM) and a foam analyzer.

4. Perform experimental investigation of the adsorption behaviour of surfactants on typical reservoir rocks (positively charged carbonate, negatively charged sandstones) with and without the presence of nanoparticles. It is recommended that experiments be conducted at high temperature and pressure to replicate actual reservoir conditions.

5. Conduct a comprehensive study of the damage of nanoparticle-surfactant-stabilized foams to different reservoir rock types.

6. Undertake a comprehensive investigation to mitigate the effects of wall slippage on the viscosity measurements at low shear rates. Grooved couette and crosshatched geometries are recommended to replace the smooth surface one. Oscillation methods are suggested to be implemented to identify and monitor the impacts of wall slippage.

9. Appendix

9.1 GOHFER software – Application, advantages and limitations

Application of GOHFER:

GOHFER is a finite element-based reservoir simulator that specializes in modelling hydraulic fracturing processes in unconventional reservoirs. This software is designed to simulate the complex interactions that occur during hydraulic fracturing treatments. The application of GOHFER primarily revolves around hydraulic fracturing simulations, specifically in unconventional reservoirs such as shale formations. It allows engineers and researchers to model the behavior of fluids, proppants, and rock formations during hydraulic fracturing operations. Some of its key applications and capabilities include:

1) Fracture Propagation: GOHFER can model the initiation, growth, and propagation of fractures within subsurface rock formations under the influence of hydraulic pressure.

2) Proppant Transport: It can simulate the transport and placement of proppant materials within fractures to understand their distribution and effectiveness in keeping fractures open.

3) Fluid Flow: The software can model the flow of hydraulic fracturing fluids within fractures and porous media, helping to optimize fluid injection strategies.

4) Stress Analysis: GOHFER can analyze the stress distribution within the reservoir, which is crucial for understanding how fractures interact with pre-existing natural fractures and faults.

5) Wellbore Interactions: It considers interactions between fractures and wellbores, helping to optimize well placement and completion designs.

6) Parametric Studies: Engineers can use GOHFER to conduct parametric studies, assessing the impact of different factors such as fluid properties, injection rates, and rock properties on fracture behavior.

Inherent model employed in GOHFER:

GOHFER employs a cohesive zone model (CZM) to simulate fracture propagation. The CZM is a widely accepted approach in fracture mechanics. It divides fractures into cohesive elements that can open and close based on stress conditions. This model considers the energy release rate, fracture toughness, and the constitutive behavior of rocks and fluids. It accurately captures the initiation, growth, and interaction of fractures in response to hydraulic fracturing operations.

Advantages of GOHFER:

1) Accurate fracture propagation modelling: GOHFER is renowned for its ability to accurately model fracture propagation in various reservoir conditions. It employs a cohesive zone model (CZM) to simulate the opening and closing of fractures, capturing the complex behavior of fractures under stress.

2) Flexibility in fluid and proppant modelling: GOHFER allows for the modeling of various fracturing fluids and proppants, providing a comprehensive understanding of how different fluid and proppant properties influence fracture behavior. This flexibility is crucial in optimizing hydraulic fracturing operations.

3) Realistic reservoir considerations: The software incorporates real reservoir data, such as rock mechanics properties, stress profiles, and geological features, to create highly realistic simulations. This ensures that the simulations closely match actual reservoir conditions.

4) Sensitivity analysis: GOHFER enables sensitivity analysis, allowing users to investigate the impact of different parameters on fracture behavior. This capability is valuable for optimizing fracture design and well performance.

5) User-friendly interface: Despite its advanced capabilities, GOHFER offers a user-friendly interface that makes it accessible to engineers and researchers with varying levels of expertise. It simplifies the process of setting up and running simulations.

Limitations of GOHFER:

1) Computational intensity: GOHFER's high level of accuracy comes at the cost of computational intensity. Running simulations with fine grids and complex reservoir models can be time-consuming and computationally demanding.

2) Data requirements: To achieve accurate results, GOHFER relies on detailed reservoir data, including rock properties, stress profiles, and geological information. Obtaining and inputting this data can be challenging and time-consuming.

3) Complexity: The software's complexity may pose a learning curve for new users. Training and experience are necessary to fully harness its capabilities.

9.2 GOHFER software – Step-by-step guide

Working with GOHFER involves several key steps to effectively set up and run simulations. Below is a step-by-step guide to help you navigate the process:

Step 1: Installation and setup:

- Begin by installing the GOHFER software on your computer. Follow the installation instructions provided by the software vendor.
- Launch the software and ensure that you have all the necessary licenses and access to required modules.

Step 2: Import reservoir data:

- Before running simulations, import the reservoir data, including geological information, stress profiles, and rock properties, into GOHFER. This data is crucial for creating an accurate reservoir model.
- Ensure that your data is in the appropriate format and that units compatible with GOHFER.

Step 3: Define simulation parameters:

- Set up your simulation parameters, including the fracture fluid properties (e.g., viscosity, density), wellbore information (e.g., well trajectory, completion design), and fracture geometry (e.g., initial fracture dimensions).
- Specify the time step size and duration for your simulation.

Step 4: Fluid and proppant modelling:

- Choose the fluid and proppant models that best represent your fracturing fluid and proppant types. Input their respective properties, such as viscosity, density, and size distribution.
- GOHFER allows you to simulate various fracturing fluid and proppant combinations, providing flexibility in your simulations.

Step 5: Set boundary conditions:

- Define the boundary conditions for your simulation, including the reservoir boundaries, initial stress conditions, and any external forces or pressures.
- Ensure that boundary conditions align with your reservoir data and real-world conditions.

Step 6: Mesh generation:

- Create a computational mesh that divides your reservoir into discrete elements. The mesh's granularity affects the simulation's accuracy and computational demands.
- Use mesh generation tools within GOHFER or import pre-generated meshes if available.

Step 7: Cohesive zone model (CZM):

- GOHFER employs a Cohesive Zone Model (CZM) to simulate fracture propagation. Define CZM parameters based on your reservoir and rock mechanics data, such as fracture toughness and cohesive zone properties.

Step 8: Simulation run:

- Start the simulation and monitor its progress. Simulations may take varying amounts of time depending on your chosen parameters and mesh complexity.
- GOHFER provides visualization tools to track fracture propagation, fluid flow, and other relevant parameters during the simulation.

Step 9: Analyze results:

- Once the simulation is complete, analyze the results to understand fracture behavior, proppant placement, and other relevant performance metrics.
- Utilize GOHFER's post-processing capabilities to extract valuable insights from the simulation data.

Step 10: Optimization and reporting:

- Optimize your hydraulic fracturing design based on the simulation results by adjusting parameters such as fluid properties, well completion, or proppant selection.
- Generate reports and visualizations to communicate your findings and recommendations effectively.

Step 11: Iteration and validation:

- If necessary, iterate through steps 3 to 10 to refine your fracture design further.
- Validate your simulations by comparing the results with field data to ensure accuracy and reliability.
- By following these step-by-step instructions, you can effectively work with GOHFER to simulate hydraulic fracturing operations, optimize designs, and gain valuable insights into fracture behavior and well performance.